

Mutual Coupling Reduction between Closely Spaced U-slot Patch Antennas by Optimizing Array Configuration and its Applications in MIMO

Nahal Niakan

Submitted to the graduate degree program in the Department of Electrical Engineering
& Computer Science and the Graduate Faculty of the University of Kansas

In partial fulfillment of the requirements for the degree of
Master of Science.

Committee:

Sarah Seguin

Christopher Allen

James Stiles

Date Defended: 03/31/2014

The Thesis Committee for Nahal Niakan
certifies that this is the approved version of the following thesis:

**Mutual Coupling Reduction between Closely Spaced U-slot Patch
Antennas by Optimizing Array Configuration and its Applications in
MIMO**

Chairperson ,Sarah Seguin

Date approved: <<04/01/2013 >>

Page left intentionally blank.

Abstract

Multiple-input, multiple-output (MIMO) systems have received considerable attention over the last decade. There are some limitations when obtaining the most from MIMO, such as mutual coupling between antenna elements in an array. Mutual coupling and therefore inter-element spacing have important effects on the channel capacity of a MIMO communication system, its error rate, and ambiguity of MIMO radar system. There is a huge amount of research that focuses on reducing the mutual coupling in an antenna array to improve MIMO performance.

In this research, we focus on the antenna section of the system. Antenna design affects the performance of Multiple-Input–Multiple-output (MIMO) systems. Two aspects of an antenna's role in MIMO performance have been investigated in this thesis. Employing suitable an antenna or antenna array can have a significant impact on the performance of a MIMO system. In addition to antenna design, another antenna related issue that helps to optimize the system performance is to reduce mutual coupling between antenna elements in an array. Much research has focused on the reduction of mutual coupling.

In this research, the effect of the antenna configuration in array on mutual coupling has been studied and the main purpose is to find the array configuration that provides the minimum mutual coupling between elements.

The U-slot patch antenna is versatile antennas that because of its features like wide bandwidth, multi-band resonance and the ease of achieving different polarizations. This research first investigated the u-slot patch antenna, its features and capabilities. Second a CAD optimization to design a low profile, dual band U-slot patch antenna is provided. Designed antenna is a dual band antenna that is intended to work at 3.5 and 5 GHz and have sufficient gain of at least 3 dB.

The effect of mutual coupling on MIMO systems is studied and then different array configurations were considered for two closely spaced U-slot patch antennas. Different configurations show different mutual coupling behavior. After modeling and simulation, the array was designed, implemented and finally tested in an anechoic chamber. These results are compared to both simulation and theoretical results and the configuration with minimum amount of mutual coupling was found. Some radar experiments also have been done to prove the effect of mutual coupling on radar performance.

Page left intentionally blank.

Acknowledgments

This thesis would not have been possible without the guidance and the help of several individuals who in one way or another contributed and extended their valuable assistance in the preparation and completion of this study.

First and foremost, my gratitude to Dr. Sarah Seguin whose sincerity and guidance have been my inspiration in the completion of this research .

I also would like to say thank you to my friends, colleagues, especially graduate student, Brian Cordill, professors, staffs and many others at the EECS department of University of Kansas for supporting me.

I also want to thank Prof. Esfandiar Mehrshahi who introduced me to the fascinating world of Electromagnetic at very early stages of my college education.

Last but not the least I would like to express my deepest appreciation and gratitude to my parents and two brothers. They were miles away from me but always there cheering me up, stood by me through the good times and bad.

Page left intentionally blank.

Contents

ABSTRACT	IV
ACKNOWLEDGMENTS	VI
CONTENTS	VIII
LIST OF FIGURES	X
LIST OF TABLES	XIII
CHAPTER 1	1
INTRODUCTION	1
1.1 PROJECT MOTIVATION	1
1.2 BACKGROUND OF ANTENNA THEORY	2
1.2.1 Impedance Bandwidth	2
1.2.2 Gain and Radiation Efficiency	2
1.2.3 Radiation Pattern.....	2
1.2.4 Smith chart.....	3
1.3 BACKGROUND OF MIMO THEORY.....	4
1.3.1 MIMO wireless communications.....	4
1.3.2 MIMO Radar	5
1.3.3 MIMO and Mutual Coupling	6
1.3.4 MIMO System Model	7
CHAPTER 2	10
SINGLE U-SLOT PATCH ANTENNA	10
2.1 OVERVIEW	10
2.2 SLOT ANTENNA	10
2.3 PATCH ANTENNA	12
2.3.1 Design Equations and Procedures.....	13
2.4 U-SLOT PATCH ANTENNA	15
2.4.1 Other studies about u-slot.....	16
2.4.2 Antenna Design.....	18
2.4.3 Antenna Simulation in HFSS.....	19
2.4.4 Optimization	22
CHAPTER 3	30
U-SLOT PATCH ANTENNA ARRAY	30
1.1 MUTUAL COUPLING	30
1.2 ARRAY CONFIGURATIONS.....	32
Configuration 1	33
Configuration 2	35
Configuration 3	37
Configuration 4	39
Configuration 5	41

<i>Configuration 6</i>	43
<i>Configuration 7</i>	45
<i>Configuration 8</i>	47
<i>Comparison of the results</i>	49
CHAPTER 4	55
MUTUAL COUPLING AND MIMO	55
4.1 SYSTEM MODEL	55
4.2 SIMULATION RESULTS.....	59
CHAPTER 5	60
EXPERIMENTAL RESULTS AND COMPARISONS	60
5.1 SINGLE U-SLOT PATCH ANTENNA.....	60
5.2 MUTUAL COUPLING MEASUREMENTS.....	65
5.3 MIMO CAPACITY	68
5.3 MIMO RADAR RANGE –ANGLE AMBIGUITY.....	70
5.4 THREE ELEMENTS ARRAY	73
CHAPTER 6	76
CONCLUSION AND FUTURE WORK	76
BIBLIOGRAPHY	77

List of Figures

Figure 1 .Radiated field regions for an antenna of maximum dimension D	3
Figure 2 .Smith chart important points [From antenna from theory to practice]	3
Figure 3 .MIMO Spatial Multiplexing	4
Figure 4. MIMO Spatial Diversity	5
Figure 5 .Jakes Model for correlation based on antenna separation.....	7
Figure 6.MIMO system	8
Figure 7 .A slot antenna, its radiation pattern and its complementary dipole [Antenna from theory to practice]	11
Figure 8.Geometry of Microstrip patch antenna [Antennas: From Theory to Practice]	12
Figure 9 . Generic Impedance Loci for U-Slot Microstrip Antenna [14].	15
Figure 10 . Geometry of Wideband v-slot patch antenna with two parallel edge slot (Rafi and Shafai IEEE 2003)	16
Figure 11.Geometry of non-rectangular microstrip antenna with v-slot (Rafi and Shafai IEEE 2003).....	16
Figure 12.Configuration of double U-slot antenna.....	17
Figure 13 .Geometry of the circularly polarized U-slot patch antenna [16].....	17
Figure 14 .Geometry of coaxially fed rectangular patch with a U –shaped slot	18
Figure 15.DESIGN PARAMETERS OF SINGLE U-SLOT PATCH ANTENNA	19
Figure 16.Different views of the designed antenna in HFSS	19
Figure 17.Radiation pattern of a probe fed U-slot patch antenna in dB	20
Figure 18.Surface current distribution on of a probe fed U-slot patch antenna	20
Figure 19.VSWR of a probe fed U-slot patch antenna in frequency range of [1GHz to 3GHz].....	21
Figure 20. Return Loss for Initial Design of U-Slot Microstrip Patch.....	21
Figure 21 .Impedance Locus for center fed Design U-Slot Microstrip Patch	23
Figure 22.Effect of Probe Location on the Return loss Behavior of the U-Slot.....	23
Figure 23 .Effect of Probe Location on the Impedance Behavior of the U-Slot.....	24
Figure 24 .Effect of Probe radius on the Impedance Behavior of the U-Slot	24
Figure 25 .Effect of Slot width on the Return loss of the U-Slot.....	25
Figure 26 .Effect of slot width on the Impedance Behavior of the U-Slot	25
Figure 27 .Effect of slot length on the Impedance Behavior of the U-Slot.....	26
Figure 28 .Effect of slot length on the return loss behavior of the U-Slot	26
Figure 29 .Simulated return loss of the optimized design.....	27
Figure 30.Impedance behavior of dual band final design	28
Figure 31 .Radiation pattern of dual band final design.....	28
Figure 32.Triple band U-slot patch.....	28
Figure 33.Return loss of triple band U-slot patch antenna.....	29
Figure 34 .Different possible configurations for two u-slot patch antennas	32
Figure 35 .Geometry of configuration 1 of U-slot patch antenna array.....	33

Figure 36 .Simulated S ₁₁ of the first configuration for different values of d.....	33
Figure 37 . Simulated S ₂₁ of the first configuration for different values of d	34
Figure 38 .Electric field (top) and Magnetic field (bottom) coupling between array elements in configuration one	34
Figure 39 .Geometry of configuration 2 of U-slot patch antenna array.....	35
Figure 40 .Simulated S ₁₁ of the second configuration for different values of d	35
Figure 41 .Simulated S ₂₁ of the second configuration for different values of d.....	36
Figure 42. Electric field (top) and Magnetic field (bottom) coupling between array elements in configuration two	36
Figure 43 .Geometry of configuration 3 of U-slot patch antenna array.....	37
Figure 44 .Simulated S ₁₁ of the third configuration for different values of d.....	37
Figure 45 .Simulated S ₂₁ of the third configuration for different values of d.....	37
Figure 46. Electric field (top) and Magnetic field (bottom) coupling between array elements in configuration three.....	38
Figure 47 .Geometry of configuration 4 of U-slot patch antenna array.....	39
Figure 48 .Simulated S ₁₁ of configuration four for different values of d.....	39
Figure 49 . Simulated S ₂₁ of the configuration four for different values of d.....	40
Figure 50 .Electric field (top) and Magnetic field (bottom) coupling between array elements in configuration four	40
Figure 51 .Geometry of configuration 5 of U-slot patch antenna array.....	41
Figure 52 .Simulated S ₁₁ of the configuration five for different values of d.....	41
Figure 53 .Simulated S ₂₁ of the configuration five for different values of d.....	41
Figure 54 .Electric field (top) and Magnetic field (bottom) coupling between array elements in configuration four	42
Figure 55 .Geometry of configuration 6 of U-slot patch antenna array.....	43
Figure 56 .Simulated S ₁₁ of the configuration six for different values of d.....	43
Figure 57 .Simulated S ₂₁ of the configuration six for different values of d.....	44
Figure 58 .Electric field (top) and Magnetic field (bottom) coupling between array elements in configuration six	44
Figure 59 .Geometry of configuration 7 of U-slot patch antenna array.....	45
Figure 60 .Simulated S ₁₁ of the configuration seven for different values of d	45
Figure 61 .Simulated S ₂₁ of the configuration seven for different values of d	46
Figure 62 . Electric field (top) and Magnetic field (bottom) coupling between array elements in configuration seven.....	46
Figure 63 .Simulated S ₁₁ of the configuration eight for different values of d	47
Figure 64 .Simulated S ₂₁ of the configuration eight for different values of d.....	47
Figure 65 .Electric field (top) and Magnetic field (bottom) coupling between array elements in configuration eight	48
Figure 66.Return loss for different configurations.....	49
Figure 67 .Simulated S ₂₁ for different configurations for antenna spacing of d=0mm	49
Figure 68 .Simulated S ₂₁ for different configurations for antenna spacing of d=11mm	50
Figure 69 .Simulated S ₂₁ for different configurations for antenna spacing of d=44mm	51
Figure 70 .Surface current distribution on the terminated antenna due to the coupling from left side excited antenna.....	52
Figure 71 .Simulated S ₁₂ in different configurations versus antenna spacing (d/λ)	54

Figure 72 .Simulated cumulative distribution function for MIMO capacity in 8 proposed array configurations in the case of $d=\lambda/2$	59
Figure 73 .Simulated MIMO capacity versus antenna spacing for 8 proposed array configuration.....	59
Figure 74 .Photograph of the two fabricated prototypes.....	60
Figure 75 .The simulated and measured return losses of the proposed antenna	61
Figure 76 .Radiation patterns of the single U-slot patch at plane of $\phi= 90$ at 3.429 GHz.a) Measured .b) Simulated	62
Figure 77 . Radiation patterns of the single U-slot patch at plane of $\phi= 0$ at 3.429 GHz. a) Measured .b) Simulated	62
Figure 78. Radiation patterns of the single U-slot patch at plane of $\phi= 0$ at 4.965GHz. a) Measured and b) Simulated.....	63
Figure 79. Radiation patterns of the single U-slot patch at plane of $\phi=90$ at 4.965GHz . a) Measured and .b) Simulated	63
Figure 80.antenna polarization at 3.49 GHz.	64
Figure 81 Antenna polarization at 4.9 GHz.	64
Figure 82 .Measured S ₂₁ for different configurations for antenna spacing of $d=44\text{mm}$	65
Figure 83 .Measured S ₂₁ for different configurations for antenna spacing of $d=22\text{mm}$	66
Figure 84 .Measured S ₂₁ for different configurations for antenna spacing of $d=22\text{mm}$ in shorter range of frequencies.	66
Figure 85 .Measured S ₂₁ for different configurations for antenna spacing of $d=0\text{mm}$	67
Figure 86 .Measured S ₂₁ for different configurations for antenna spacing of $d=0\text{mm}$ in smaller range of frequencies.	67
Figure 87 .Measured cumulative distribution function for MIMO capacity for eight proposed array configurations in the case of $d=\lambda/2$	68
Figure 88.Simulated cumulated distribution function for MIMO capacity for 8 proposed array configurations in the case of $d=\lambda/2$	69
Figure 89.Range-Angle ambiguity function for array configuration 3	70
Figure 90.Range-Angle ambiguity function for array configuration 2	71
Figure 91.Range-Angle ambiguity function for array configuration 4	71
Figure 92.Radiation pattern of array with configuration2.....	72
Figure 93.Radiation pattern of array with configuration4.....	72
Figure 94 .Four different three element array configurations.....	73
Figure 95.S ₁₂ measurements for four different configurations.....	74
Figure 96.S ₁₃ measurements for four different configurations.....	74
Figure 97.S ₂₃ measurements for four different configurations.....	75

List of Tables

Table 1. Wideband U-slot patch antenna dimensions	19
Table 2 . Initial design of U-Slot Microstrip Patch Antenna.	22
Table 3 . Optimized design of U-Slot Microstrip Patch Antenna.	27
Table 4 . Triple band U-slot patch antenna dimensions.....	29
Table 5. Summary of eight different configurations for antenna array.....	53
Table 6. Summary of figure 77.	61
Table 7. Average MIMO capacity based on measured S_{12} for each configuration.....	68

Chapter 1

Introduction

1.1 Project motivation

Today technology faces an era characterized by small, fast and more reliable devices. One of the main goals in communication and radar technologies is to make their systems as small as possible as long as their size does not affect their performance. This means employing more antennas and placing antennas close to each other, and, thus, leading to more mutual coupling.

Antennas play an important role in today technology and since the emergence of MIMO, antennas is even more important. Good antenna array design with low mutual coupling that satisfies the space constraints and yet provides good MIMO performance has become the motivation of our study.

Several antenna designs and techniques have been proposed to reduce mutual coupling. Techniques to modify ground structure are presented in [31], Studies such as [32] have applied lump circuits or neutralization lines [28] proposed using parasitic elements to create reverse coupling to reduce mutual coupling.

In this work, we propose using simple but highly effective antenna diversity techniques to reduce mutual coupling between array elements without changing the antenna's structure. In this method antenna structure remains unchanged and without any extra cost antennas can be fabricated. The idea is to change array configuration to find a configuration with the lowest amount of mutual coupling between elements.

In this research, first we introduce a U-slot patch antenna and then optimize the mutual coupling effects of the antennas for closely spaced elements in array by just change the array configuration which enhances MIMO performance and helps to reduce a system's size.

The purpose of this chapter is to provide sufficient background in antenna and MIMO theory to enable the reader to better understand the work detailed in this thesis. Those who are interested in more details of the concepts can refer to [1] and [2].

1.2 Background of Antenna Theory

Regardless of antenna type, its performance can be characterized by the metrics such as Impedance Bandwidth, Efficiency, Gain, Polarization and Radiation Pattern. Following discussions give brief explanation about each of these antenna parameters.

1.2.1 Impedance Bandwidth

The antenna is essentially a matching network between the characteristic impedance of the radio system (nominally 50 ohms) and the impedance of free space. It is essential that antenna presents an acceptable impedance match over the frequency band(s) of operation. Antenna impedance is most commonly characterized by either return loss or Voltage Standing Wave Ratio (VSWR).

1.2.2 Gain and Radiation Efficiency

Antenna efficiency is one of the most important antenna performance parameters. Mathematically, the gain can be written as

$$G = \frac{4\pi U}{P_{in}} \quad (1)$$

G is gain, U is the radiation intensity and P_{in} is the total input power accepted by the antenna .

1.2.3 Radiation Pattern

Radiation pattern of an antenna is a plot of the radiated field/power as a function of angle at a fixed distance, which should be large enough to be considered far field. Three radiation regions have been defined for antenna.

Figure 1 presents these three regions.

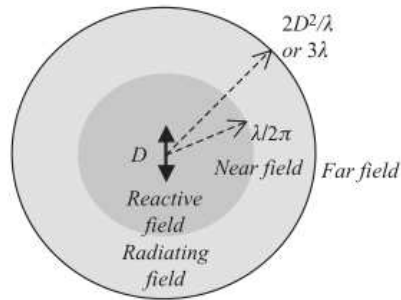


Figure 1 .Radiated field regions for an antenna of maximum dimension D

1.2.4 Smith chart

Smith chart is one of the most useful graphical tools for high frequency circuit applications. The Smith chart provides a graphical representation of Γ and quantities such as the VSWR or the terminating impedance of a device under test.

A locus of points on a Smith Chart can be employed to represent:

- How capacitive or inductive a load is across the frequency range.
- How difficult matching is likely to be at various frequencies.
- How well matched a particular component is.

Figure 2 shows important points on smith chart.

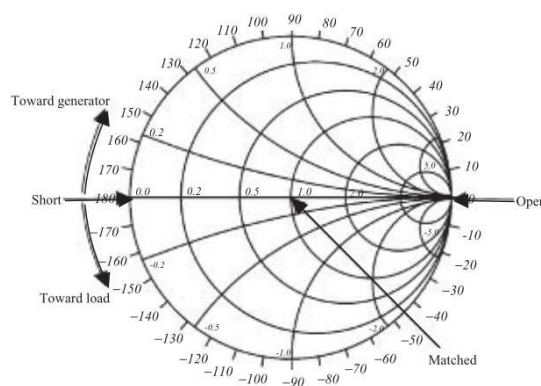


Figure 2 .Smith chart important points [From antenna from theory to practice]

1.3 Background of MIMO Theory

Having wireless communication systems offering high data rates and small error rates has always been desirable. Utilizing multiple antennas at the transmitter and/ or the receiver, Multiple-input multiple-output (MIMO), system seems to be a good idea to achieve high data rates and small error rates. Benefits of having multiple antennas are increase in data rates, decrease in error rates, improvement in signal-to-noise ratios, and beam forming.

1.3.1 MIMO wireless communications

Two categories can be considered for MIMO communication systems.

- Spatial Multiplexing Techniques
- Spatial Diversity Techniques

In Spatial Multiplexing systems the goal is to increase data rates while in Spatial Diversity goal is to decrease error rates. Transmitter in Spatial multiplexing system split the data into M sub-sequences and transmits them simultaneously using the same frequency band and therefore data rate will increase by M.

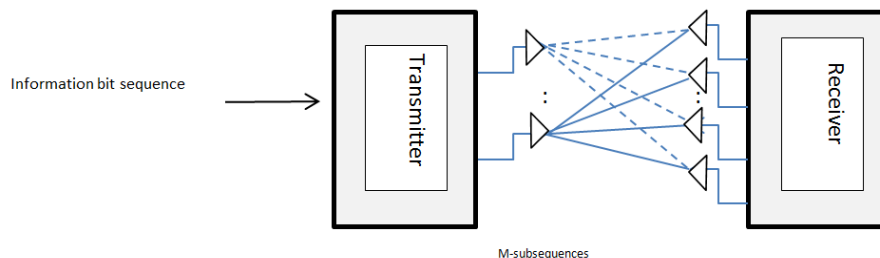


Figure 3 .MIMO Spatial Multiplexing

In Spatial Diversity the transmitter and the receiver send and the receiver multiple redundant versions of the same data sequence. At the receiver end, the receiver combines the signals and if the redundant signals are statistically independent, the likelihood of receiving error decreases significantly.

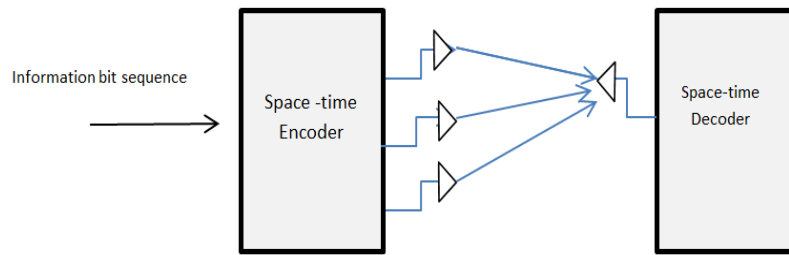


Figure 4. MIMO Spatial Diversity

The performance of a MIMO system is dependent on the availability of independent multiple channels. Channel correlation is damaging to the performance and the capacity of a MIMO system. Channel correlation is a measure of similarity between the channels. If the channels are fully correlated, then the MIMO system will have no difference from a single-antenna communication system. So the greater the channel correlation, the smaller the channel capacity.

The channel correlation of a MIMO system is mainly due to two components:

- (1) Spatial correlation
- (2) Antenna mutual coupling

The spatial correlation depends on the multipath signal environment.

MIMO system capacity

One of the primary measures of quality for a MIMO communication is the system capacity, or the maximum rate of information transfer between a transmitter and receiver. The goal of the system design is to engineer an architecture that achieves maximum capacity, which dramatically changes as design parameters and their associated electromagnetic effects are changed. Chapter 4 talks more about MIMO capacity.

1.3.2 MIMO Radar

Radar ambiguity function represents the output of the matched filter, and it describes the interference caused by the range and/or Doppler shift of a target when compared to a reference target of equal RCS.

The radar ambiguity function is used by radar designers as a way to study different waveforms. It provides insight about how different radar waveforms may be suitable for the various radar applications.

The following integral equation is defined as the “range ambiguity function,”

$$\square_{\mathbf{R}}(\tau) = \int_{-\infty}^{\infty} u^*(t)u(t - \tau)dt \quad (2)$$

The maximum value of $\square_{\mathbf{R}}(\tau)$ is at $\tau = 0$.

If $|\square_{\mathbf{R}}(\tau)| = \square_{\mathbf{R}}(0)$ for some nonzero value of τ , then the two targets are indistinguishable. As a consequence, the most desirable shape for $\square_{\mathbf{R}}(\tau)$ is a very sharp peak centered at $\tau = 0$ and falling very quickly away from the peak.

1.3.3 MIMO and Mutual Coupling

Multiple inputs multiple outputs (MIMO) system performance has been explored considerably but recently the researchers pay more attentions to the electromagnetic concepts. Due to the fact that MIMO systems have multi antennas, electromagnetic concepts such as mutual coupling can affect performance of MIMO system. The electromagnetic effects due to placing antennas together and MIMO systems are not new topics. However, incorporating their effects together is fairly a new topic.

Following discussions try to model the mutual coupling between antennas. In the transmitter antenna array, antenna mutual coupling causes the input signals being coupled into neighboring antennas. This Effect can be represented by a mutual coupling impedance matrix Z_t .

$$\mathbf{Z}_t = \begin{bmatrix} 1 & \frac{Z_t^{12}}{Z_t} & \dots & \frac{Z_t^{1N}}{Z_t} \\ \frac{Z_t^{21}}{Z_t} & 1 & \dots & \frac{Z_t^{2N}}{Z_t} \\ \vdots & \vdots & \ddots & \vdots \\ \frac{Z_t^{N1}}{Z_t} & \frac{Z_t^{N2}}{Z_t} & \dots & 1 \end{bmatrix} \quad (3)$$

The number of antennas and their separation are two important factors in multi-antenna systems. There are a number of limits on the number of antennas in MIMO systems.

Correlation could be a measure of how close antennas can be placed. In order to get satisfactory performances, the antennas should be spaced apart at least 0.5λ [6].

Jake's Model is another way to quantify antenna separation based on correlation.

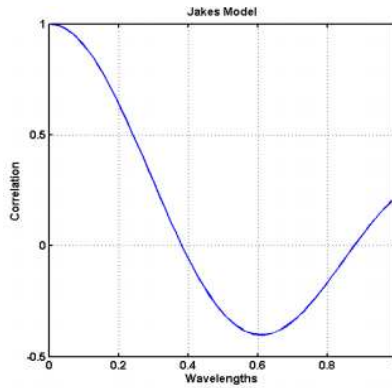


Figure 5 .Jakes Model for correlation based on antenna separation

1.3.4 MIMO System Model

Channel capacity depends on the number of transmit and receive antennas M and N , channel matrix H , and the signal-to-noise ratio (SNR).For a MIMO system we have:

$$Y = H X \quad (4)$$

Channel matrix has N rows as many as there are transmitting antennas with index i . Then transmitted signal vector is written as

$$X = [x_1, x_2 \dots x_N] \quad (5)$$

Channel matrix has M columns, as there are receiving antennas with index j . Then the received signal vector is

$$Y = [y_1, y_2 \dots y_M] \quad (6)$$

The channel matrix contains

$$\mathbf{H} = \begin{pmatrix} h_{11} & h_{12} & \dots & h_{1M} \\ h_{21} & h_{22} & \dots & h_{2M} \\ \vdots & \vdots & \dots & \vdots \\ h_{N1} & h_{N2} & \dots & h_{NM} \end{pmatrix} \quad (7)$$

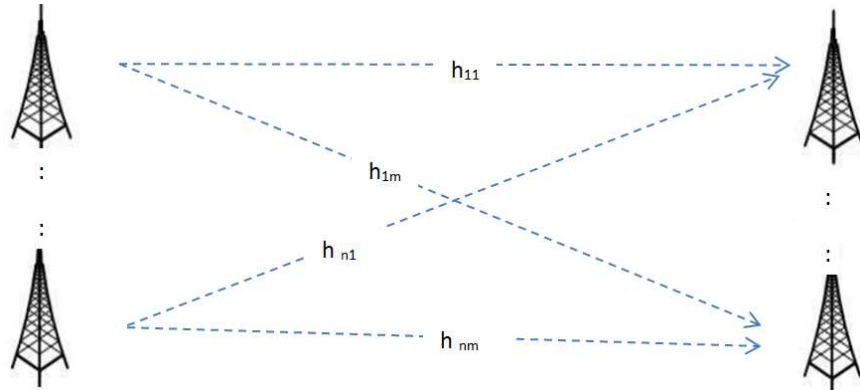


Figure 6. MIMO system

Transmitted signal \mathbf{X} can be solved if we invert the channel matrix and multiply it with the received signal \mathbf{Y} .

$$\mathbf{X} = \mathbf{H}^{-1} \mathbf{Y} \quad (8)$$

The inverse of channel matrix \mathbf{H}^{-1} can be determined by first finding the adjoint of the channel matrix and then dividing it with its determinant. Mathematically, the inverse of the channel matrix can be represented as

$$\mathbf{H}^{-1} = \frac{\text{adj}(\mathbf{H})}{\det(\mathbf{H})} \quad (9)$$

Where $\text{adj}(\mathbf{H})$ is the adjoint of the channel matrix that is formed by taking the transpose of the cofactor matrix of \mathbf{H} .

The whole MIMO system can be described by

$$\mathbf{Y} = \mathbf{H} \mathbf{S} + \mathbf{n} \quad (10)$$

Where \mathbf{n} is additive Gaussian noise vector.

The channel matrix is often normalized so that it is independent of the channel attenuation [27]. The capacity is expressed as a function of SNR at the receiver. With the assumption of the transmit power is equally spread among the transmit antennas. The channel capacity of a MIMO system in the presence of spatially uncorrelated Gaussian distributed noise can be calculated by

$$C = \log_2 \left(\det \left(\mathbf{I} + \frac{SNR}{M} \mathbf{H}_n \mathbf{H}_n^* \right) \right) \quad (11)$$

Where I is the identity matrix and $()^*$ denotes the complex conjugate transposition. The channel attenuation, which is included in the channel matrix depends on the antennas and the radio channel and has to be expressed in the SNR when normalizing the channel matrix.

In order to see the effects of antenna on channel capacity the path loss and the gains of the single antenna elements should be included in \mathbf{H} , and therefore \mathbf{H} should not be normalized.

The capacity of a MIMO system can be written as

$$C = \log_2 \left(\det \left(\mathbf{I} + \frac{Pr}{\sigma^2 n} \mathbf{H} \mathbf{H}^* \right) \right) \quad (12)$$

This equation expresses the capacity as a function of the transmit power P_T , noise power, attenuation of the transmission link which depends on the antennas and the radio channel, σ^2 . This formula allows comparison of different MIMO systems, including the influence of the transmission gain and the SNR.

Capacity depends on the correlation properties of \mathbf{H} . Power correlation coefficients are also important for MIMO systems with different antenna arrays, leading to a comparison of antenna arrays for MIMO. Usually it is difficult to show the direct relationship between the capacity distribution and the correlation properties.

Chapter 2

Single U-slot patch antenna

2.1 Overview

In order to understand the behavior of u-slot patch antenna, two different types of antennas, Slot and patch have been investigated. Using desired resonant frequencies, initial antenna dimensions have been calculated. HFSS software was used to simulate the antenna with initial dimensions and optimize antenna performance. Later effects of different parameters on the performance of U-slot antenna have been explored by the use of HFSS.

2.2 Slot antenna

Slot antennas are a special group of aperture antennas. They have found many applications such as for aircrafts and airborne radar. Slot antenna radiation pattern is omnidirectional. The slot size, shape and the cavity behind it are the design variables that should be optimized to get the best performance. One way to understand the slot antenna behavior is to look at its similarities to the dipole antenna. Slot antenna and electric dipole are dual of each other.

A thin slot in an infinite ground plane is the complement to a dipole in free space. However, the slot is a magnetic dipole rather than an electric dipole. A vertical slot has the same pattern as a horizontal dipole of the same dimensions. Thus, a longitudinal slot in the broad wall of waveguide radiates like a perpendicular dipole to the slot. E and H are the electric and magnetic fields within the slot and \hat{n} is the unit vector normal to the surface of the slot. So for electric and magnetic surface current we have:

$$\mathbf{J}_s = \hat{n} \times \mathbf{H} \quad , \quad \mathbf{M}_s = - \hat{n} \times \mathbf{E} \quad (13)$$

The surface electric current is zero $\mathbf{J}_s = \hat{n} \times \mathbf{H} = 0$, so magnetic current $\mathbf{M}_s = - \hat{n} \times \mathbf{E}$ is the only available current.

For a half wavelength slot antenna, the magnetic current looks like loop current distribution. Based on duality principle its radiation pattern looks like half wavelength dipole antenna. Equation 14 shows the electric and magnetic fields of a half wavelength dipole antenna.

$$E_{\theta} = \frac{\cos\left(\frac{\pi}{2}\cos\theta\right)}{\sin\theta}, \quad H_{\phi} = \frac{\cos\left(\frac{\pi}{2}\cos\theta\right)}{\sin\theta} \quad (14)$$

Using the duality relation, we obtain the radiated fields of a half wavelength slot antenna.

$$E_{\phi} = \frac{\cos\left(\frac{\pi}{2}\cos\theta\right)}{\sin\theta}, \quad H_{\theta} = \frac{\cos\left(\frac{\pi}{2}\cos\theta\right)}{\sin\theta} \quad (15)$$

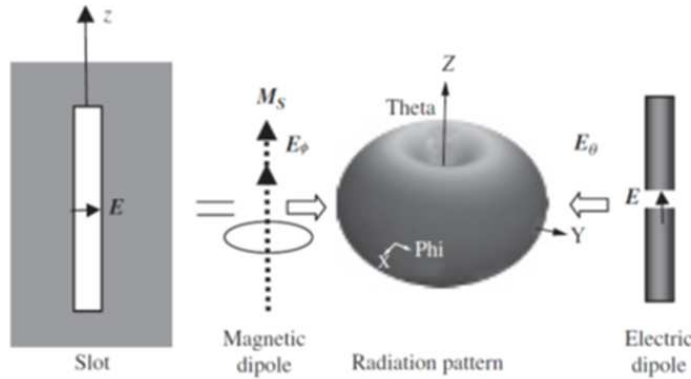


Figure 7 .A slot antenna, its radiation pattern and its complementary dipole [Antenna from theory to practice]

Based on the Babinet principle, there is a relationship between the input impedances of complementary antennas therefore we have:

$$Z_{\text{slot}} \cdot Z_{\text{dipole}} = \frac{\eta^2}{4} \quad (16)$$

Where Z_{slot} and Z_{dipole} are the antenna impedances of slot and dipole, and η is the free space impedance.

The main advantages of slot antenna are its size, design simplicity, and convenient adaptation to mass production using PC board technology.

2.3 Patch antenna

The microstrip antenna, also known as a patch antenna, consists of a metal patch on a substrate on a ground plane. There are different ways of feeding these antennas including aperture coupled, microstrip line feed and coaxial feed.

In order to resonate, microstrip patch antenna should have a length of around half wavelength. Advantages of microstrip antenna are low-profile, conformable to planar and nonplanar surfaces, simple and cheap to manufacture using modern printed-circuit technology. It is also very versatile in terms of resonant frequency, input impedance, radiation pattern and polarization. However, Low efficiency, low power handling capability, poor polarization purity, and narrow frequency bandwidth are its major disadvantages.

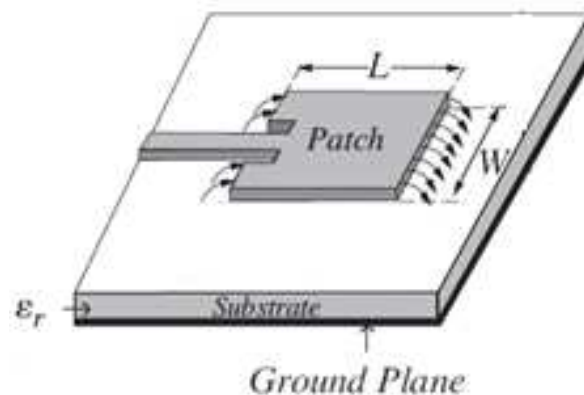


Figure 8. Geometry of Microstrip patch antenna [Antennas: From Theory to Practice]

Microstrip antennas have narrow bandwidth, typically 1–5%. There are different methods that have been used to broaden the bandwidth.

Other than increasing patch height and decreasing substrate permittivity, some of these techniques are:

- **Using Stacked patch.**
- **Use parasitic patches, either in another layer [7], or in the same layer [8], [9].**
Both has the disadvantage of increasing in antenna size
- **Matching multi-resonators to broaden the bandwidth.**
The impedance-matching techniques include planar gap-coupled, directly coupled, stacked electromagnetically coupled and aperture-coupled patches.

There is an empirical formula that can be used to estimate the impedance bandwidth for $VSWR < 2$ [4]:

$$\frac{\Delta f}{f} = \frac{16}{3\sqrt{2}} \frac{\epsilon_r - 1}{\epsilon_r^2} \frac{Ld}{\lambda W} \quad (17)$$

d is the substrate height; W and L are width and length of the patch.

From the formula, the bandwidth is proportional to the thickness of the substrate. Also the higher the permittivity, the smaller the bandwidth, which means there is a trade-off between the size (Ld/W) and bandwidth.

2.3.1 Design Equations and Procedures

Electrically patch antenna looks larger than its physical dimensions; the enlargement on L is given by equation 18.

$$\Delta L = \frac{0.412 d (\epsilon_{r\text{eff}} + 0.3) \left(\frac{W}{d} + 0.264\right)}{(\epsilon_{r\text{eff}} - 0.258) \left(\frac{W}{d} + 0.8\right)} \quad (18)$$

This enlargement is due to the fringing effects. Effective relative permittivity is

$$\epsilon_{r\text{eff}} = \frac{\epsilon_r + 1}{2} + \frac{\epsilon_r - 1}{2 \sqrt{1 + 12 \frac{d}{W}}} \quad (19)$$

So based on equation 19 the larger the $\frac{d}{w}$, the smaller the effective permittivity. The effective length of the patch is now

$$L_{\text{eff}} = L + 2 \Delta L \quad (20)$$

For the TM_{100} mode we have:

$$f_r = \frac{1}{2 L_{\text{eff}} \sqrt{\epsilon_{r\text{eff}}} \sqrt{\epsilon_0 \mu_0}} \quad (21)$$

For optimized width:

$$W = \frac{1}{2 f_r \sqrt{\epsilon_0 \mu_0}} \sqrt{\frac{2}{1 + \epsilon_r}} \quad (22)$$

So by having substrate parameters ϵ_r and d and also the resonance frequency f_r , patch dimensions can be found based on these simplified formulas.

$$L = \frac{1}{2 f_r \sqrt{\epsilon_0 \mu_0 \sqrt{\epsilon_{r\text{eff}}}}} - 2 \Delta L \quad (23)$$

In this research, goal is to design a patch antenna to work at 3.5 GHz on FR4 substrate ($\epsilon_r = 4.4$, and $d = 1.6$ mm). Therefore we have:

$$W = \frac{1}{2 f \sqrt{\epsilon \mu}} \sqrt{\frac{2}{\epsilon + 1}} = 0.026 \text{ m} \quad (24)$$

$$\epsilon_{r\text{eff}} = \frac{\epsilon + 1}{2} + \frac{\epsilon - 1}{2 \sqrt{1 + \frac{12d}{w}}} = 3.9898, \quad \Delta L = 7.342 * 10^{-4} \text{ m} \quad (25)$$

$$L = \frac{1}{2 f \sqrt{\epsilon \mu \epsilon}} - 2 \Delta L = 0.030962 - 2 * 7.342 * 10^{-4} = 0.029 \text{ m} \quad (26)$$

So the fractional bandwidth for $VSWR < 2$ is :

$$\frac{\Delta f}{f_0} = 3.77 \frac{\epsilon_r - 1}{\epsilon_r * \epsilon_r} \frac{Ld}{W\lambda} = 0.0208 \quad (27)$$

2.4 U-Slot patch antenna

Originally the U-slot patch antenna was developed as a wide band antenna, introduced by Huynh and Lee [26]. They also are good choices for multiband applications and circular polarization operation. The basic geometry of the U-slot antenna is shown in Figure 15.

These antennas can provide impedance bandwidths of 20% to 30 % for a patch with the thickness of about $0.08 \lambda_0$. Because of broad bandwidth slot patch antennas are very useful in commercial applications like 3G and 4G.

Multi band U-slot antenna

A basic patch antenna with added slots is able to resonate in more operational bands. U-slot patch antennas with different dimensions can represent dual and triple band results. The aim of introducing the U-slot on the rectangular patch is to produce four resonance frequencies. Broad-band operation is achieved when the second and third resonance frequencies are sufficiently close [14].

Wide band

Having a wideband antenna that is electrically large has always been a desired for different applications. Ideal broad-band performance is achieved when the loop of the impedance loci, such as in 1, 2 and 3 in figure 9, shrinks to the $VSWR = 1$ point on the Smith Chart. For practical applications, the size and location of the loop of impedance loci is required to be such that $VSWR \leq 2$, as in locus 4. $VSWR \leq 2$ corresponds to a return loss of 10 db. Figure 9 shows the smith chart for four different impedance loci. Locus number 4 is the desired locus for the wideband design [14].

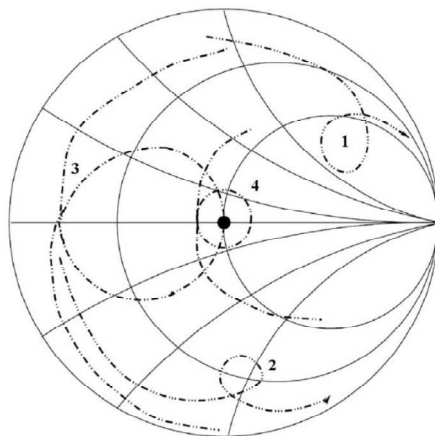


Figure 9 . Generic Impedance Loci for U-Slot Microstrip Antenna [14].

Locus 1 indicates that the design has too much inductance. Locus 2 indicates that the design has too much capacitance. Locus 3 indicates narrowband behavior. Locus 4 indicates broad-band performance [14].

2.4.1 Other studies about u-slot

There have been several other studies on U-slot patch antenna, and some of them are mentioned in the following paragraph [27].

Edge-Slotted v-Slot Antenna:

The V-slot antenna was studied in Rafi and Shafai [15], which showed that the V angle can be used to improve its performance. The main advantage of using V slot instead of U-slot is the increase in the bandwidth. And like U-slot antenna, one major problem of V-slot antennas is the cross polarization in the H -plane that is severe at high frequencies. Figure 10 shows the geometry of wideband V-slotted microstrip patch antenna.

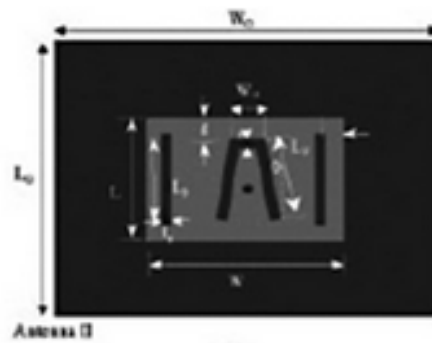


Figure 10 . Geometry of Wideband v-slot patch antenna with two parallel edge slot (Rafi and Shafai IEEE 2003)

Circular-Arc V- Slot Antenna:

The bandwidth of this antenna is increased to 40 percent, from 30 percent of the U -slot antenna. Other parameters remain similar.

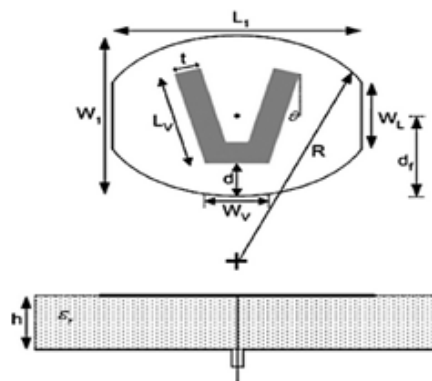


Figure 11. Geometry of non-rectangular microstrip antenna with v-slot (Rafi and Shafai IEEE 2003)

Double U-Slot Antenna:

Two or more resonant structures can be closely located or even co-located with a single feed point in order to achieve multiband operation. This is illustrated in Figure 12 .A second *U*-slot is placed inside the first one to increase its bandwidth up to 44 percent.



Figure 12. Configuration of double U-slot antenna

Circularly polarized U-Slot Antenna

Asymmetrical U-slot structure which excited two orthogonal modes for radiation; has been proposed in [16].It is shown that by adjusting the length of an arm of U-slot ,circular polarization is achievable for U-slot.

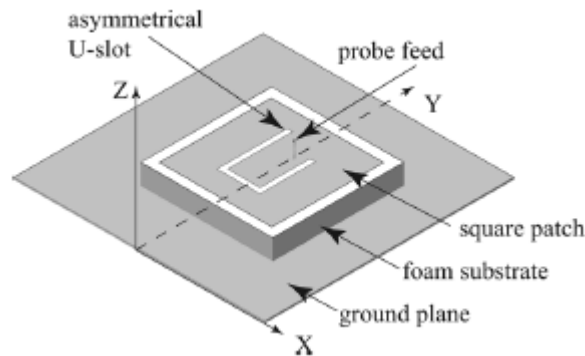


Figure 13 . Geometry of the circularly polarized U-slot patch antenna [16].

2.4.2 Antenna Design

Approximate expressions of resonance frequencies for the *U*-slot antenna were proposed and investigated. They are given in equation 28 and 29 [27].

$$f_1 = \frac{c}{\left(\frac{w_s}{2} + w + \frac{3\Delta w}{2} - \frac{b}{2}\right)\sqrt{\epsilon_{eff}}} \quad (28)$$

$$f_2 = \frac{c}{\left(\frac{L}{2} - \frac{w_s}{4} + w + \frac{3\Delta w}{2} - a\frac{b}{2} + F + \frac{t}{2}\right)\sqrt{\epsilon_{eff}}} \quad (29)$$

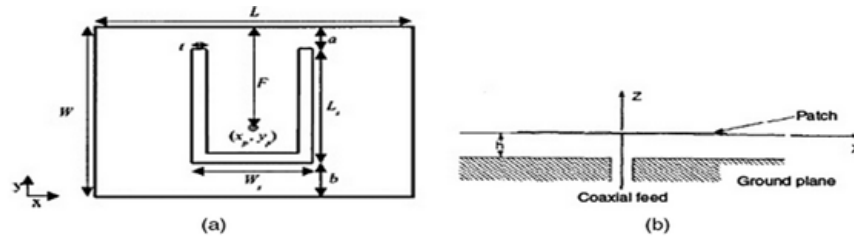


Figure 14 .Geometry of coaxially fed rectangular patch with a U –shaped slot

a)Top view b)side view (after R. Bhalla and L. Shafai, Microwave and Optical Technology Letters 2002)

In this section first the geometry and the features of a single patch *U*-slot antenna such as radiation pattern and reflection coefficient are shown. In addition effects of different terms on the *U*-slot patch antenna have been studied.

Figure 15 shows the topology of the *U*-slot microstrip patch antenna investigated in this thesis. Table 1 represents the initial values for different design parameters.

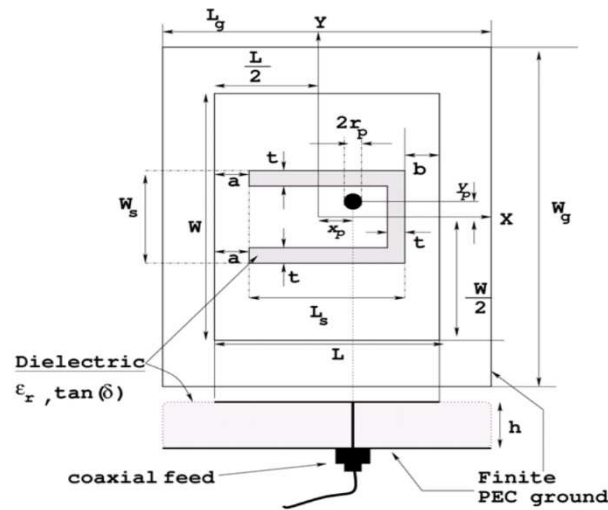


Figure 15.DESIGN PARAMETERS OF SINGLE U-SLOT PATCH ANTENNA

Frequency (GHz)	ϵ_r	H (cm)	L (cm)	W (cm)	L_s (cm)	W_s (cm)	t (cm)	a (cm)	b (cm)	L_g (cm)	W_g (cm)
3	4.5	0.762	1.96	2.72	1.36	1.06	0.152	0.3	0.3	5	5

Table 1. Wideband U-slot patch antenna dimensions

2.4.3 Antenna Simulation in HFSS

Here is the U-slot patch antenna structure in HFSS, which was created to simulate the behavior of U-slot patch antenna.

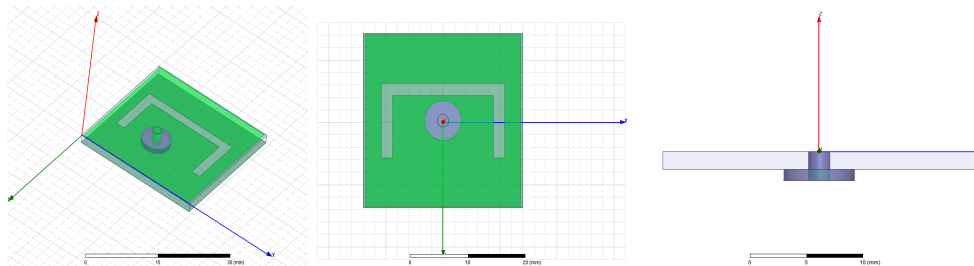


Figure 16.Different views of the designed antenna in HFSS

This section presents the initial designed wide band u-slot patch antenna characteristics:

- Radiation pattern

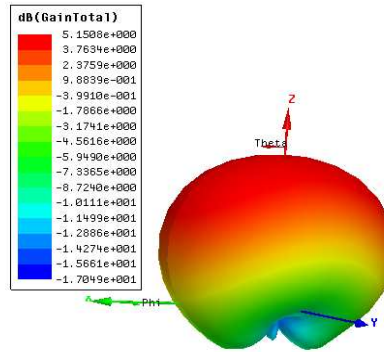


Figure 17. Radiation pattern of a probe fed U-slot patch antenna in dB

It is evident from Figure 17 that the radiation pattern of a U-slot patch antenna is omnidirectional and it is almost like a patch antenna.

- Current distribution.

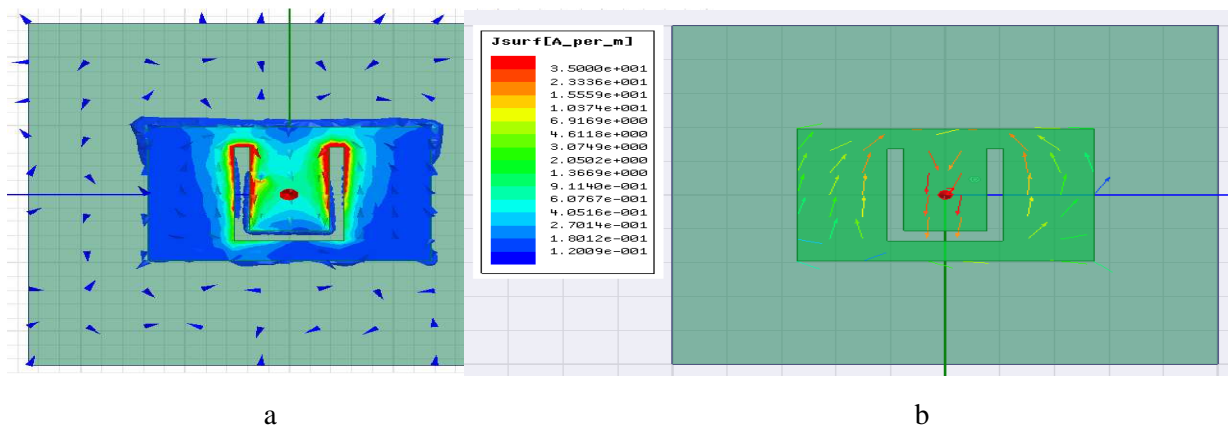


Figure 18. Surface current distribution on of a probe fed U-slot patch antenna

From figure 18 it is evident that slots on patch change the path that current takes.

- VSWR

The VSWR of the broad band U-slot antenna is shown in figure 19 which shows that the antenna of figure 16 is a broadband antenna of about 500 MHz bandwidth.

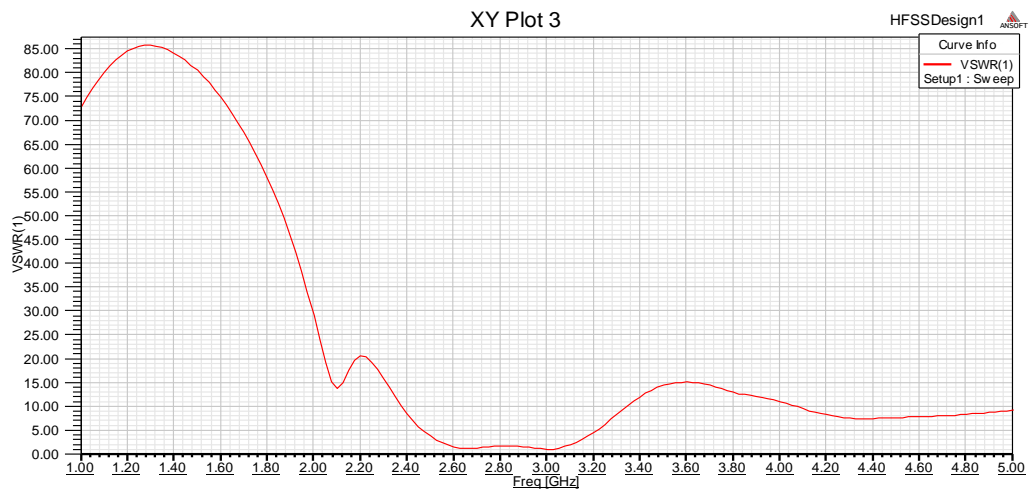


Figure 19. VSWR of a probe fed U-slot patch antenna in frequency range of [1GHz to 3GHz]

- S_{11}

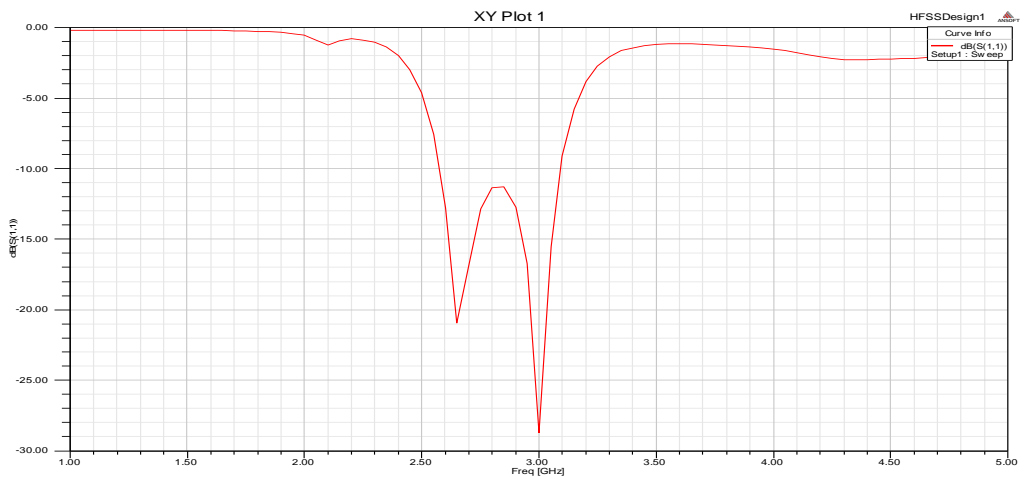


Figure 20. Return Loss for Initial Design of U-Slot Microstrip Patch

U-slot patch antenna is a suitable candidate for dual band applications. Band width is 500 MHz. The key advantage of the U-slot design is that it produces broad-band characteristics with a very simple topology.

Initial dimensions¹

There is no accurate analytical procedure for U-slot microstrip patch antenna design .So creating initial design and optimize its performance by changing the dimensions seems reasonable. The mentioned calculations described in chapter 3 for patch antenna are used to create an initial design with center frequency of 3.5 GHZ and 5GHz.The dimensions of initial design are shown in table 2.

<i>Frequency (GHz)</i>	ϵ_r	H (mm)	L (cm)	W (cm)	L_s (cm)	W_s (cm)	t (cm)	a (cm)	b (cm)	L_g (cm)	W_g (cm)
3.5	4.4	1.6	2.9	2.6	1.36	1.06	0.152	0.3	0.3	2.9	2.6

Table 2 . Initial design of U-Slot Microstrip Patch Antenna.

2.4.4 Optimization

Experimentally, it has been shown that variations in parameters such as the width and length of the U-slot, height and size of the patch, probe size and location as well as Substrate permittivity can dramatically change the antenna's behavior. Effect of following factors on antenna behavior has been studied and CAD simulation used to optimize the design [14].

- **Width of the U-slot**
- **Length of the U-slot,**
- **Substrate height (h)**
- **Size of the patch**
- **Feed point size**
- **Feed point location**

¹ In order to reduce the fabrication cost, common FR4 board thickness has been chosen .So instead of using board with 0.76 cm thickness, board with 1.6 mm thickness has been chosen for antenna fabrication. This makes the antenna narrow band.

➤ **Optimization of feed point location (X_p, Y_p)**

Figure 21 shows the smith chart for center fed u-slot patch antenna .It is evident that the antenna is single band.

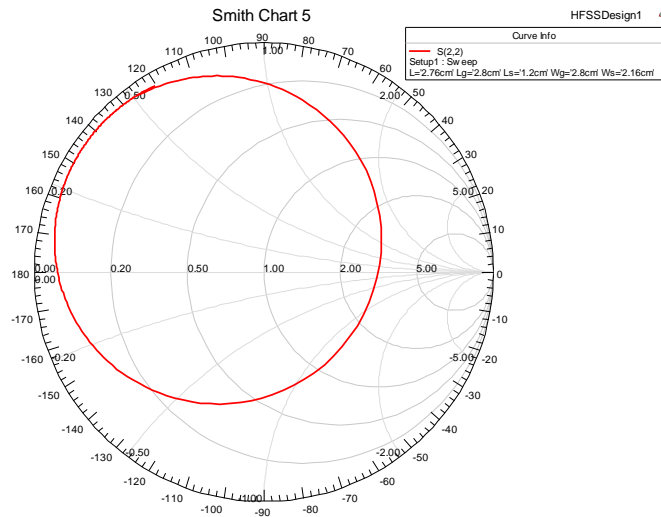


Figure 21 .Impedance Locus for center fed Design U-Slot Microstrip Patch

In order to find best location for feed point, X_p has been changed from -0.2 to 0.2 and Y_p has been changed from -0.35 to 0.35. Figures 22 and 23 represent the return loss and smith chart for different amount of X_p and Y_p .

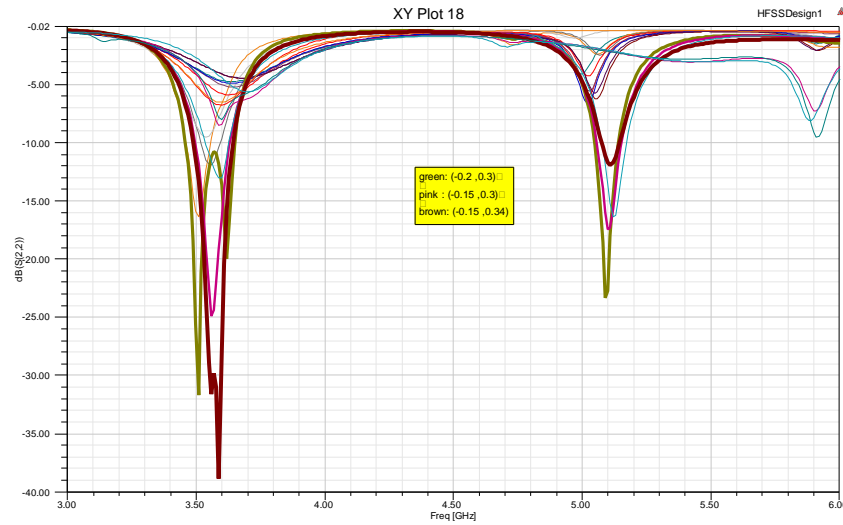


Figure 22.Effect of Probe Location on the Return loss Behavior of the U-Slot

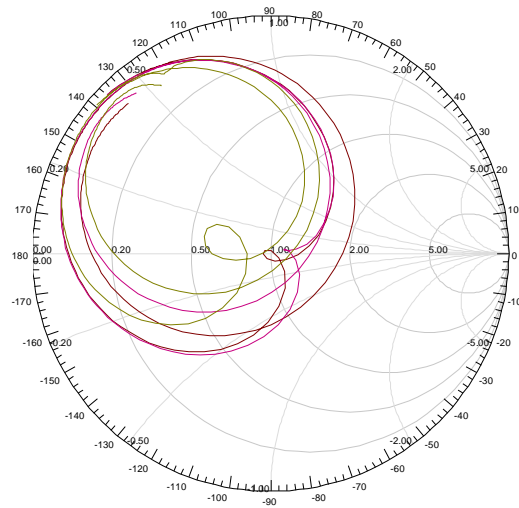


Figure 23 .Effect of Probe Location on the Impedance Behavior of the U-Slot

So based on Figure 22 and Figure 23 best place to put probe feed is $X_p = -0.15$, $Y_p = 0.34$.

➤ *Effect of Probe Radius (radi)*

Figure 24 shows the effects of varying the probe radius on the return loss behavior of the U-slot. The results indicates that by reducing the probe radius better return loss and broader band width is achievable .However due to fabrication limits it cannot be very small.

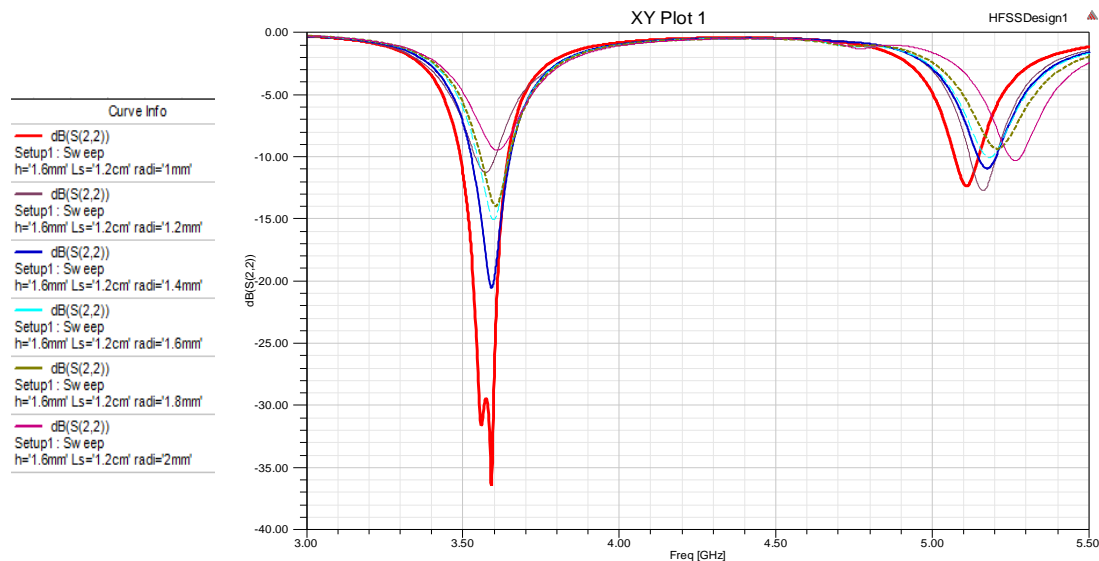


Figure 24 .Effect of Probe radius on the Impedance Behavior of the U-Slot

Red trace which is for probe with the radius of 1 mm and is the best compared to the others. Variations in the probe radius do not change the size of the impedance loop. Decreasing the probe radius causes the loop to become more inductive.

➤ **Optimization of slot width(t)**

Figure 25 shows the effects of varying the slot width on the impedance behavior of the U-slot. T has been varied from 0.1 cm to 0.4 cm with the steps of 0.05cm. Results indicate that the blue trace that is for a slot width of 0.2 cm represents the best results.

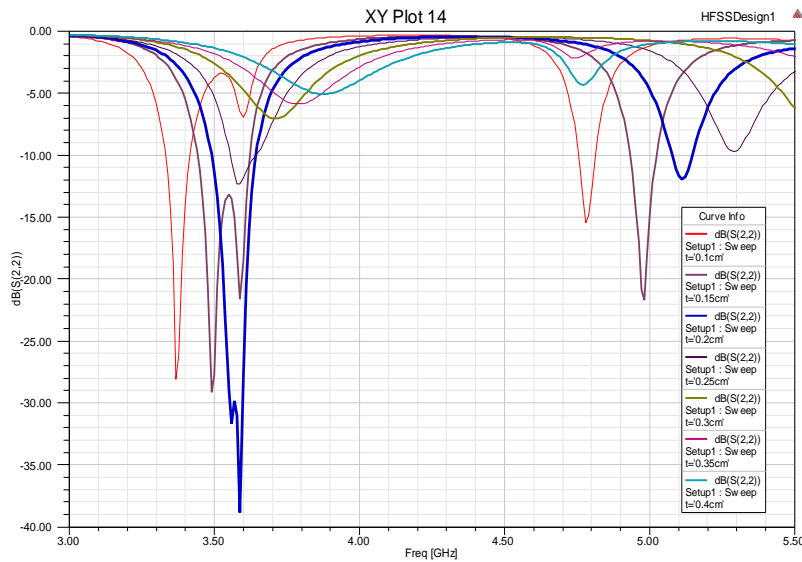


Figure 25 .Effect of Slot width on the Return loss of the U-Slot

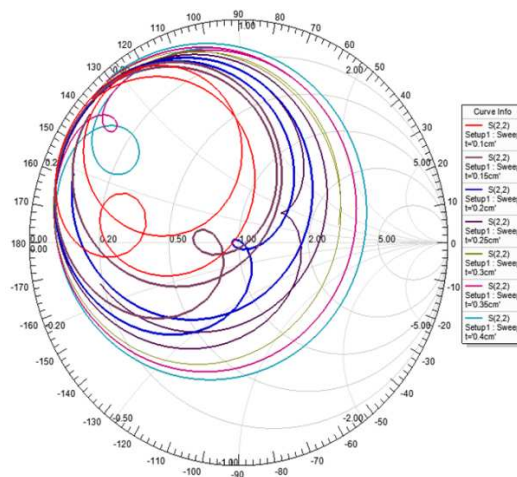


Figure 26 .Effect of slot width on the Impedance Behavior of the U-Slot

As Slot width decreases, the impedance loop becomes more inductive and its size decreases.

➤ OPTIMIZATION OF THE SLOT length(l_s)

Variations of return loss as a function of frequency for different slot dimensions are shown in Figure 27. It is found that blue trace ($L_s=1.2$ cm) has both wide band performance, Figure 27 and dual band operation at 3.57 GHz and 5.1 GHz, Figure 28.

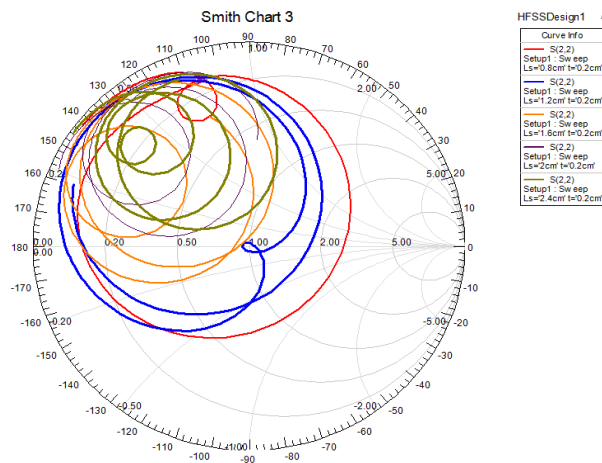


Figure 27 .Effect of slot length on the Impedance Behavior of the U-Slot

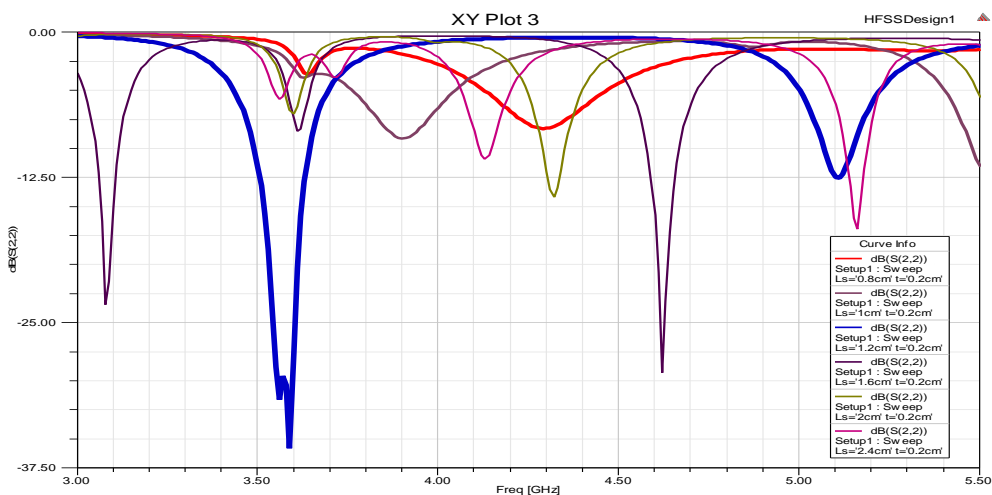


Figure 28 .Effect of slot length on the return loss behavior of the U-Slot

Optimized Design

Table 3 shows the optimized dimensions.

Frequency (GHz)	ϵ_r	H (mm)	L (cm)	W (cm)	L_s (cm)	W_s (cm)	t (cm)	a (cm)	b (cm)	L_g (cm)	W_g (cm)	Radi (mm)	X_p
3.5	4.5	1.6	2.76	2.72	1.2	2.16	0.2	0.3	0.3	2.8	2.8	1	-0.15

Table 3 . Optimized design of U-Slot Microstrip Patch Antenna.

Figure 29 shows dual band performance of the antenna with center frequencies of 3.57 GHz and 5.1 GHz for each band.

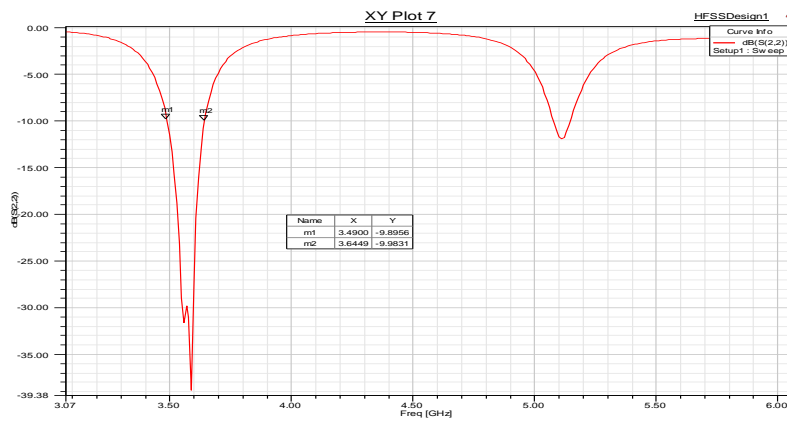


Figure 29 .Simulated return loss of the optimized design

Figure 30 shows the smith chart for dual band final design

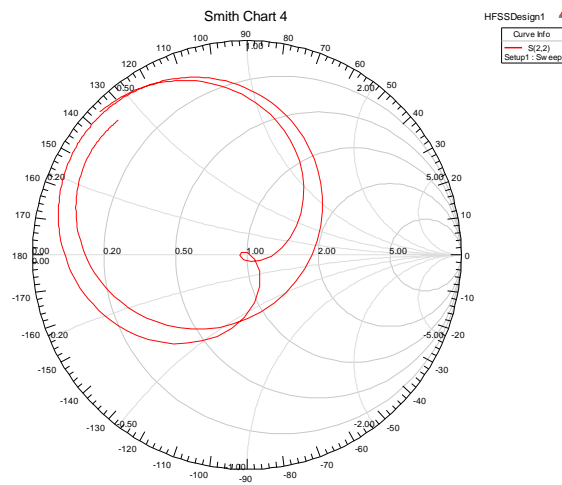


Figure 30. Impedance behavior of dual band final design

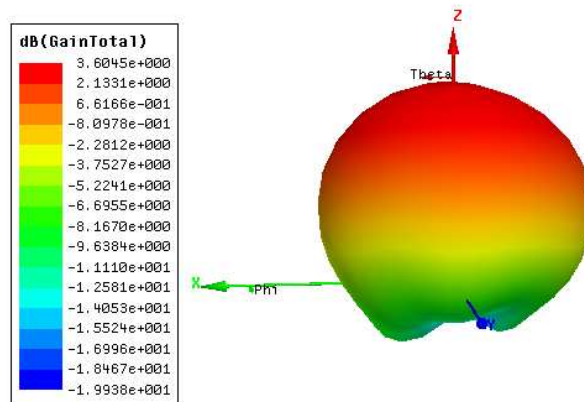


Figure 31 .Radiation pattern of dual band final design

As mentioned previously by changing dimensions, single, double, and triple band U-slot patch antenna can be achieved. Following pictures represent a triple band U-slot patch antenna.

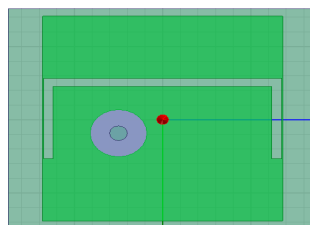


Figure 32. Triple band U-slot patch

ϵ_r	H (mm)	L (cm)	W (cm)	L_s (cm)	W_s (cm)	t (cm)	a (cm)	b (cm)	L_g (cm)	W_g (cm)	Radi (mm)	Xp	Yp
4.5	1.6	2.8	2.72	1.1	2.7	0.11	0.3	0.3	3	3.5	1	-0.2	0.5

Table 4 .Triple band U-slot patch antenna dimensions

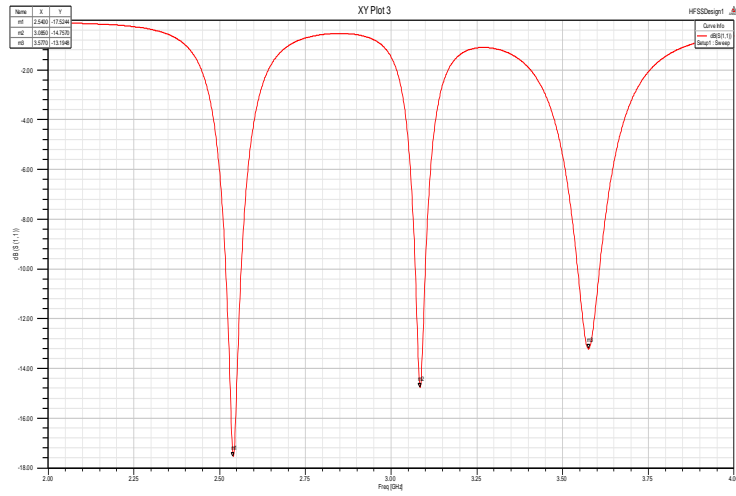


Figure 33.Return loss of triple band U-slot patch antenna

Chapter 3

U-slot patch antenna Array

1.1 Mutual coupling

The energy absorbed by one antenna from the nearby antenna is called mutual coupling that exists in antenna arrays. It can have bad effects on Antenna performance, such as antenna efficiency reduction and altering antenna radiation's pattern and can cause some limitations in antenna array size. In applications like beam steering, high mutual coupling it also makes array antenna elements highly correlated, and this makes beam steering inefficient .Mutual coupling is a good measure of antenna isolation [1].

The effect of mutual coupling on an antenna array's performance has become important in many areas such as multiple-input multiple-output (MIMO) systems, diversity systems, and medical imaging, sonar and radar systems. In today ever-decreasing size technology mutual coupling has become more important since antennas have to be closer to each other and this means high mutual coupling. The inter element mutual coupling can be reduced by optimizing array configuration, using ground structures and optimizing impedance matching networks [17, 18].

In order to gain some insight into the coupling mechanism, first a single element of the array has been considered. Current distribution, radiation pattern and other characteristics of the single element isolated from rest of the array have been shown in previous chapter. When the same element is placed among the other elements in the array, the boundary condition is not the same as that of the single element alone. It can be determined by all the elements of the array . The mutual coupling between antennas is due to the induced current on one antenna because of the other antenna. These induced currents are due to

1) Near field coupling from the other antennas

The near-field coupling arises when an antenna is placed in the near-field zone of another antenna. The near-field coupling is strong in situations where the antennas are printed on dielectric substrates with very low permittivity. Coupling space-waves dominate and show strong coupling when antennas are in close proximity.

2) The common-ground current, surface waves

Surface waves are weakly excited in very thin grounded dielectric substrates and can cause mutual coupling between antennas.

Network formulation of antenna Arrays

Consider an array of N identical elements, each has a self-impedance of Z_{11} .

$$I = \begin{bmatrix} I_1 \\ \vdots \\ I_N \end{bmatrix} \quad (30)$$

Elements of I represent the current on each element.

$$I_0 = \begin{bmatrix} I_{01} \\ \vdots \\ I_{0N} \end{bmatrix} \quad (31)$$

Elements of I_0 represent the current on each element, when it is isolated from the array, and there is no mutual coupling.

$$I_{\text{induced}} = \frac{-Z_{mn} \cdot I_m}{(Z_{11} + Z_0)} \quad (32)$$

Where I_{induced} is the induced current on the n^{th} element because of the m^{th} element of the array.

I_m is the current on the m^{th} element, $Z_{mn} I_m$ is the voltage induced across the open circuited terminals of the n^{th} element.

Therefore the induced current on the n^{th} element can be calculated as

$$I_{n_induced} = - \sum_{\substack{m=1 \\ m \neq n}}^N \frac{Z_{mn}}{Z_{11} + Z_0} I_m \quad (33)$$

Now consider C as an N by N coupling matrix with

$$C_{mn} = \frac{Z_{mn}}{Z_{11} + Z_0} \text{ and } C_{mm} = 0 \quad (34)$$

1.2 Array Configurations

Antenna diversity is a simple approach for reducing the mutual coupling between antenna elements, which is used in this project to find the configuration of two U-slot patch antenna with lowest mutual coupling.

Antenna array's inter-element mutual coupling is affected by factors such as the antenna configuration and the relative position of the feed points. The purpose of this chapter is to answer following question:

Of all the various antenna configurations illustrated in Figure 34 which combinations provide minimum mutual coupling?

The designed two element antenna array is presented in this section. This consists of two U-slot patch antennas positioned reasonably apart to satisfy the limitation related to array size and mutual coupling between elements. Eight configurations of this antenna array are investigated and shown in Figures 34(a-h).

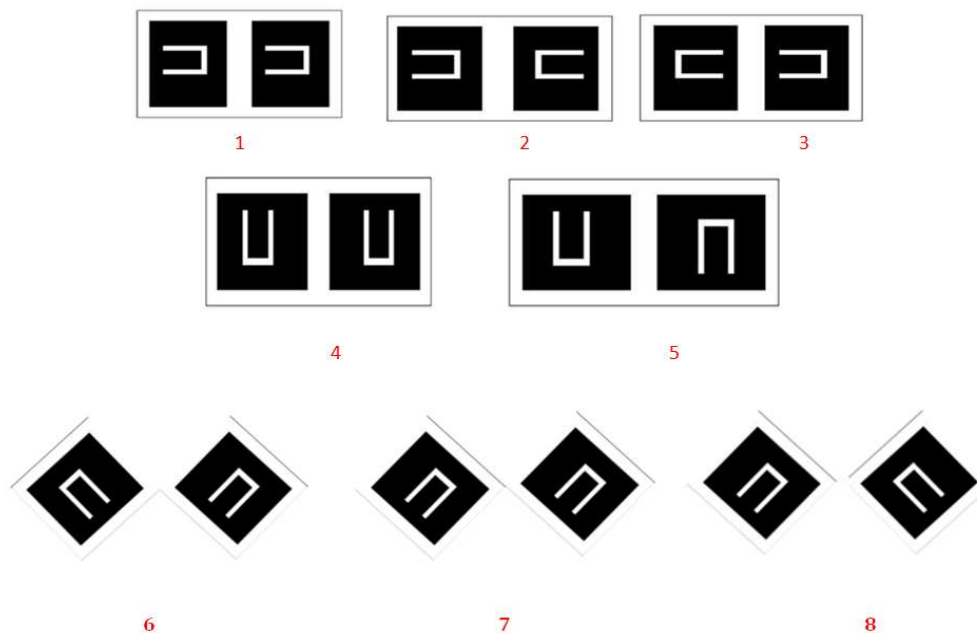


Figure 34 .Different possible configurations for two u-slot patch antennas

PERFORMANCE OF VARIOUS ANTENNA CONFIGURATIONS

In each configurations set up 4 different antenna spacing have been considered

$$(d=0, \frac{\lambda}{8}, \frac{\lambda}{4}, \frac{\lambda}{2}).$$

Configuration 1

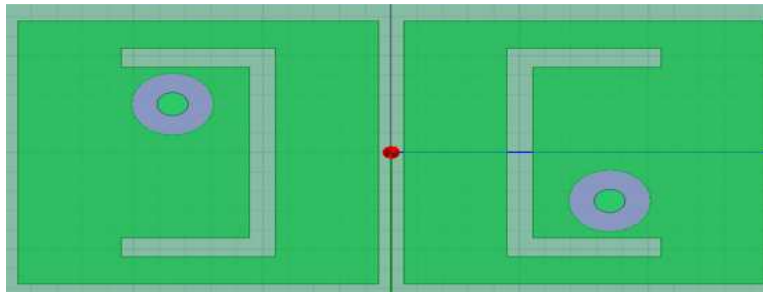


Figure 35 .Geometry of configuration 1 of U-slot patch antenna array

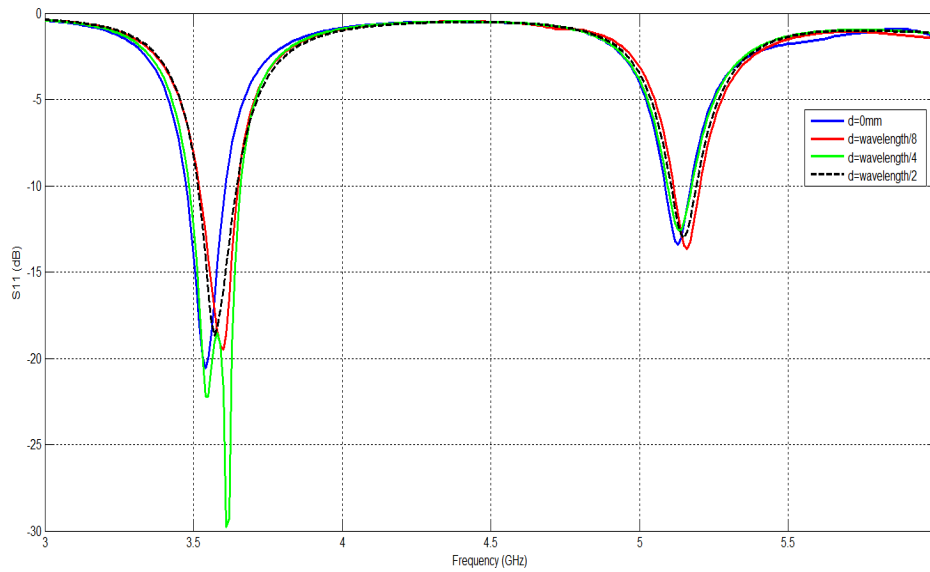


Figure 36 .Simulated S11 of the first configuration for different values of d

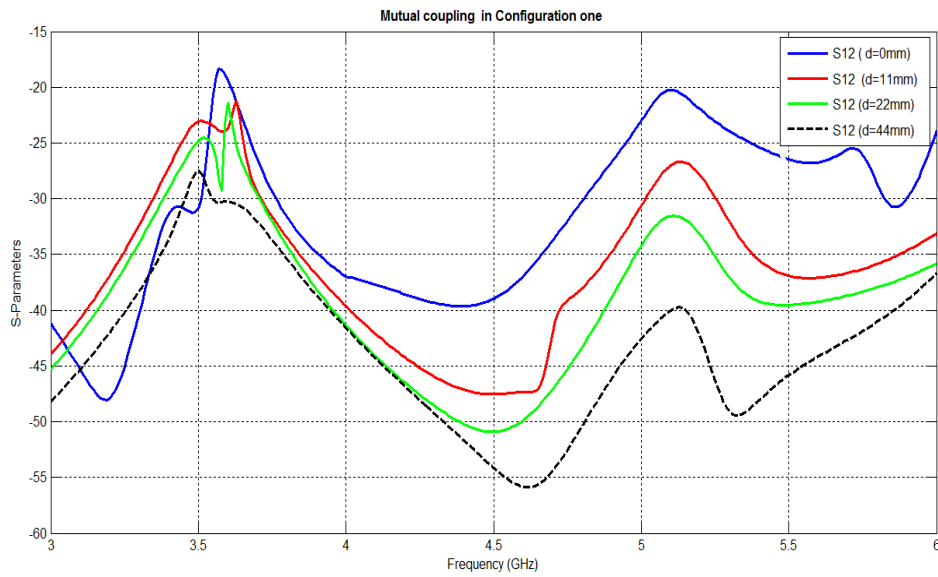


Figure 37 . Simulated S_{21} of the first configuration for different values of d

As we expected, mutual coupling decreased as the spacing between antennas increased. The significant effect of d on the mutual coupling is clearly indicated in Figure 37. Increasing the spacing between the elements decreases the mutual coupling between the elements. At 3.57 GHz there is 14 dB and in 5.2 GHz there is 20 dB improvements from the array with smallest spacing to the array with largest spacing between elements.

Figure 38 shows the E field and H field respectively on a plane 0.1mm above the antenna array when just element 1(left) is excited. Following figures represent the E and H field coupling on the other antenna.

It is evident that E field coupling is dominated in the case of configuration 1.

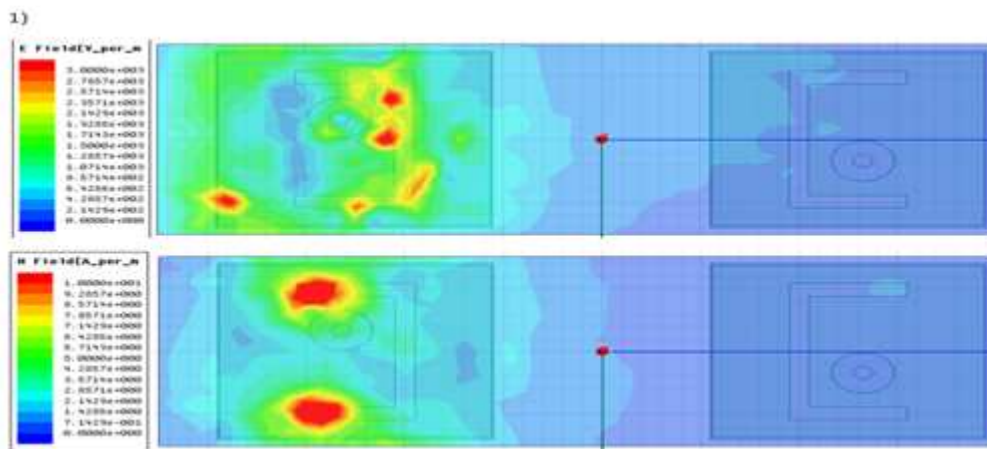


Figure 38 .Electric field (top) and Magnetic field (bottom) coupling between array elements in configuration one

Configuration 2

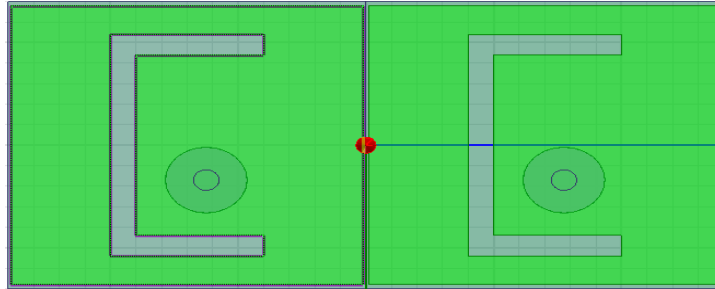


Figure 39 .Geometry of configuration 2 of U-slot patch antenna array

It is important to note that in configuration 2 feed points are closer to each other compare to configuration one. This could be a good reason for mutual coupling to be more in configuration 2.

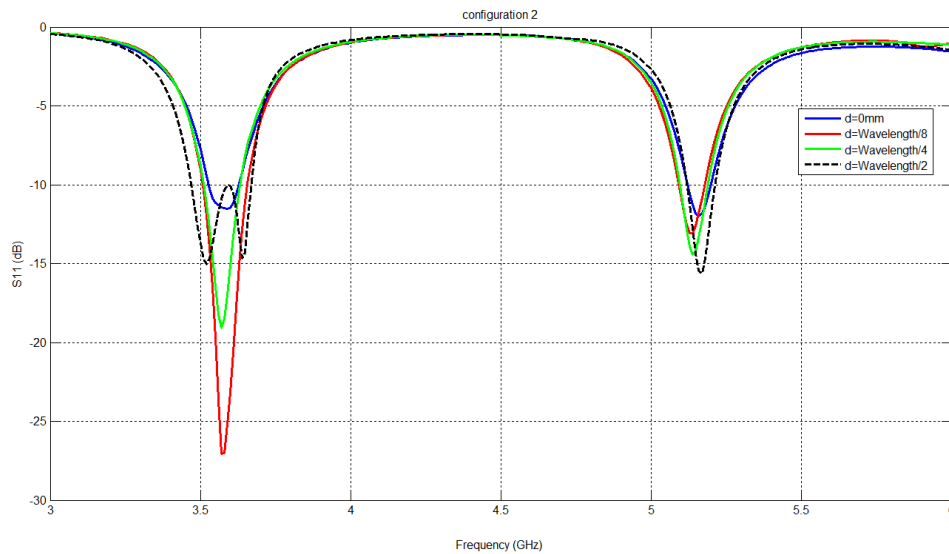


Figure 40 .Simulated S11 of the second configuration for different values of d

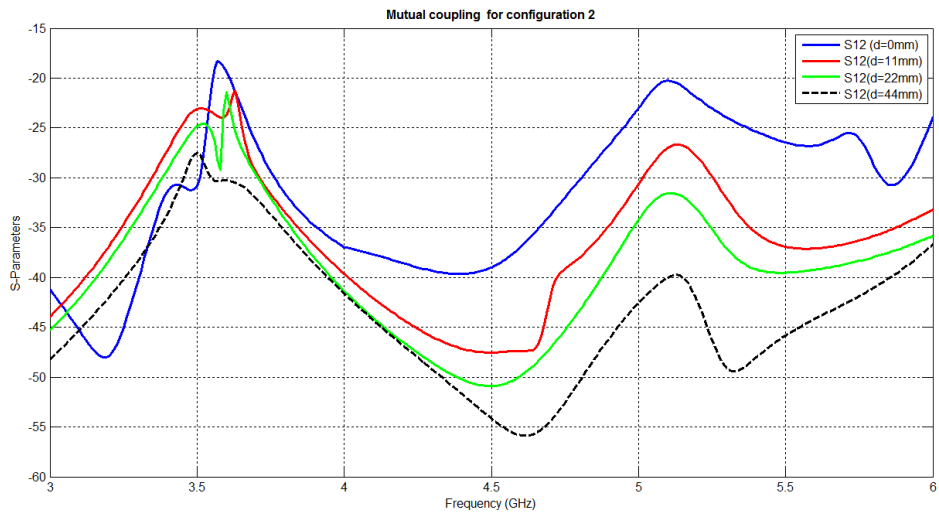


Figure 41 .Simulated S21 of the second configuration for different values of d

By comparing Figure 41a and b it is obvious that E field coupling is stronger than H field coupling in configuration 2.

In compare to figure 38 mutual coupling is more than configuration one.

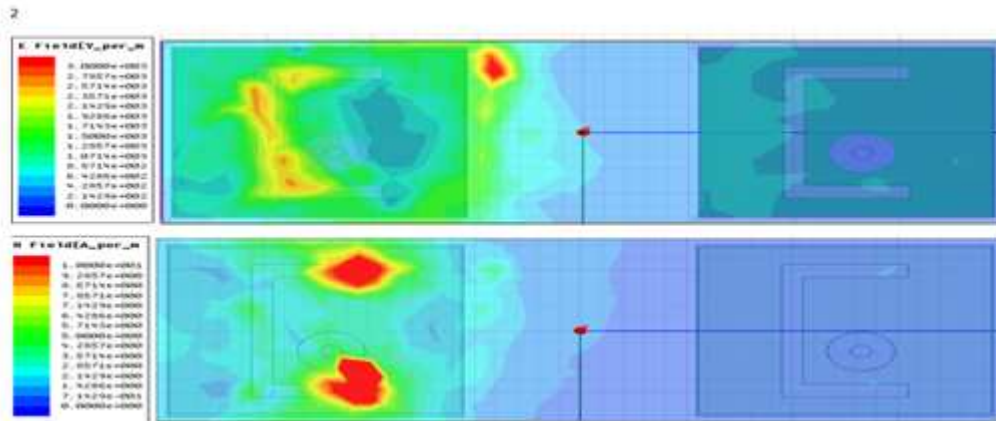


Figure 42. Electric field (top) and Magnetic field (bottom) coupling between array elements in configuration two

Configuration 3

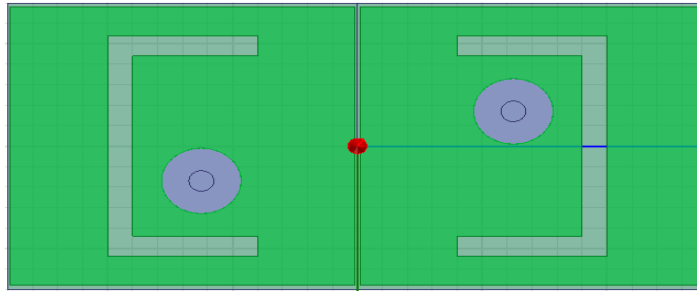


Figure 43 .Geometry of configuration 3 of U-slot patch antenna array

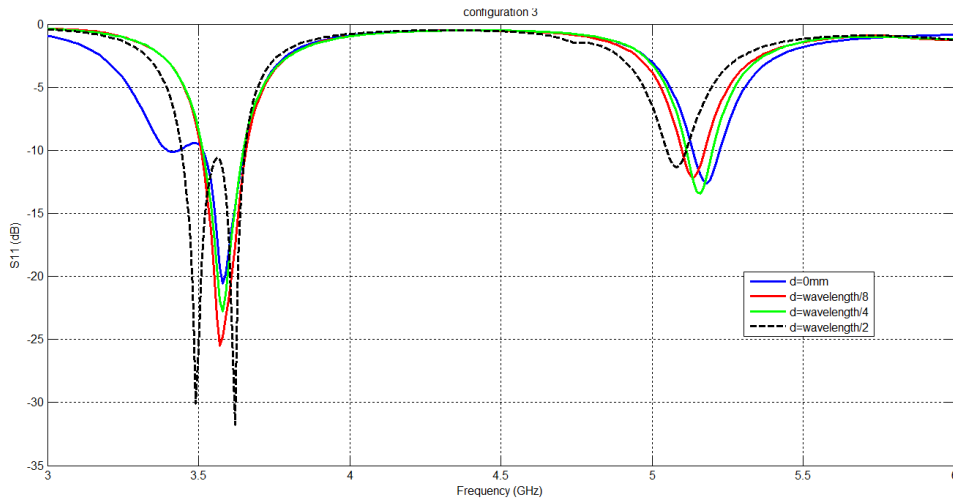


Figure 44 .Simulated S11 of the third configuration for different values of d

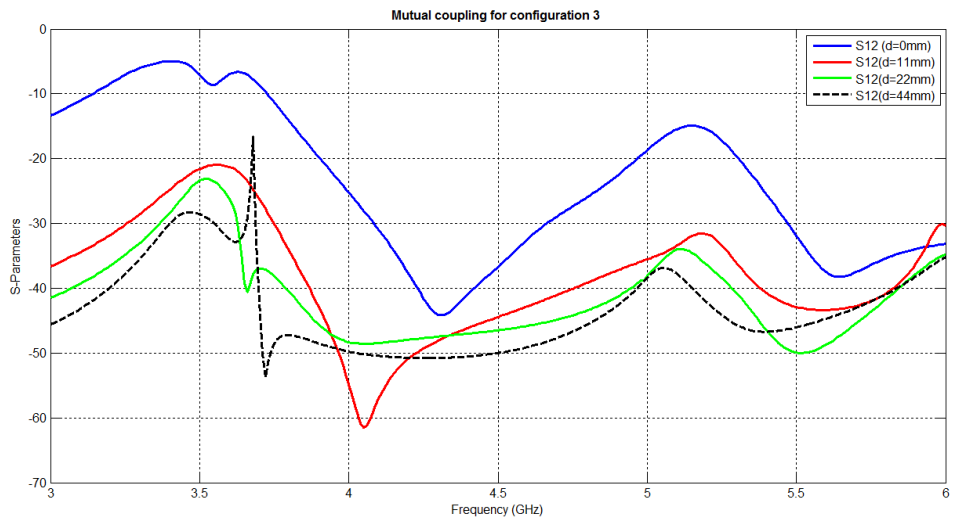


Figure 45 .Simulated S21 of the third configuration for different values of d

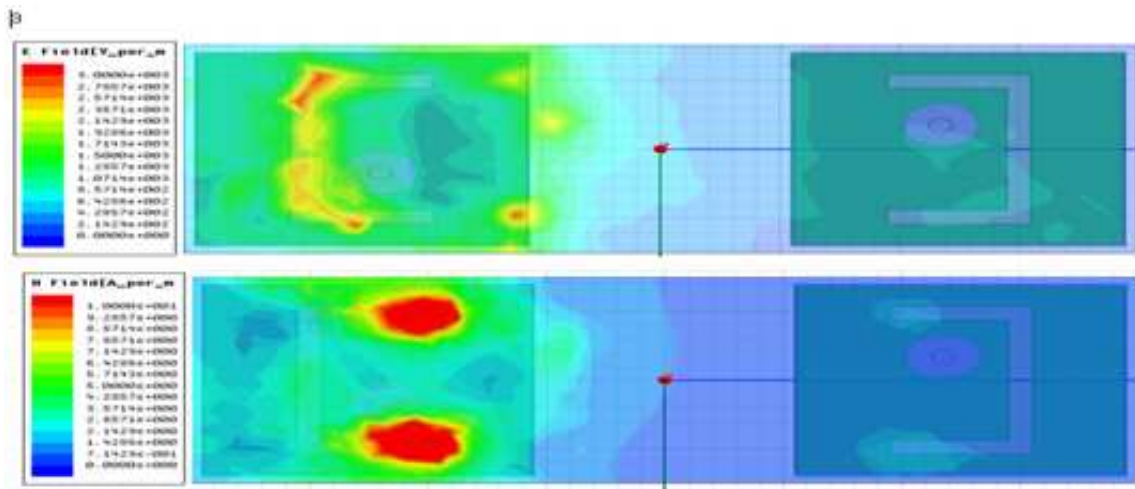


Figure 46. Electric field (top) and Magnetic field (bottom) coupling between array elements in configuration three.

Most of the mutual coupling is due to Electric field coupling.

Configuration 4

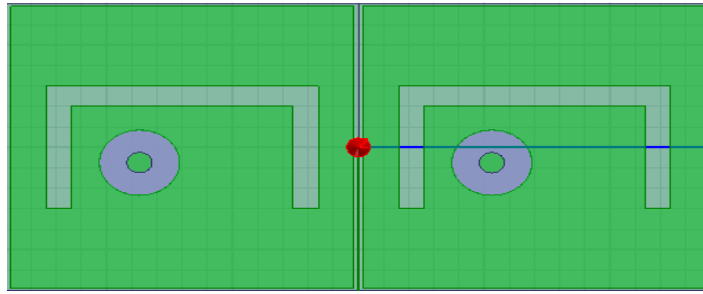


Figure 47 .Geometry of configuration 4 of U-slot patch antenna array

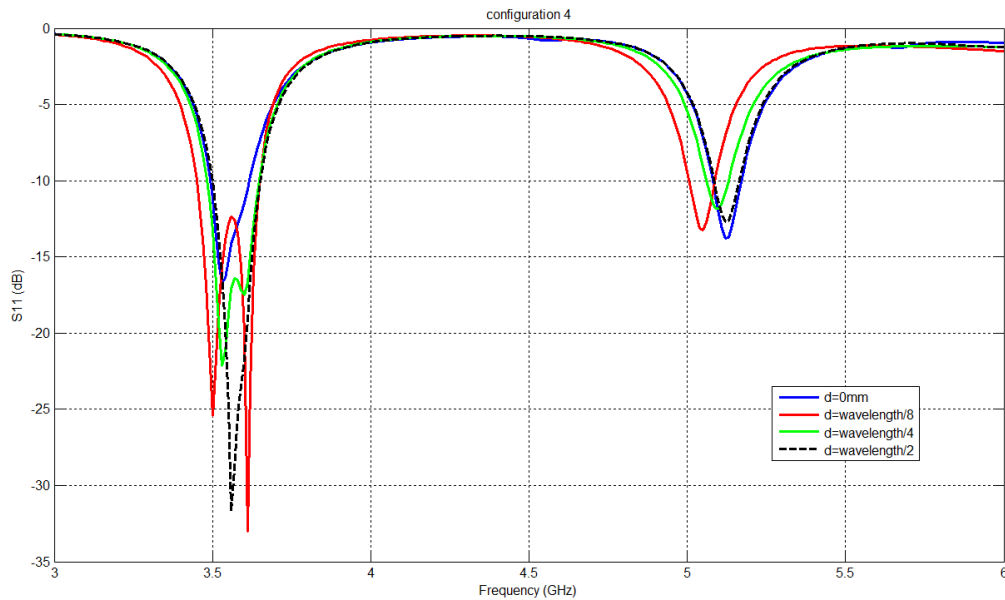


Figure 48 .Simulated S_{11} of configuration four for different values of d

Figure 48 shows the mutual coupling between elements for different antenna spacings . It is interesting to see a null in the mutual couplings at 3.57 GHz that is the lower resonance frequency. This provides a mutual coupling of about -34 dB when antennas are placed in distance of only $\lambda/8$ from each other .This means 10 dB improvement compare to configuration 1.

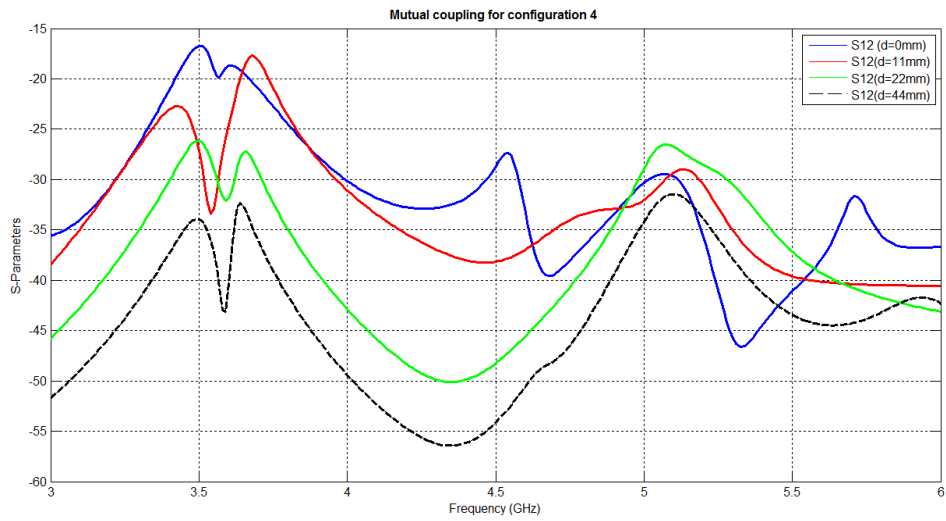


Figure 49 . Simulated S_{21} of the configuration four for different values of d

Unlike the three previous configurations, it seems the H field has more coupling than E fields. So in this configuration antennas are coupled by their H fields.

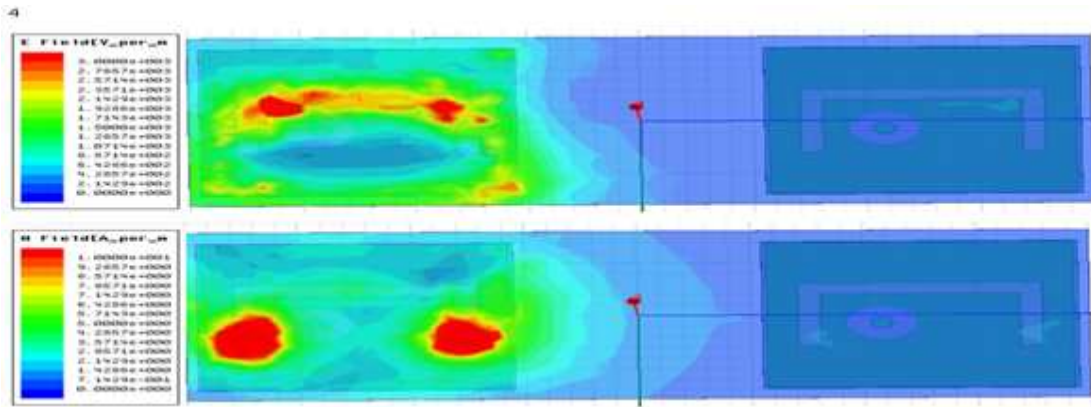


Figure 50 .Electric field (top) and Magnetic field (bottom) coupling between array elements in configuration four

Configuration 5

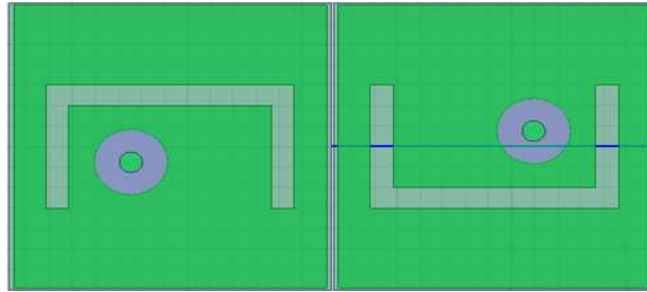


Figure 51 .Geometry of configuration 5 of U-slot patch antenna array

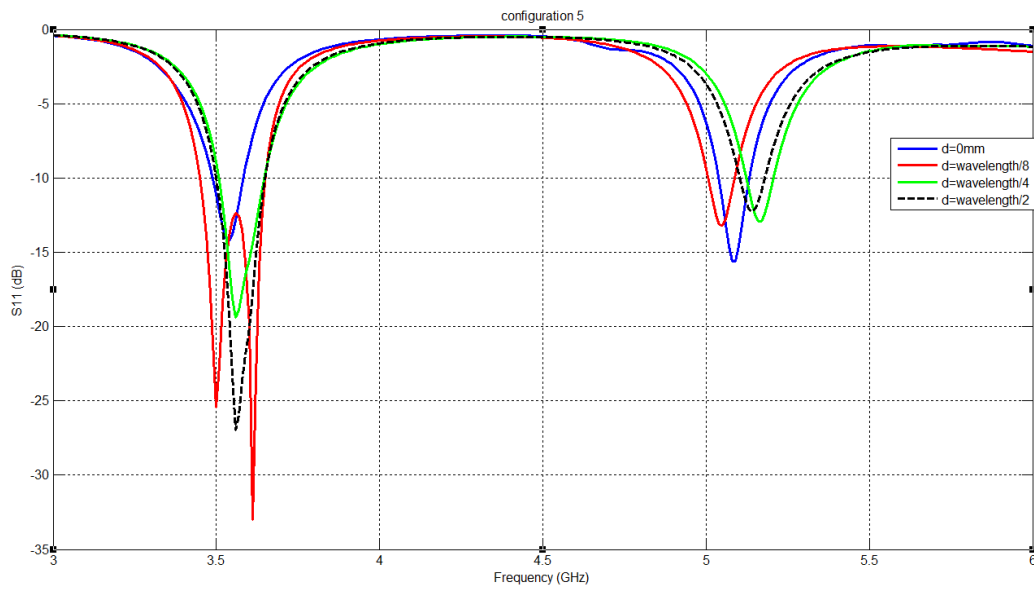


Figure 52 .Simulated S11 of the configuration five for different values of d

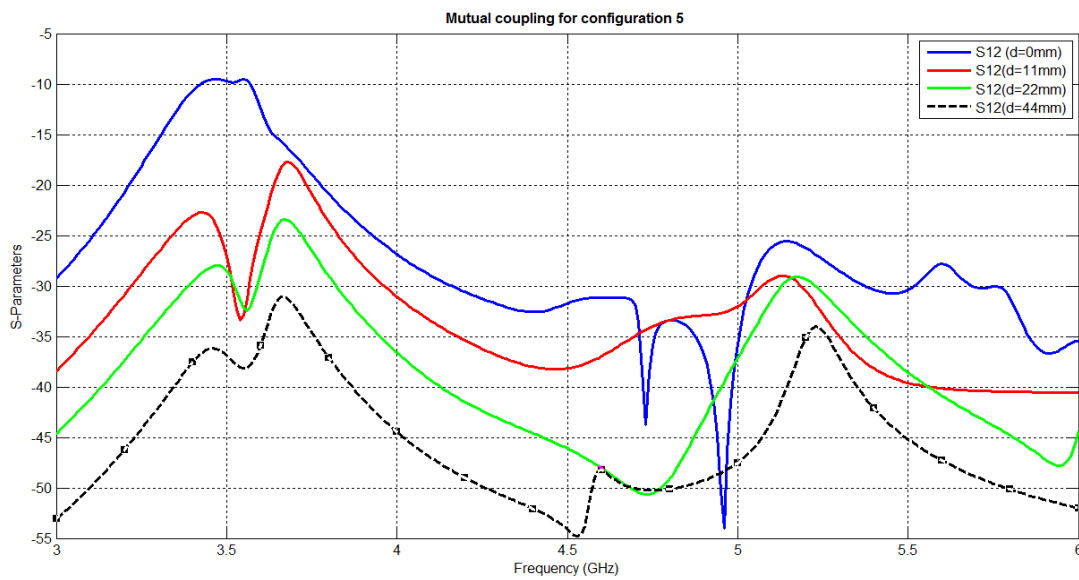


Figure 53 .Simulated S21 of the configuration five for different values of d

In this configuration although feed points are far from each other compare to configuration 4 ,the mutual coupling at lower resonant frequency is worse than configuration 4. But in higher frequencies it shows better mutual coupling results.

Similar to configuration 4, the H field coupling is dominant in configuration 5.

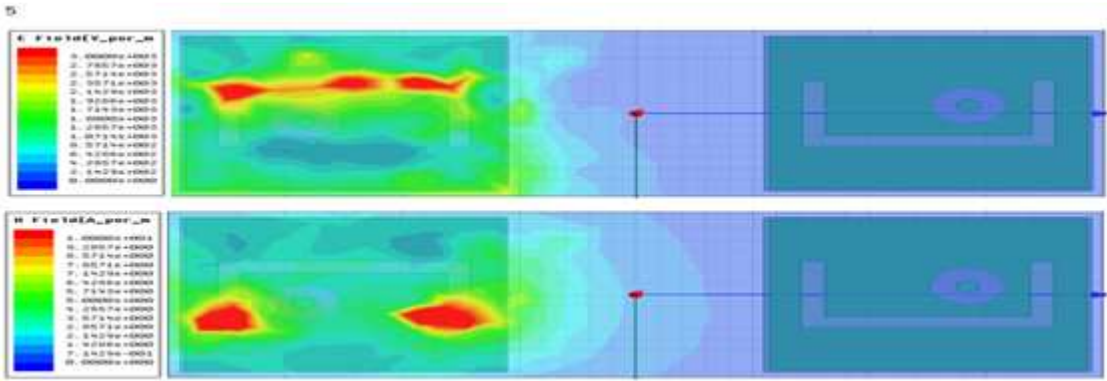


Figure 54 .Electric field (top) and Magnetic field (bottom) coupling between array elements in configuration four

Configuration 6

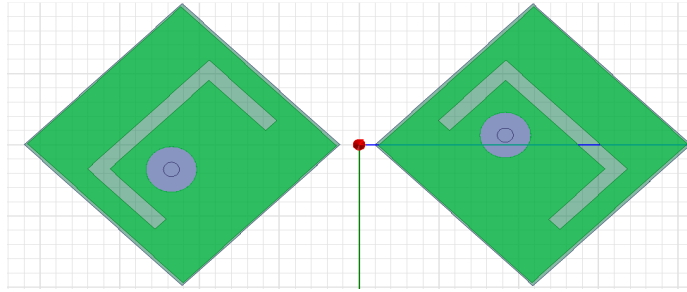


Figure 55 .Geometry of configuration 6 of U-slot patch antenna array

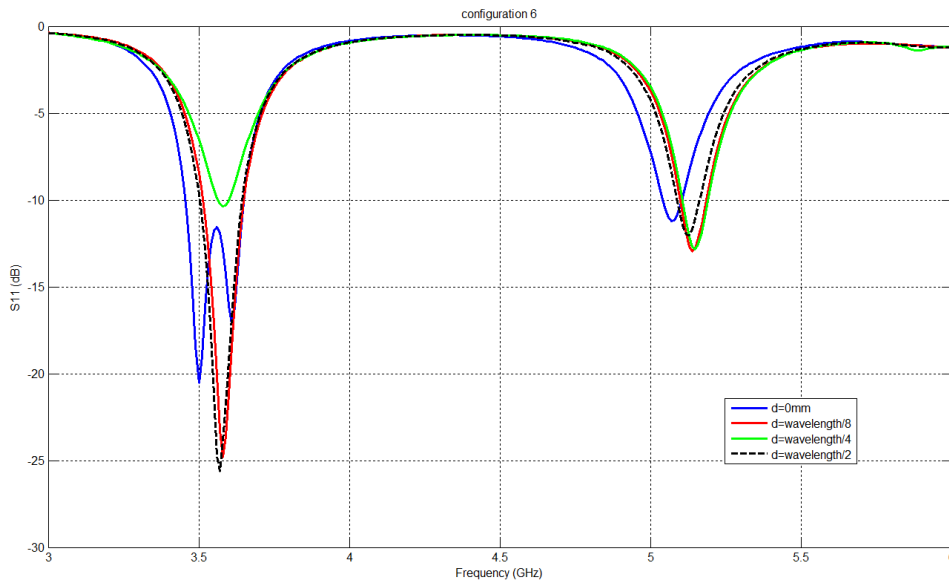


Figure 56 .Simulated S_{11} of the configuration six for different values of d

From Figure 56 it is found that at a quarter wavelength the antenna spacing reflection coefficient increased at lower frequency. So $d = \lambda/4$ is not a good option in case of configuration 6.

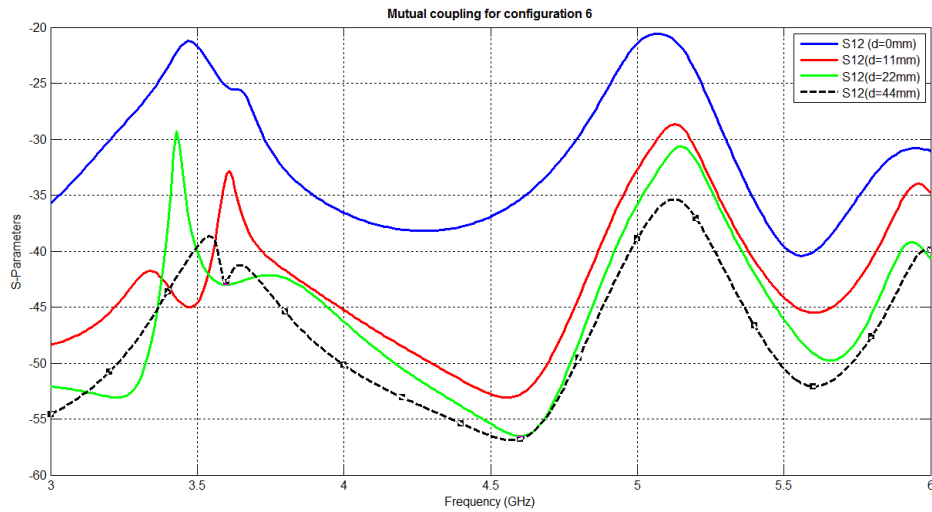


Figure 57 .Simulated S21 of the configuration six for different values of d

The whole mutual coupling amounts for all frequencies dropped in case of configuration 6. In this configuration even at $d=0$, the maximum mutual coupling is -21 dB which is an extremely good number for mutual coupling of two antennas that are close to each other.

It seems in configuration 6, E and H fields contribute evenly in coupling mechanism.

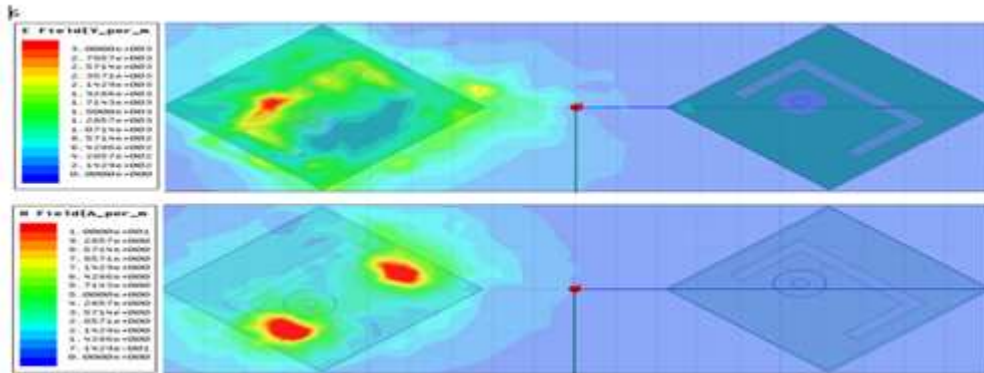


Figure 58 .Electric field (top) and Magnetic field (bottom) coupling between array elements in configuration six

Configuration 7

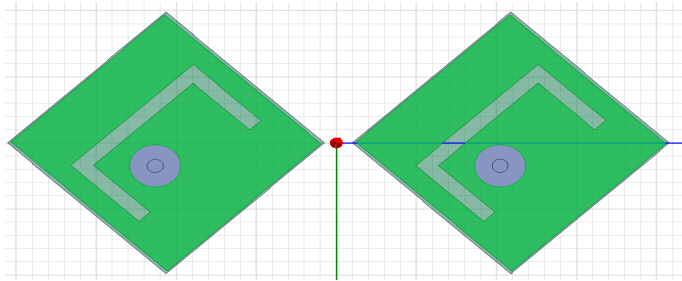


Figure 59 .Geometry of configuration 7 of U-slot patch antenna array

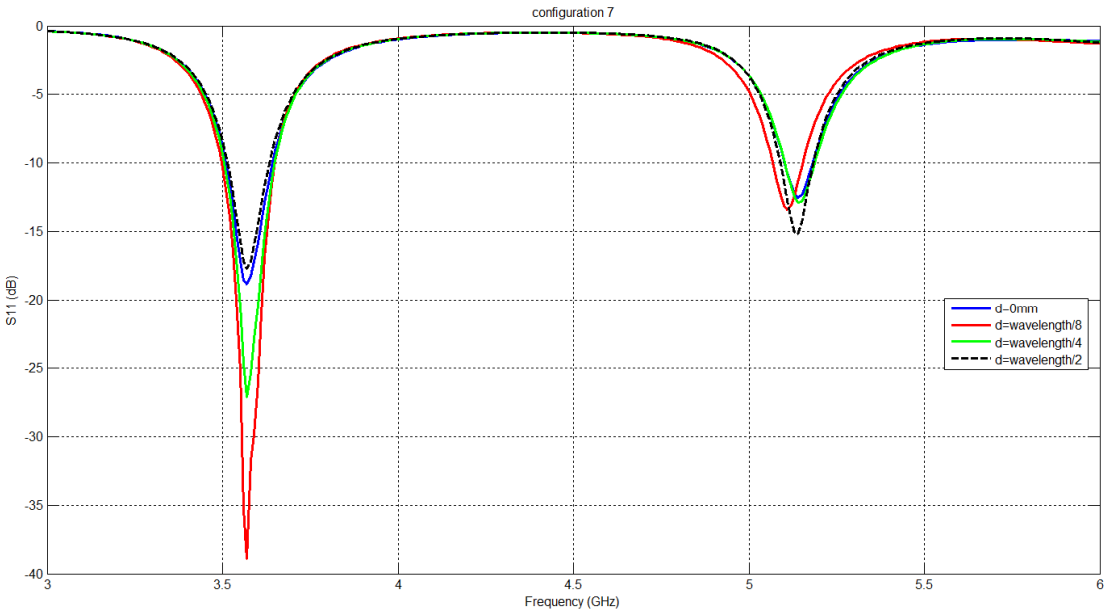


Figure 60 .Simulated S11 of the configuration seven for different values of d

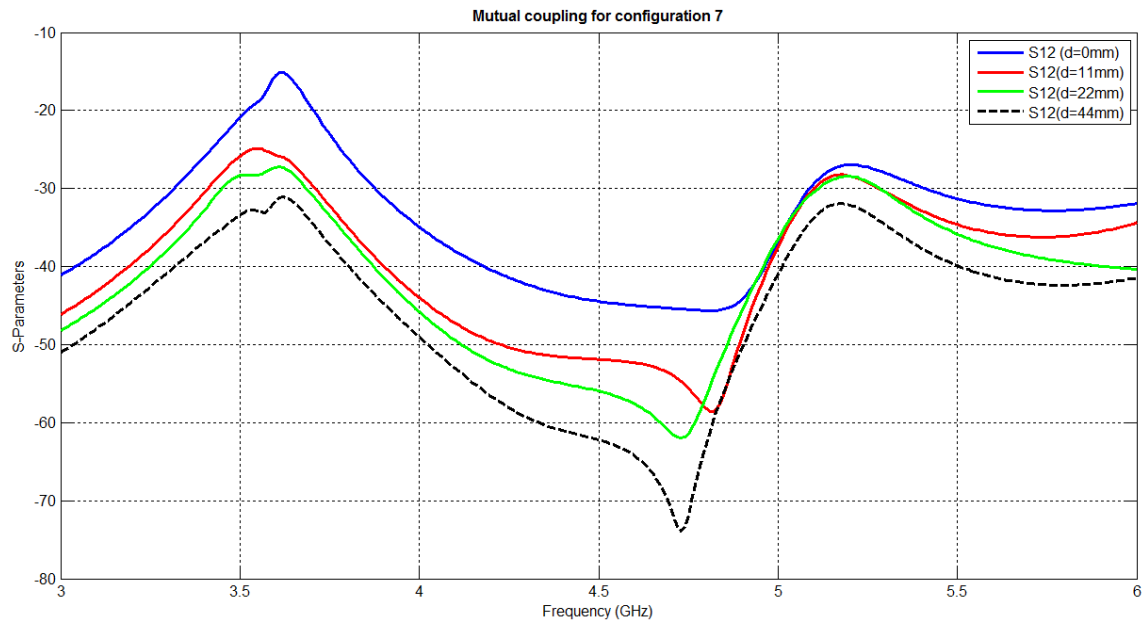


Figure 61 .Simulated S21 of the configuration seven for different values of d

It is evident from this figure that the isolation has improved by 20 dB by increasing the distance between elements in expense of increasing the reflection response.

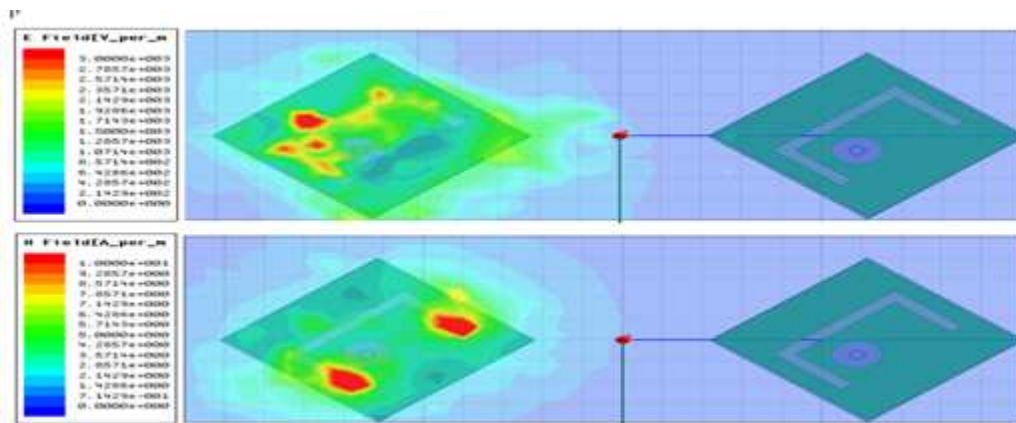


Figure 62 . Electric field (top) and Magnetic field (bottom) coupling between array elements in configuration seven

Configuration 8

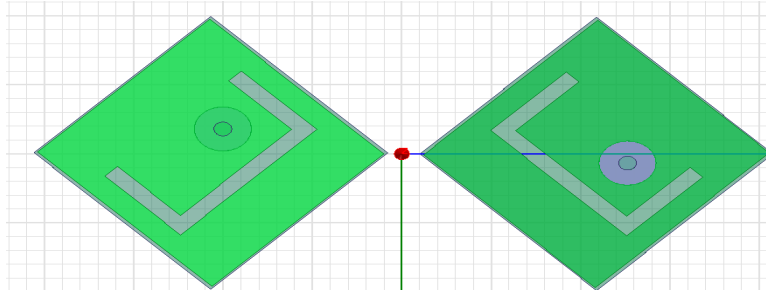


Figure 60 .Geometry of configuration 8 of U-slot patch antenna array

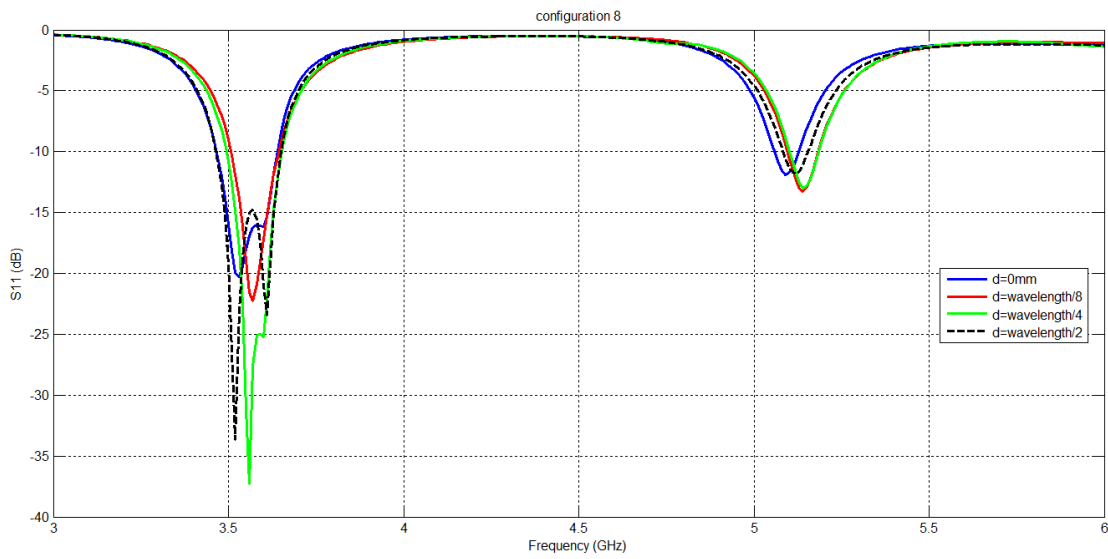


Figure 63 .Simulated S11 of the configuration eight for different values of d

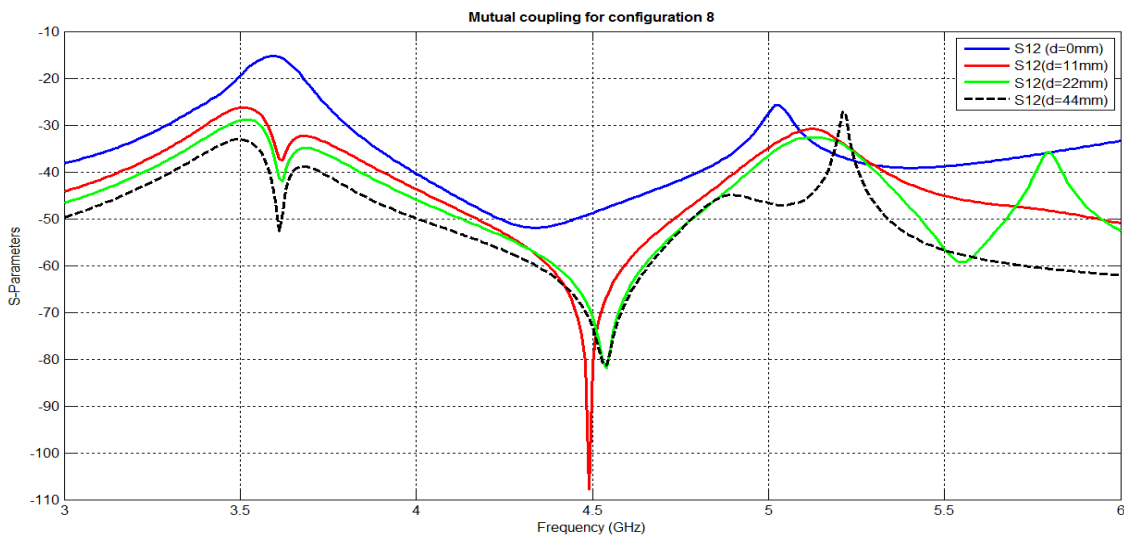


Figure 64 .Simulated S₂₁ of the configuration eight for different values of d

Using configuration 8 does not seem to be a good option for $d=0$. But at $d=\text{half wave length}$ it shows the lowest mutual coupling among all other configurations. At 3.57 GHz and $d=\text{half wavelength}$, S_{12} is -52 dB which is better than the required mutual coupling for most of the applications.

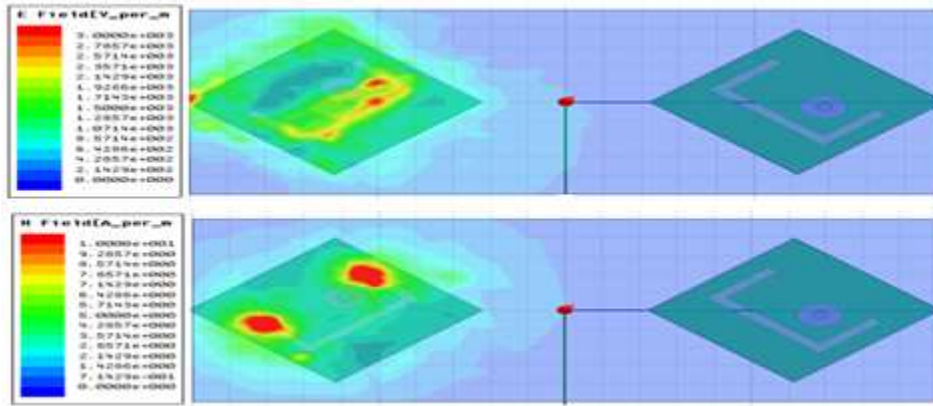


Figure 65 .Electric field (top) and Magnetic field (bottom) coupling between array elements in configuration eight

Comparison of the results

D=0

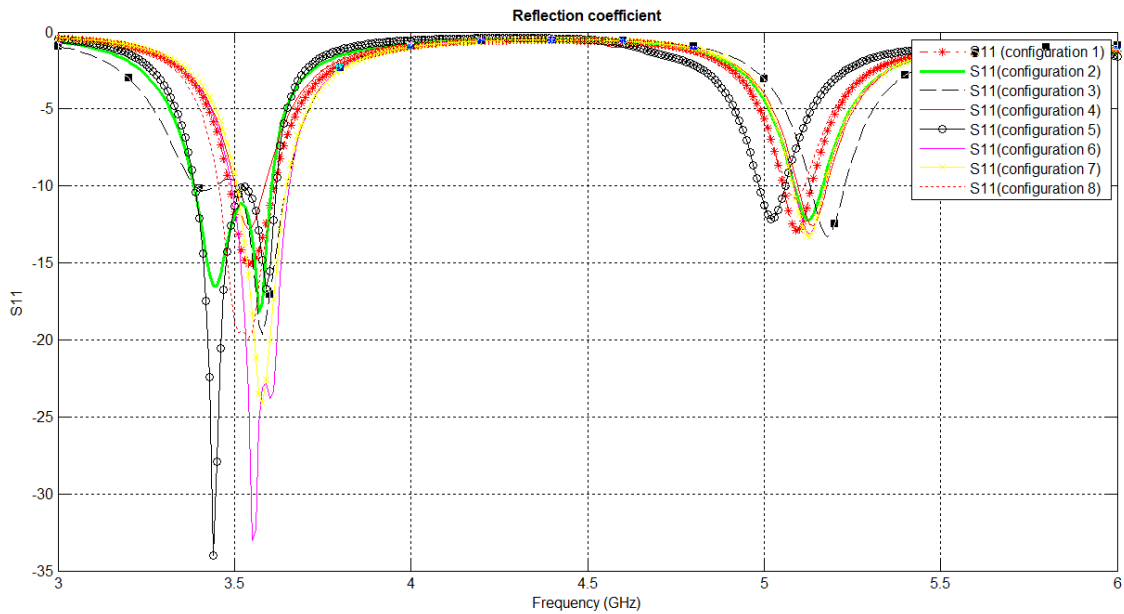


Figure 66. Return loss for different configurations

Figure 67 – 72 show the comparison between 8 proposed configurations at different antenna spacing.

When there is no space between antennas, antennas are attached together, configuration 3 shows the highest and configuration 6 has the lowest mutual coupling. An improvement of 16 dB is achievable by using configuration 6 instead of configuration 3.

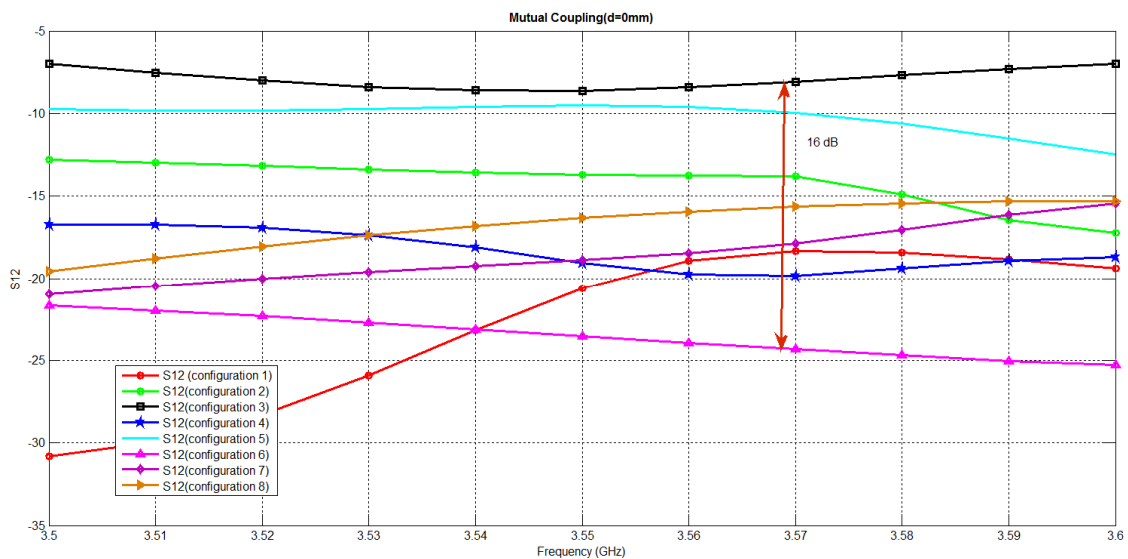


Figure 67 .Simulated S21 for different configurations for antenna spacing of d=0mm

By separating the antenna elements 11 mm $(\frac{\lambda}{8})$, overall mutual coupling decrease at least 10 dB for all configurations. Similar to the previous results still antenna 3 is the worst and antenna 6 is the best configurations. However at the resonant frequency, configuration 2 represents the mutual coupling of -43 dB which is very desirable for two antennas that are placed very close to each other.

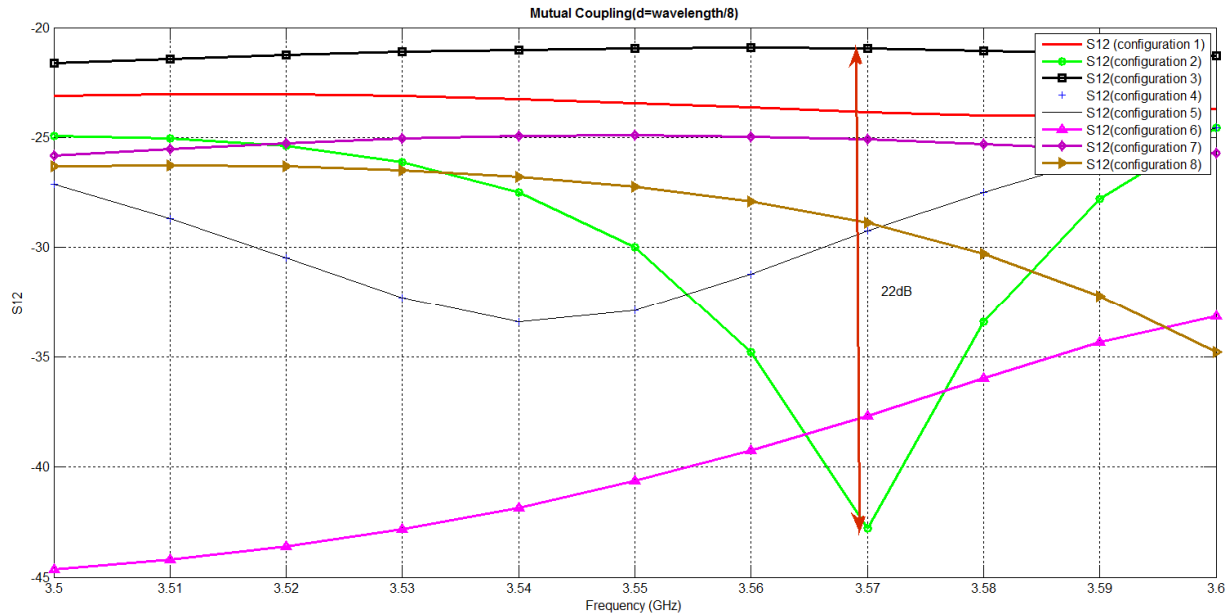


Figure 68 .Simulated S21 for different configurations for antenna spacing of d=11mm

By changing d to a quarter wavelength still configuration 6 shows the best performance in terms of mutual coupling. Mutual coupling in configuration 6 is less than 40 dB for the entire band of 3.5 to 3.6 GHz. In applications that even more antenna isolation is required, configuration 2 with minimum mutual coupling amount of about -50 dB seems to be a good option.

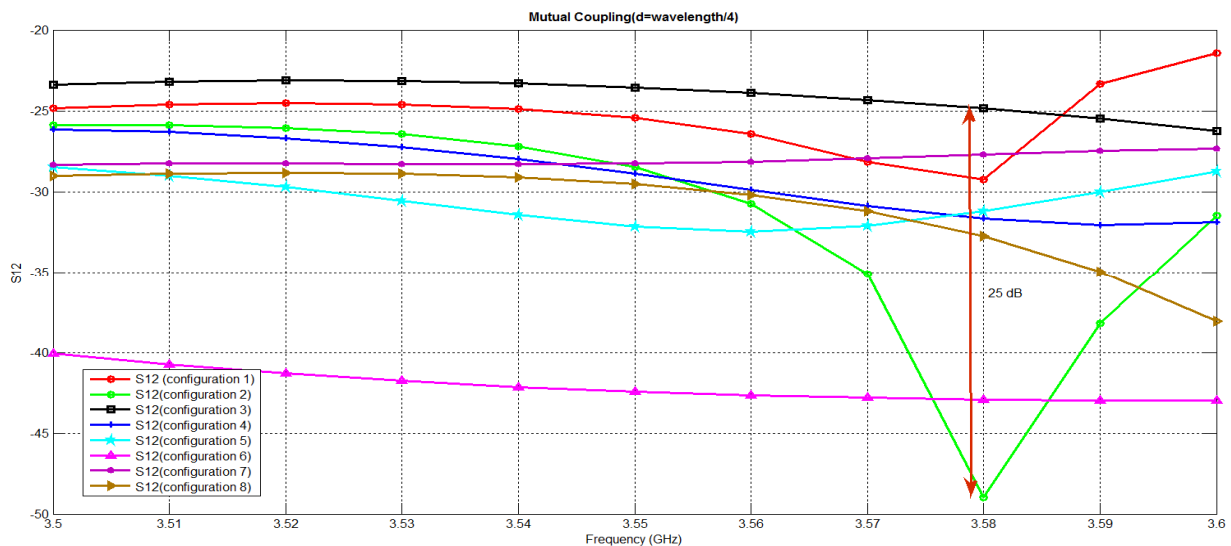


Figure 67 .Simulated S21 for different configurations for antenna spacing of d=22mm

Figure 71 shows mutual coupling between two elements in different configurations. In this case configuration 4 and 6 represent the lowest amount of mutual coupling. An improvement of 12 dB is achievable by the changing configuration.

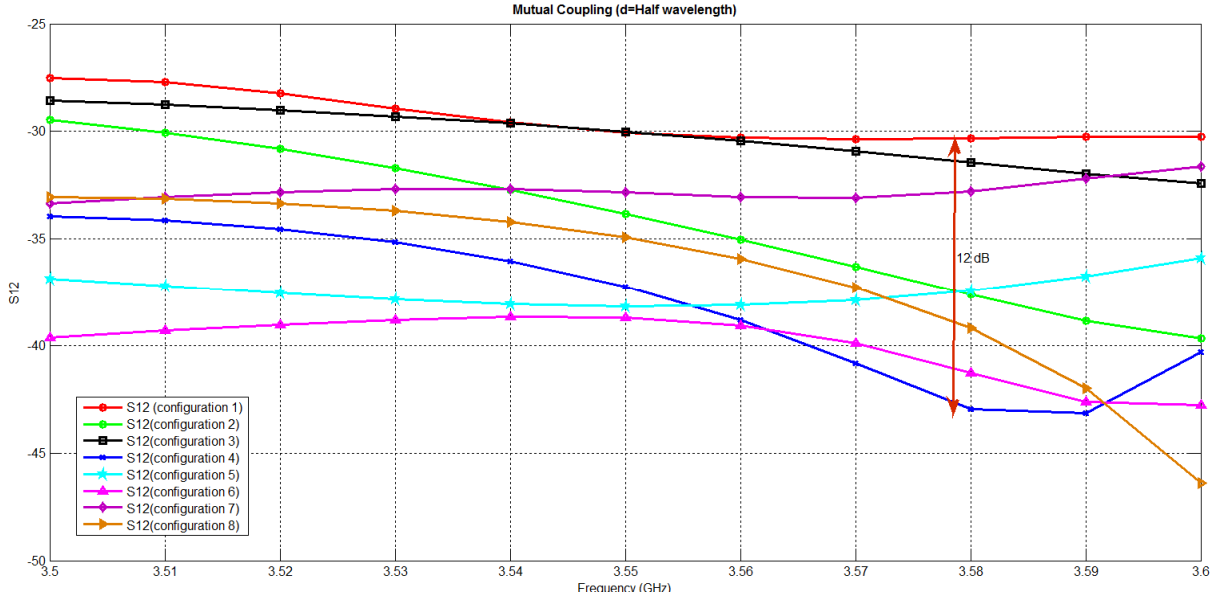
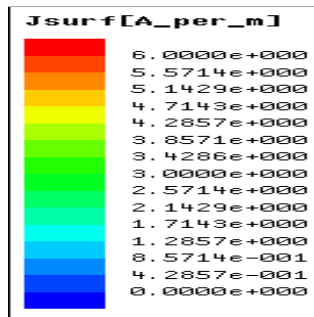


Figure 69 .Simulated S21 for different configurations for antenna spacing of d=44mm

The variations of the space-wave coupling by changing array element configurations is clearly observed in Figure 72, in which the distribution of the surface currents on the second antenna is plotted when antenna one (port 1) is excited while the other antenna is terminated with a 50 Ω impedance. High concentration of the surface currents is seen in the loaded antenna in configuration 2 and 3 [see Figure 72].



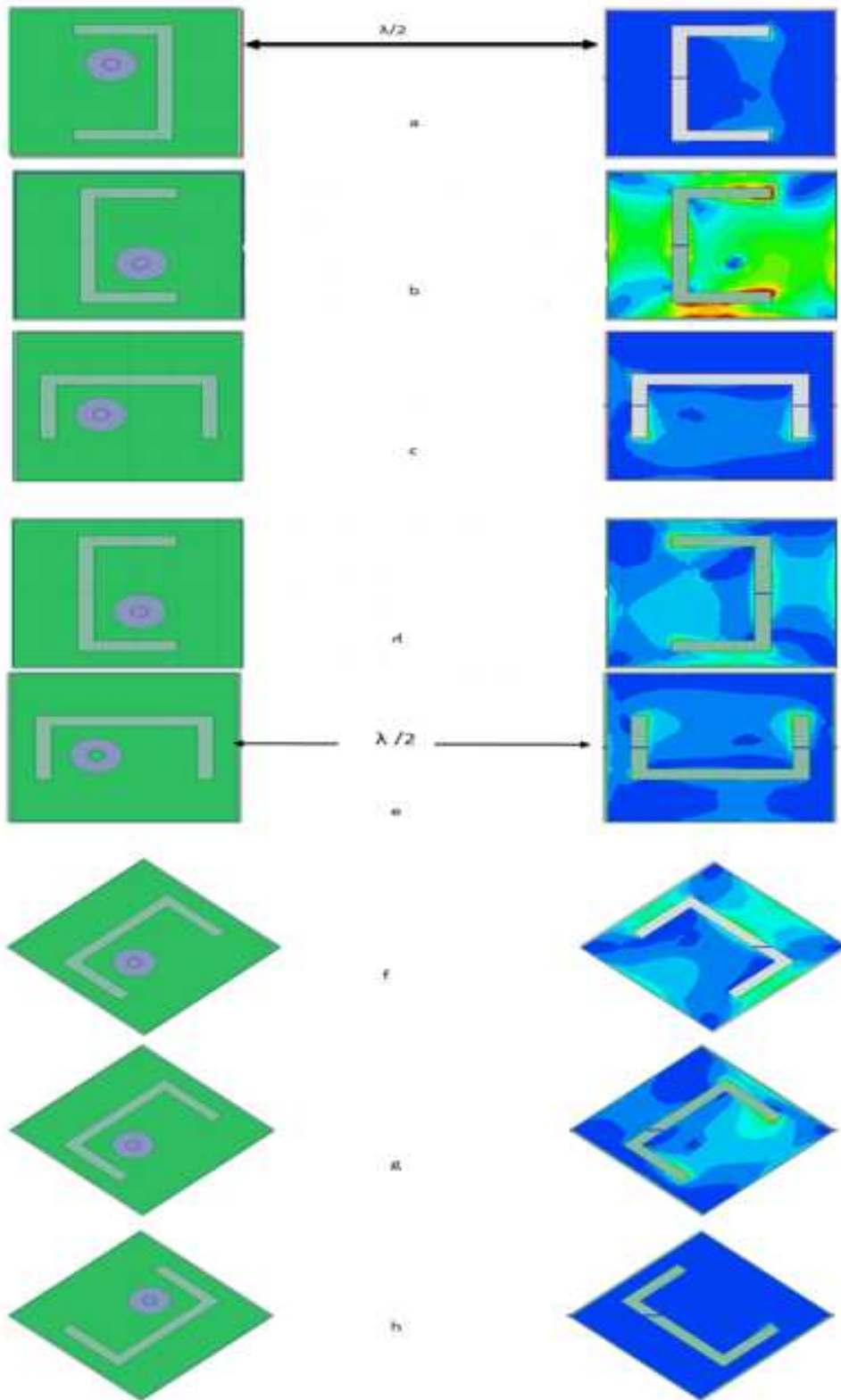


Figure 70 .Surface current distribution on the terminated antenna due to the coupling from left side excited antenna.

It is evident from this figure that the isolation has improved in configuration 1 and 8 .

Table 5. Summary of eight different configurations for antenna array

Configuration #	Lower resonant frequency (GHz)	S_{21} d=0	S_{21} d= $\lambda/8$	S_{21} d= $\lambda/4$	S_{21} d= $\lambda/2$
1	3.58	-17 dB	-24dB	-28 dB	-31 dB
2	3.58	-13 dB	-45 dB	-48 dB	-37.5 dB
3	3.58	-7 dB	-22 dB	-25 dB	-32 dB
4	3.58	-20 dB	-29 dB	-32 dB	-43 dB
5	3.58	-10 dB	-29 dB	-31 dB	-37.5 dB
6	3.58	-24 dB	-37 dB	-43 dB	-42 dB
7	3.58	-16 dB	-25 dB	-27.5 dB	-33 dB
8	3.58	-16.7 dB	-28.5 dB	-32 dB	-38 dB

Configuration 6 and 4 seem to be the best cases for all different antenna spacing.

Spacing Between antennas

The spacing (d) between two adjacent antennas is very critical. If the Antennas are too close to each other, mutual coupling will increase, which affects the polarization purity, and the antenna performance. Spacing is limited due to the available array grid space that is very small in hand held devices.

The following figure shows the effect of spacing on mutual coupling for different array configurations.

From Figure 73 it is obvious that as the spacing increased, the mutual coupling will be reduced. Generally configuration 6 has the lowest mutual coupling among other configurations for different antenna spacing. Configurations 4 and 8 seems to be the next configurations with the least amount of mutual coupling.

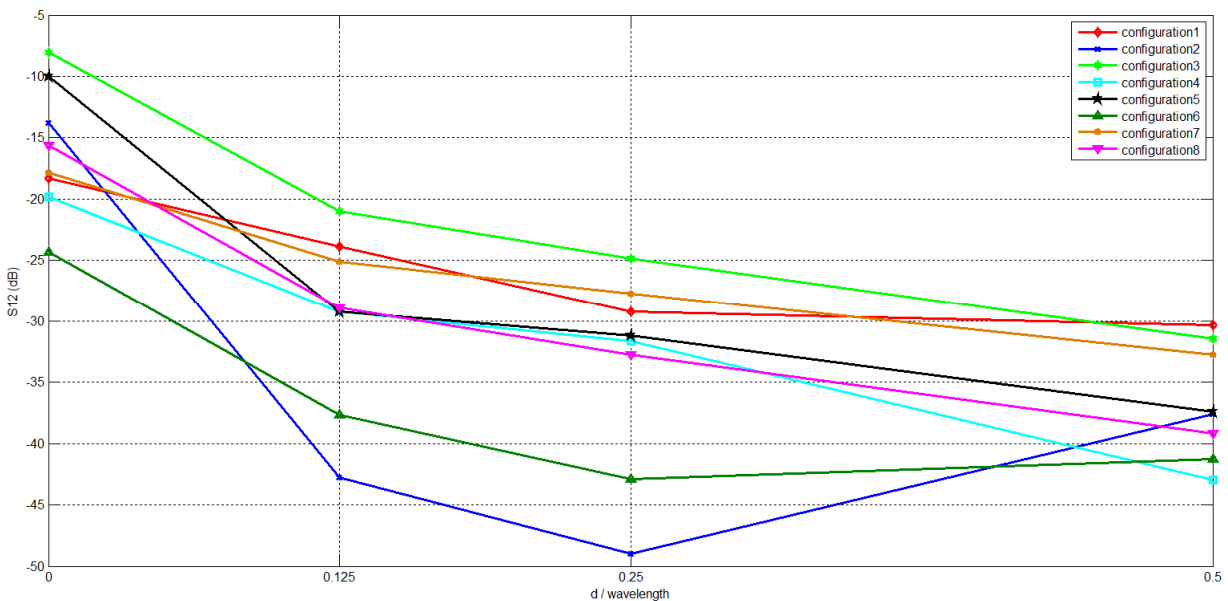


Figure 71 .Simulated S12 in different configurations versus antenna spacing (d/λ)

Chapter 4

Mutual coupling and MIMO

Multiple Input Multiple Output, MIMO, is a technology that has been improving the performance of wireless communication systems and radars. In order to get a good results from MIMO systems, channels between different transmit and receive antennas should be independent and identically distributed (i.i.d). Therefore antennas should be far from each other. Usually MIMO studies neglect the influence of antennas on each other and on MIMO performance. But recently by the growing popularity of smaller and lighter devices, antenna elements have to be placed close to each other, so antenna radiation characteristics as well as mutual coupling become a very important factor in arrays.

Considering mutual coupling is even more important in MIMO studies, since mutual coupling not only affects the antenna efficiency but also influences the correlation, and makes the channel between antennas correlated. Having correlated channels in MIMO systems reduces both the capacity and the diversity gain.

There is an extensive interaction between antennas and the propagation channel in MIMO systems, antenna configuration has to be chosen carefully. Antenna type as well as the arrangement of the elements in a MIMO array strongly influence the performance. Achieving high efficiency in terms of power and a low correlation between propagation paths are major challenges in MIMO systems with multiple antennas in small handheld devices and radars.

In chapter three among 8 different possible configurations, the configuration with the lowest amount of mutual coupling was introduced. The subject of this chapter is to investigate the effect of antenna orientation and mutual coupling on MIMO capacity for communication applications and range ambiguity for radar applications. It is shown that using antenna configuration with minimum amount of mutual coupling enhances the capacity of a MIMO system.

4.1 System Model

In the case of this research, there are two transmitting antennas and one receiving antenna.

The received signal can written as

$$\mathbf{r} = \mathbf{H} \mathbf{s} + \mathbf{n} \quad (35)$$

n: AWGN noise

s: Transmitted signal

H: $N \times M$ channel matrix consist of complex Gaussian random variables.

For correlated MIMO channel we have

$$\mathbf{H} = \mathbf{H}_{\text{iid}} ([\mathbf{R}_{\text{tx}}]^{1/2})^T \quad (36)$$

\mathbf{R}_{tx} is the transmit correlation matrix. \mathbf{H}_{iid} is the channel matrix generated using zero mean unit variance i.i.d complex Gaussian random variables.

$$\mathbf{R}_{\text{tx}} = \begin{bmatrix} 1 & \rho_{\text{tx} 1,2} \\ \rho_{\text{tx} 2,1} & 1 \end{bmatrix} \quad (37)$$

Where $\rho_{\text{tx} i,j}$ is the correlation coefficient between the i^{th} and j^{th} transmitting antennas.

By considering following assumptions

- 1) Angle of Arrival is uniformly distributed between 0 and 360 degree.
- 2) Antenna is omnidirectional

Correlation coefficient between the two antennas is

$$\rho_{i,j} = J_0 \left(\frac{2\pi d}{\lambda} \right) \quad (38)$$

Now in presence of Mutual coupling, channel matrix can be presented as

$$\mathbf{H}_C = \mathbf{C}_p \mathbf{H}_U = (\mathbf{Z}_{\text{load}} + \mathbf{Z}_s) \begin{bmatrix} \mathbf{Z}_{\text{load}} + \mathbf{Z}_s & \mathbf{Z}_m \\ \mathbf{Z}_m & \mathbf{Z}_{\text{load}} + \mathbf{Z}_s \end{bmatrix}^{-1} \mathbf{H}_U \quad (39)$$

$\mathbf{Z}_s = \mathbf{R}_s + j\mathbf{X}_s$: self-impedance of the antenna;

$\mathbf{Z}_m = \mathbf{R}_m + j\mathbf{X}_m$: mutual impedance between the antennas;

$\mathbf{Z}_{\text{load}} = \mathbf{R}_{\text{load}} + j\mathbf{X}_{\text{load}}$: loading impedance of the antennas.

Where \mathbf{H}_C and \mathbf{H}_U are the coupled and uncoupled channel matrices with loading impedance \mathbf{Z}_{load} , and \mathbf{C}_p is the coupling matrix.

The capacity of a MIMO system not only depends on the number of channels (N.M) but also depends on the correlation between the channels.

The greater the channel correlation, the smaller is the channel capacity. The channel correlation of a MIMO system is mainly due to two components:

(1) Spatial correlation

(2) Antenna mutual coupling

We can write

$$\mathbf{R}_{\text{tx}} = \mathbf{C}_{\text{tx}} \mathbf{A}_{\text{tx}} \mathbf{C}_{\text{tx}}^H \quad (40)$$

\mathbf{C}_{tx} is the mutual coupling matrix for the transmit antenna

\mathbf{A}_{tx} is the correlation matrix of transmit antenna

We can write the transmit correlation matrix for a 2 transmit antenna system as

$$\mathbf{R}_{tx} = \begin{bmatrix} C_{tx,1,1} & C_{tx,1,2} \\ C_{tx,2,1} & C_{tx,2,2} \end{bmatrix} \begin{bmatrix} 1 & J_0\left(\frac{2\pi d}{\lambda}\right) \\ J_0\left(\frac{2\pi d}{\lambda}\right) & 1 \end{bmatrix} \begin{bmatrix} C_{tx,1,1}^* & C_{tx,1,2}^* \\ C_{tx,2,1}^* & C_{tx,2,2}^* \end{bmatrix} \quad (41)$$

The capacity of the MIMO channel is given by

$$C(\mathbf{H}) = \log_2 \left[\det \left(\mathbf{I} + \frac{SNR}{N} \mathbf{H}\mathbf{H}^H \right) \right] \quad \text{b/s/Hz} \quad (42)$$

4.2 Simulation Results

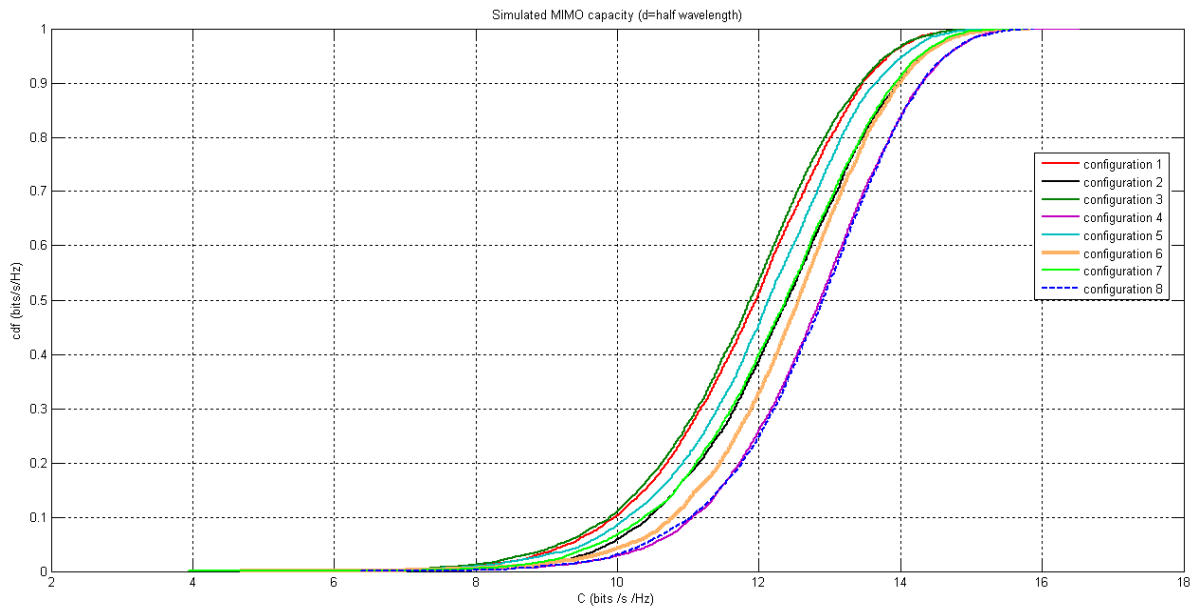


Figure 72 .Simulated cumulative distribution function for MIMO capacity in 8 proposed array configurations in the case of $d=\lambda/2$

Figure 74 shows that based on simulations configurations 8, 4 and 6 have the higher amounts of channel capacities. This was predictable, since these three configurations have the lower amount of mutual couplings between their elements.

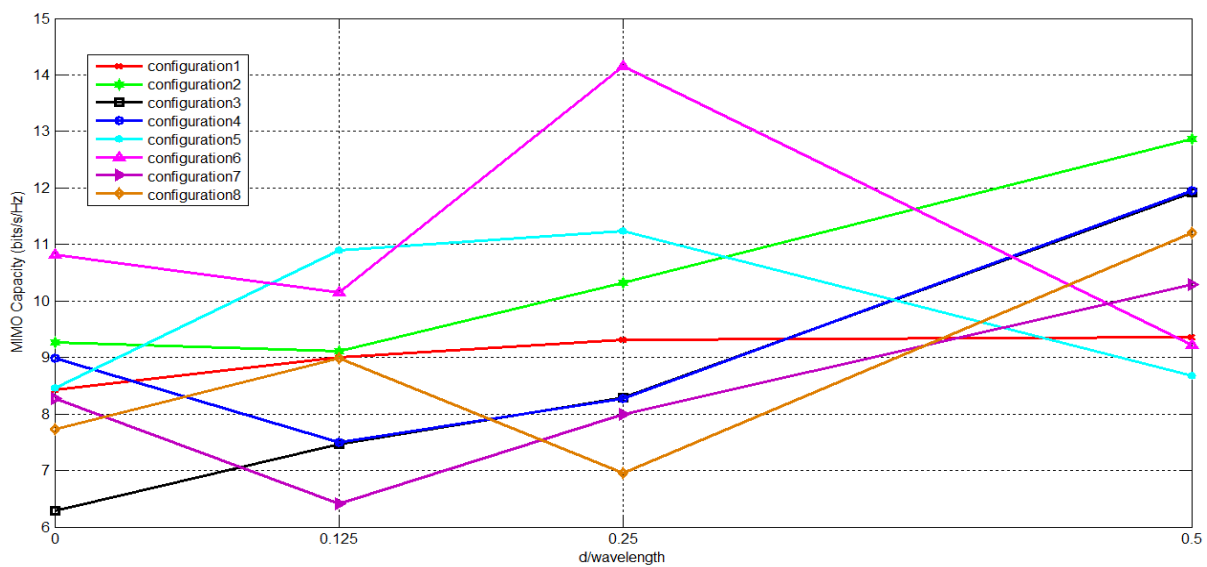


Figure 73 .Simulated MIMO capacity versus antenna spacing for 8 proposed array configuration

CHAPTER 5

EXPERIMENTAL RESULTS AND COMPARISONS

It is now obvious that mutual coupling between antenna elements in array affects MIMO performance. Thus, an experiment on MIMO system in presence of mutual coupling between array elements will provide useful information about the mutual coupling effects in MIMO applications.

Chapter 2 deals with simulation results about the performance of a Single U-slot patch antenna. Next in Chapter 3, different array configurations are considered and their mutual interactions are studied. In chapter 4 the effect of the simulation results on MIMO performance in each array configuration was investigated. In this chapter the experimental results and their correspondence with simulation and theory are presented.

Finally in section 5.2 some interesting conclusions are drawn from the comparison of experimental and computed results.

5.1 Single U-slot patch Antenna

Three sample prototype antennas were built to verify repeatability of the results obtained. Figure 76 shows top view of two of the samples side by side. 50 –Ohm SMA connectors are connected to the input of the antennas.

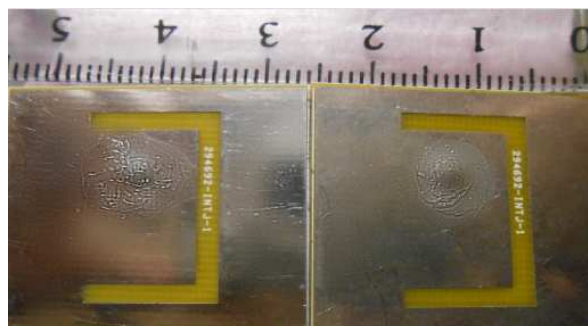


Figure 74 .Photograph of the two fabricated prototypes

The experimentation started with the measurement of the antenna return loss response (S11) using the network analyzer. Since the antennas are designed to operate at frequencies of 3.5GHz and 5 GHz the reflection response of the device was observed for a frequency range of 2 to 6 GHz. Figure 77 plots the reflection response (S11) of the single antenna. From the figure, it is evident

that the antenna is a dual resonator resonating at 3.43 GHz and, 4.9 GHz. In addition the $|S_{11}|$ is -8.8 dB at 3.43 GHz and -9.1 at 4.9GHz.

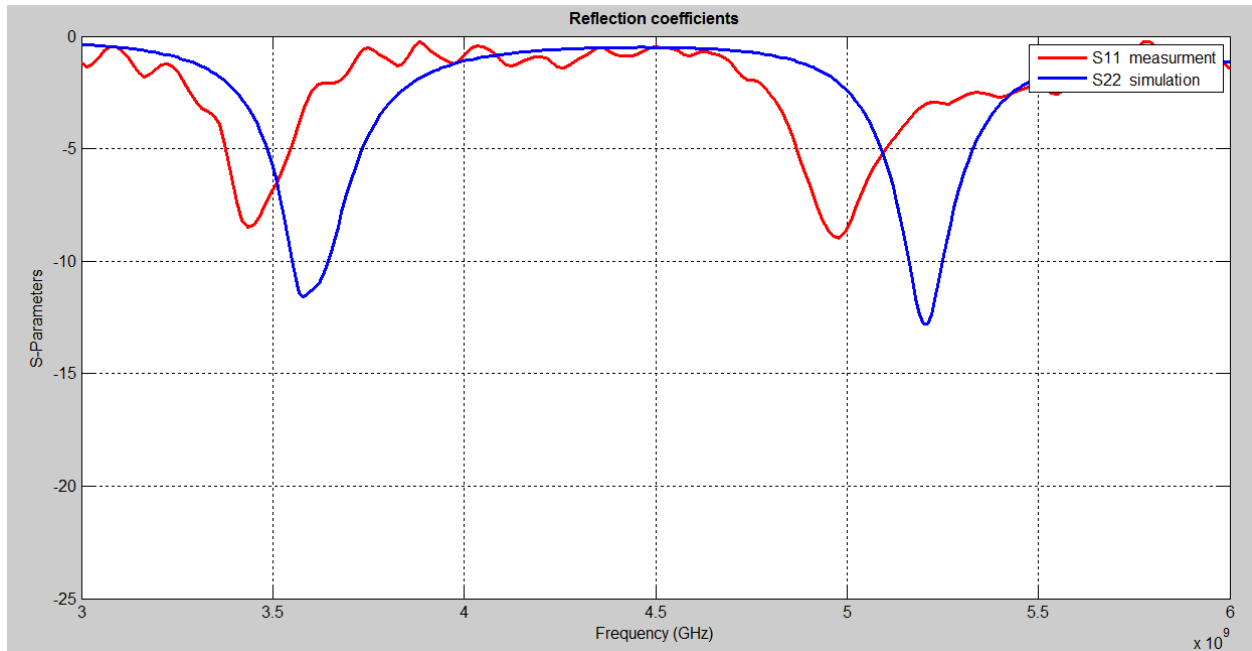


Figure 75 .The simulated and measured return losses of the proposed antenna

Based on our simulation results we are expecting to see the resonances at 3.57 GHz and 5.2 GHz. Thus the resonant frequencies have been shifted about 130 MHz and also there is a reduction in the amplitude t of the reflection coefficient. In order to have a good resonator S_{11} should be at least -10 dB.

Table 6. Summary of figure 77.

	Frequency (GHz)	Reflection Coefficient (dB)
Simulation	3.57 and 5.013	-12.4 and -13.7
Experimentation	3.43 and 4.9	-8.8 and -9.1

As mentioned before in order to reduce the fabrication cost, a thin substrate was chosen and therefore the bandwidth of the antenna was significantly decreased. By choosing substrates with the thickness of 0.76cm, wide bandwidth behavior would be guaranteed.

Other antenna characteristics, such as mutual coupling were measured in University of Kansas anechoic chamber.

Radiation patterns of the single antenna at 3.429 GHz in two planes are presented in Figure 78 a and 79 a.

Figure 80 a and figure 81a shows radiation pattern of a single u slot patch at 4.965GHz.

It is evident that the simulated radiation pattern result and measured ones are in good agreement with each other.

F=3.429 GHz

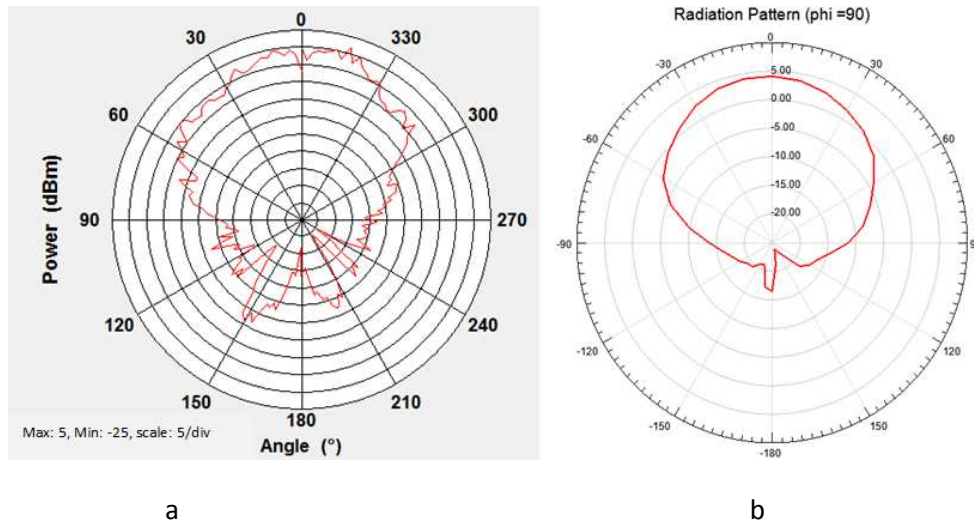


Figure 76 .Radiation patterns of the single U-slot patch at plane of phi= 90 at 3.429 GHz.a) Measured .b) Simulated

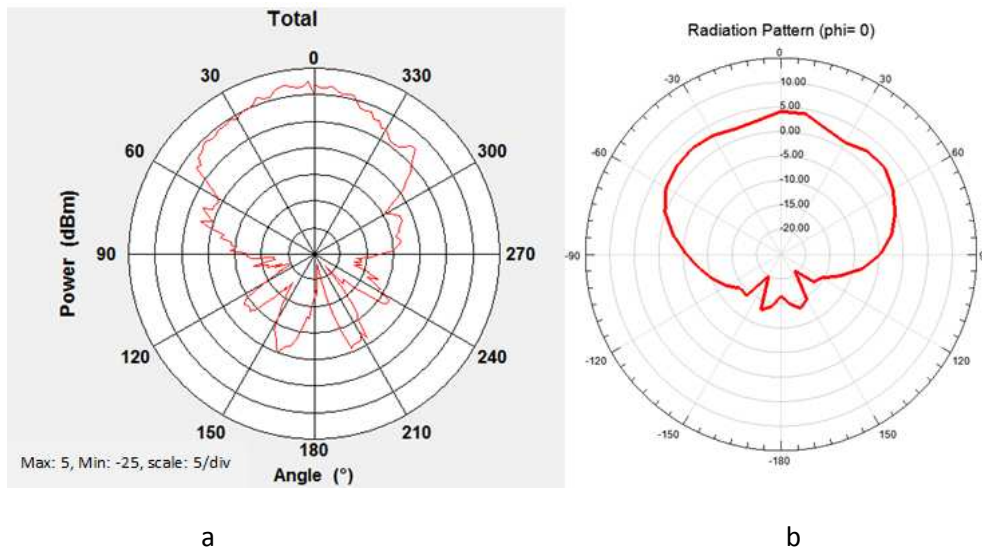


Figure 77 . Radiation patterns of the single U-slot patch at plane of phi= 0 at 3.429 GHz. a) Measured .b) Simulated

F=4.965GHz

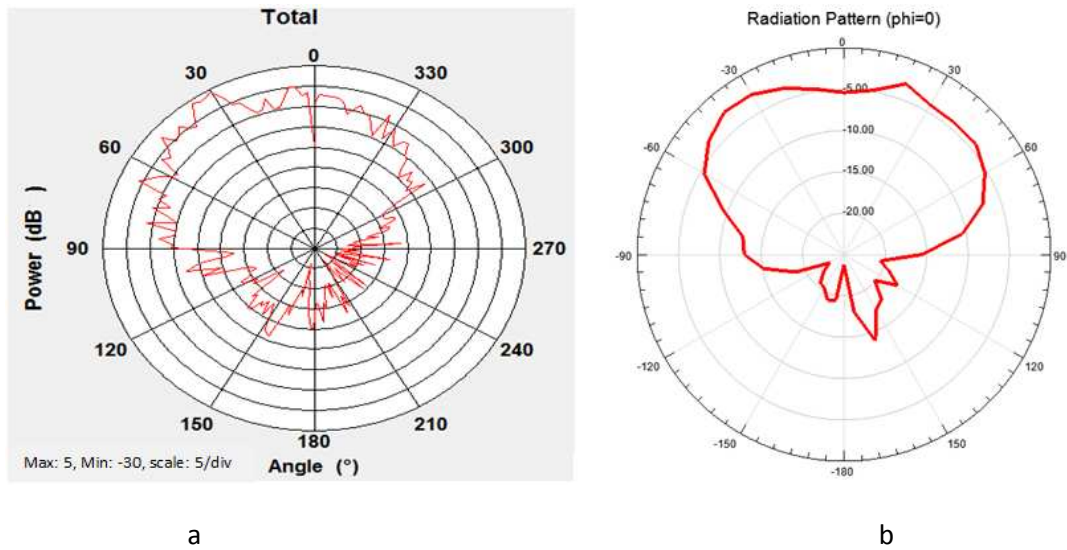


Figure 78. Radiation patterns of the single U-slot patch at plane of $\phi=0$ at 4.965GHz. a) Measured and b) Simulated

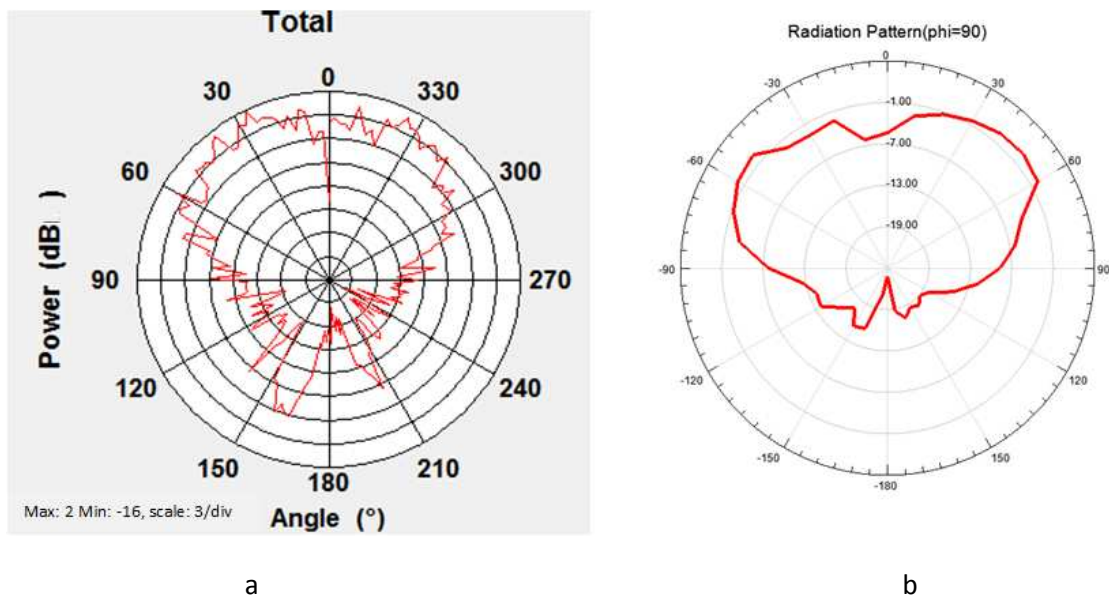


Figure 79. Radiation patterns of the single U-slot patch at plane of $\phi=90$ at 4.965GHz . a) Measured and .b) Simulated

One interesting observation from these radiation pattern measurements is of the polarization of the antenna at different frequencies. From Figure 82 and 83, the antenna has vertical polarization at higher frequency (4.965 GHz) and horizontal polarization at lower frequency, 3.429 GHz.in Figure

82 at 210 degrees there is a peak for the vertical polarization measurements that is due to the antenna holding structure inside the chamber.

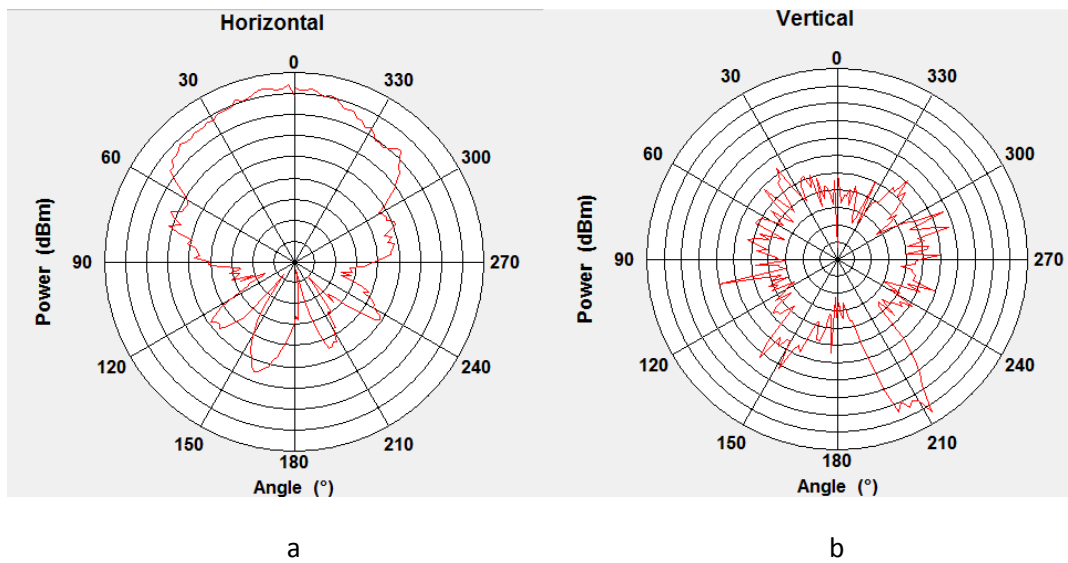


Figure 80. antenna polarization at 3.49 GHz.

Antenna polarization is horizontal in lower resonant frequency.

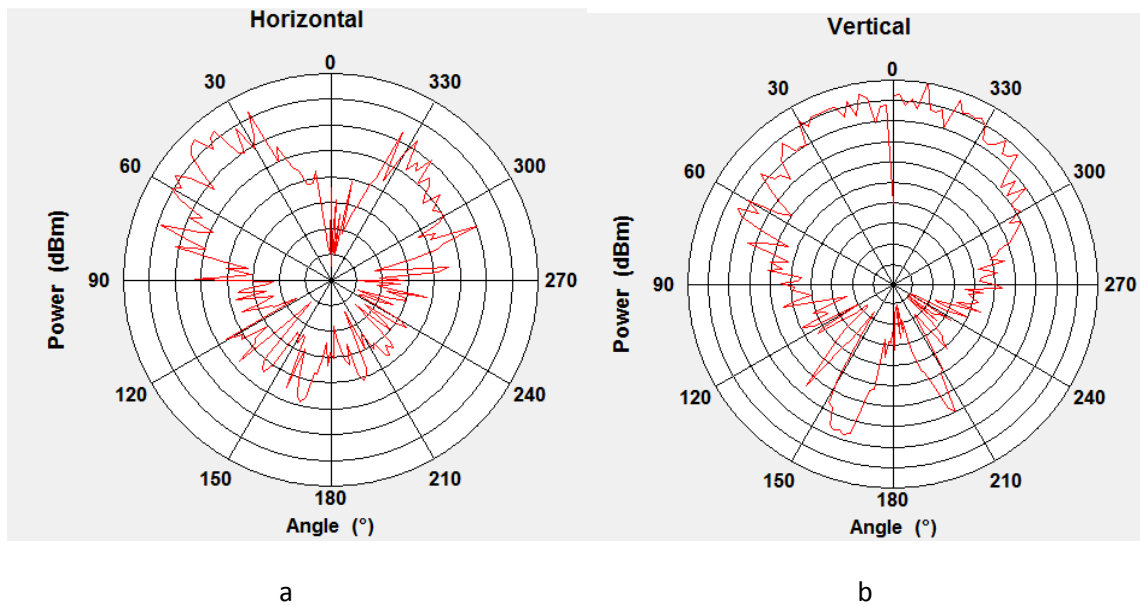


Figure 81 Antenna polarization at 4.9 GHz.

At higher resonant frequencies the polarization is horizontal.

5.2 Mutual coupling Measurements

All measured results of mutual coupling of the design for different configurations are presented in Figure 84. In the case of Figure 84 the edge-to-edge distance between two antennas is about the half wavelength at the lower resonant frequency.

By changing the array configuration from three to four, the configuration with highest and lowest mutual coupling respectively, mutual coupling is decreased from -17 dB to about -48 dB at 3.4 GHz.

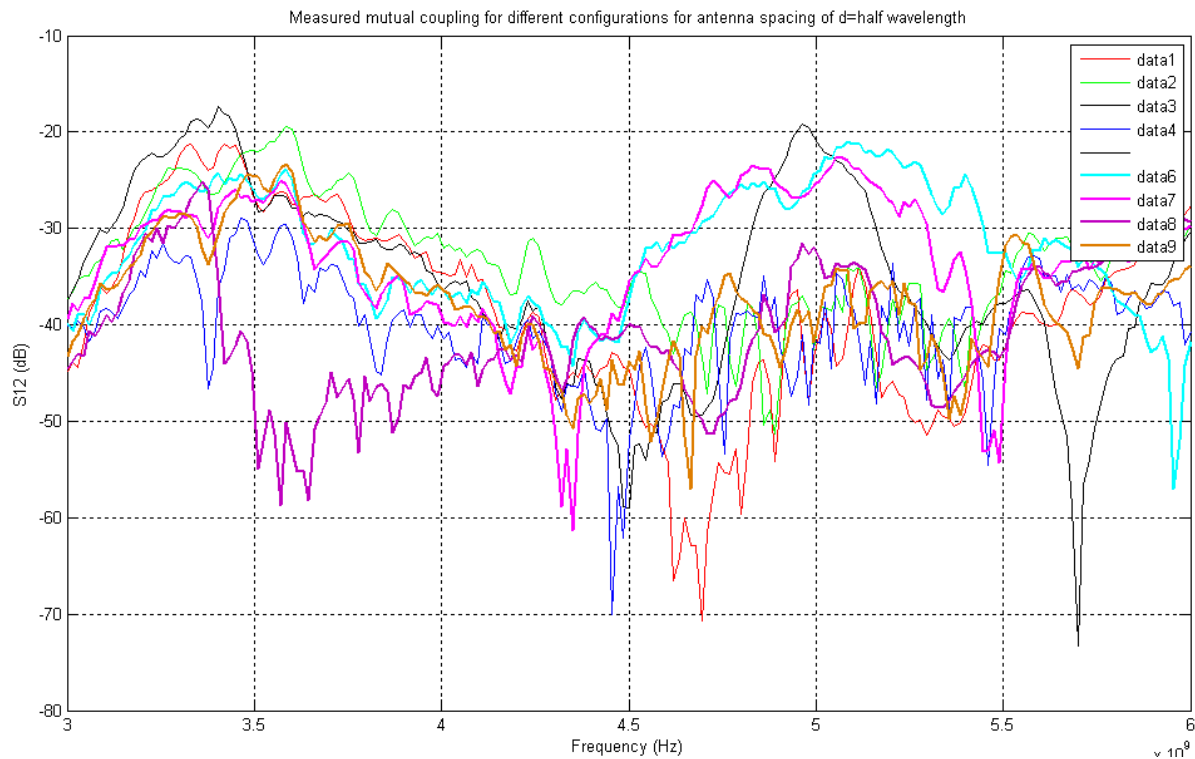


Figure 82 .Measured S21 for different configurations for antenna spacing of d=44mm

The S12 measurements for lower spacing between antennas are represented in Fig 85 and 87.

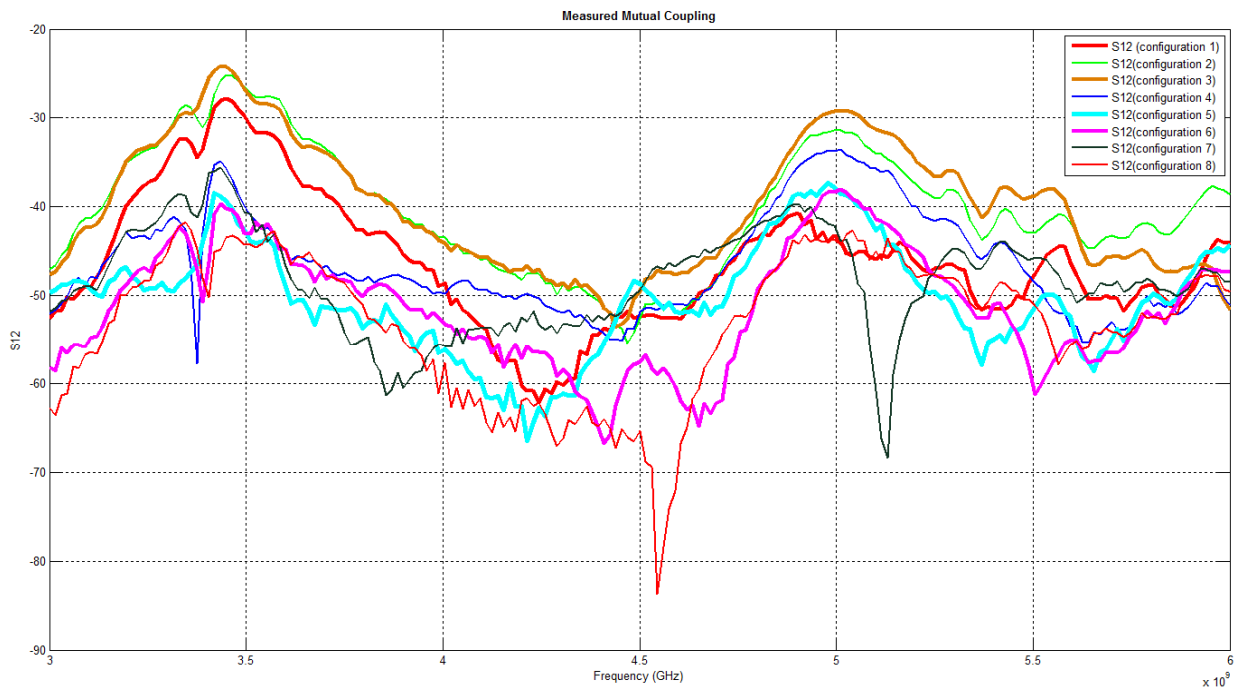


Figure 83 .Measured S_{21} for different configurations for antenna spacing of $d=22\text{mm}$

While figure 85 represents the mutual couplings in the entire frequency range, Figure 86 gives a better view of mutual coupling in smaller range of frequency which enclosed lower resonance frequency.

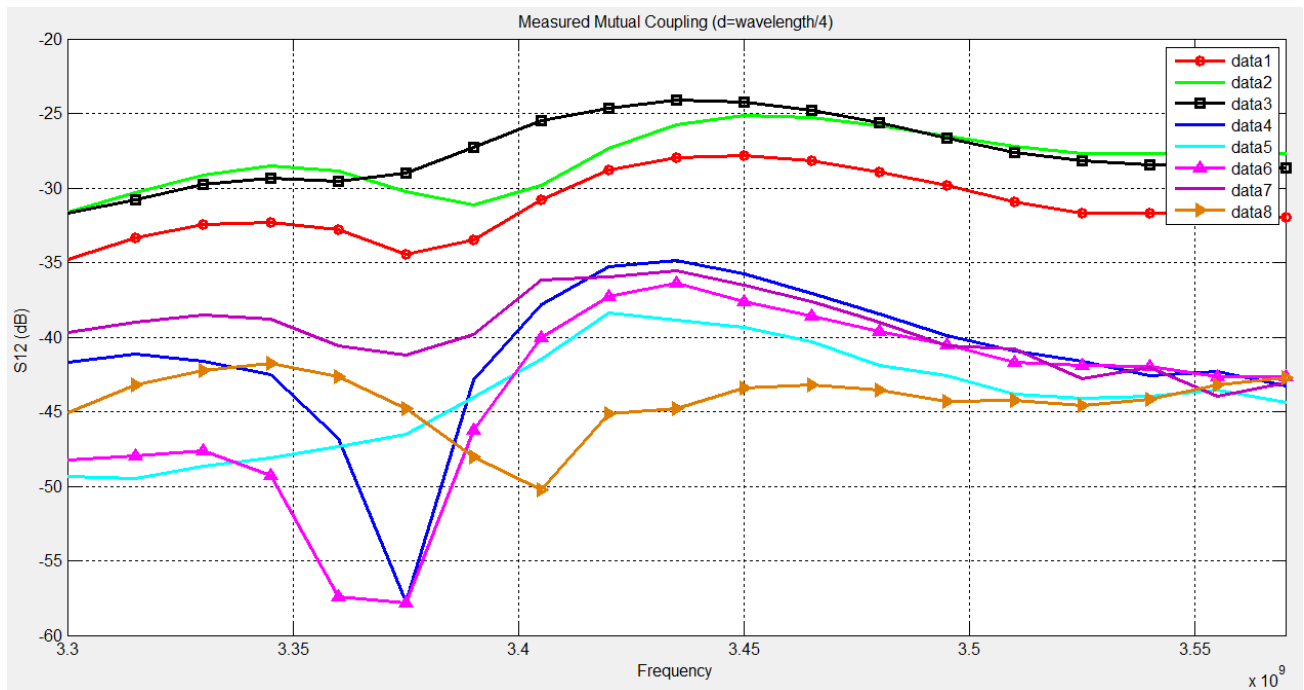


Figure 84 .Measured S_{21} for different configurations for antenna spacing of $d=22\text{mm}$ in shorter range of frequencies.

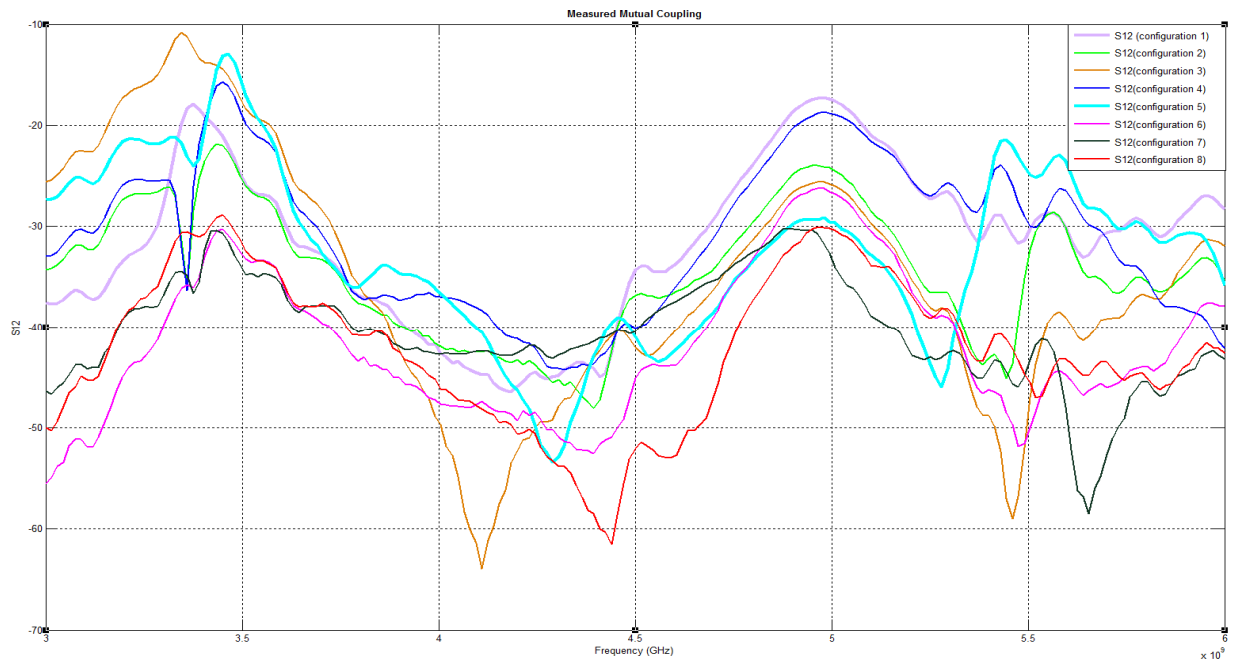


Figure 85 .Measured S21 for different configurations for antenna spacing of d=0mm

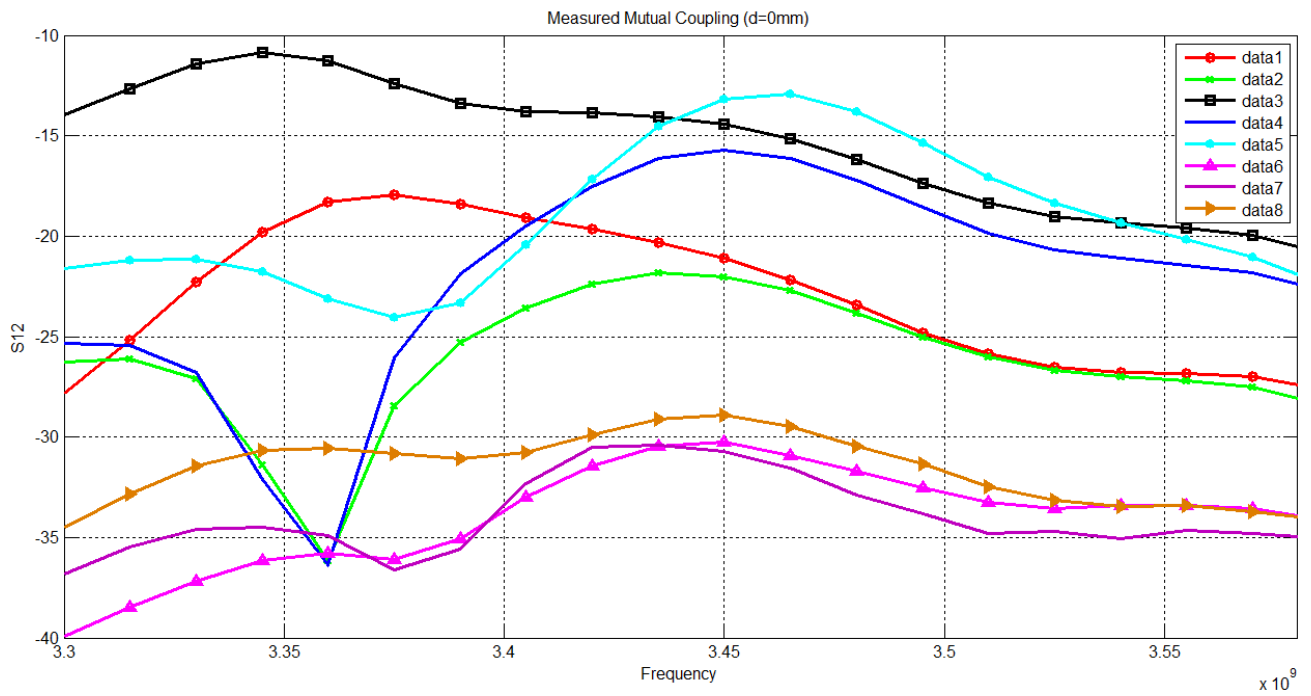


Figure 86 .Measured S21 for different configurations for antenna spacing of d=0mm in smaller range of frequencies.

5.3 MIMO capacity

In order to observe the effect of mutual coupling on MIMO, measured and simulated mutual coupling amounts used to calculate MIMO capacity in MATLAB. The calculation procedure is presented in chapter 4.

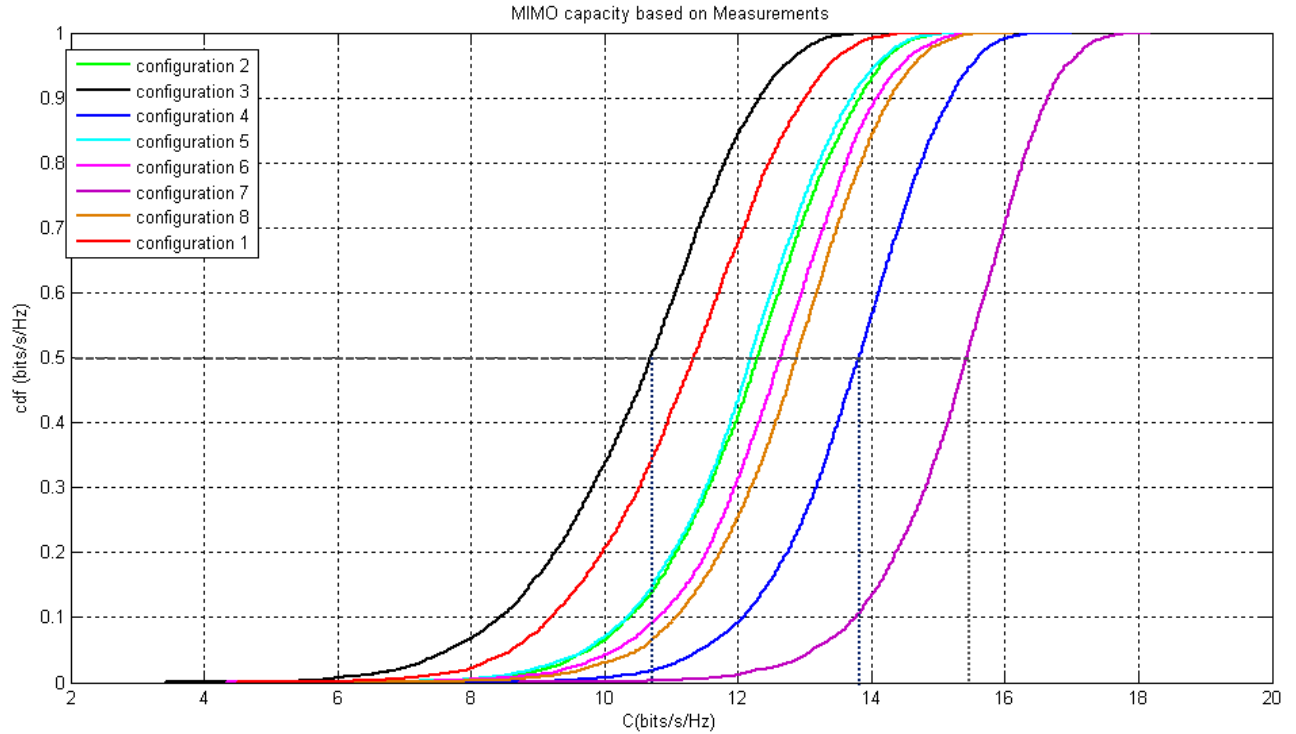


Figure 87 .Measured cumulative distribution function for MIMO capacity for eight proposed array configurations in the case of $d=\lambda/2$

Table 7. Average MIMO capacity based on measured S_{12} for each configuration

configuration	1	2	3	4	5	6	7	8
Average_Capacity	11.1989	12.1662	10.5007	13.6920	12.0821	12.5501	15.2848	12.7501

Based on measurements and simulations, configurations which have higher channel capacities are configuration 4, 8, and 6. These are the configurations that previously have been proven to have the lowest mutual couplings.

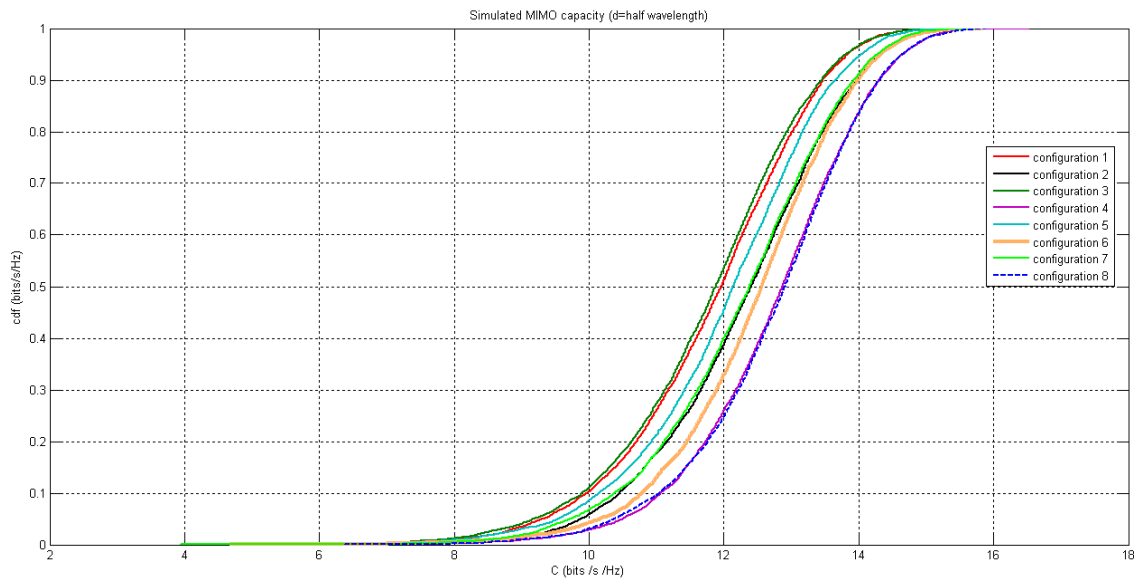


Figure 88. Simulated cumulated distribution function for MIMO capacity for 8 proposed array configurations in the case of $d=\lambda/2$

5.3 MIMO Radar Range –Angle Ambiguity

Before the invention of MIMO radars, a single waveform was transmitted from all the elements in the array. Even in the case that the mutual coupling between antenna elements had bad effects on receive mode processing. In the case of MIMO radar where different waveforms are emitted, mutual coupling should be considered both on the receive and the transmit side [24].

It is shown in [24] that mutual coupling between antenna elements in MIMO radar can cause mismatch loss. So having an array with low mutual coupling could be very useful. In order to see the effect of having different array configurations on radar system sensitivity, two random baseband codes have been generated and transmitted. In order to show that the true received waveform deviates from the ideal transmitted waveform in presence of mutual coupling the range –angle ambiguity function of the system with three different antenna array configurations has been calculated.

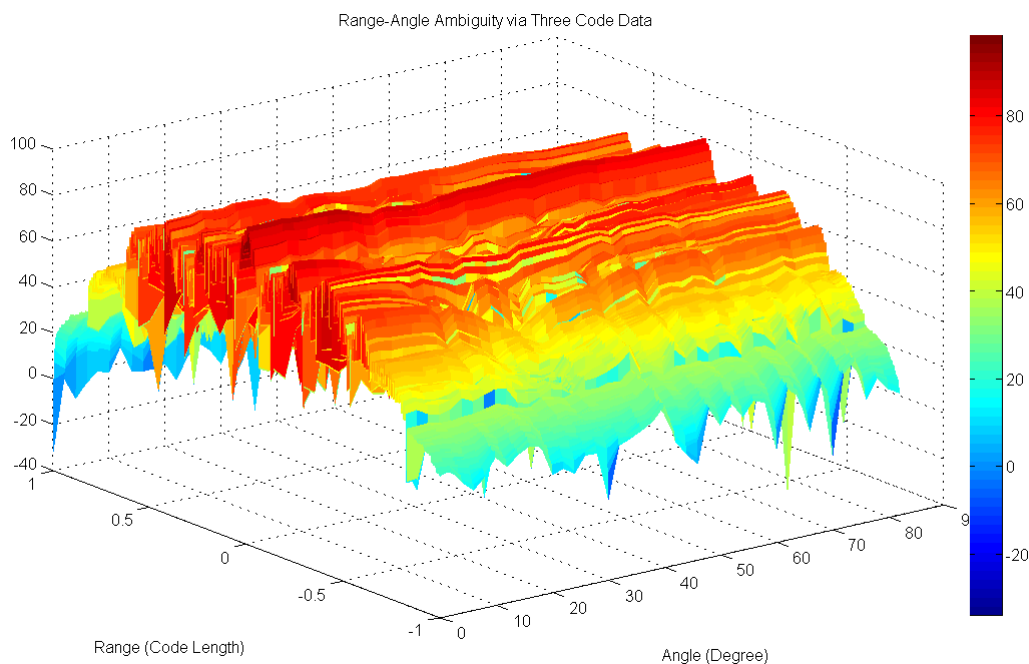


Figure 89.Range-Angle ambiguity function for array configuration 3

The range-angle ambiguity in Figure 91-92-93 illustrates the resulting distortion in terms of mismatch loss and degradation of angular resolution.

Figure 91, which shows the ambiguity function of radar with antenna array in configuration 3, represents higher mismatch loss than the other configurations that are shown in Figures 92 and 93. This could be due to high mutual coupling between antenna elements in configuration 3.

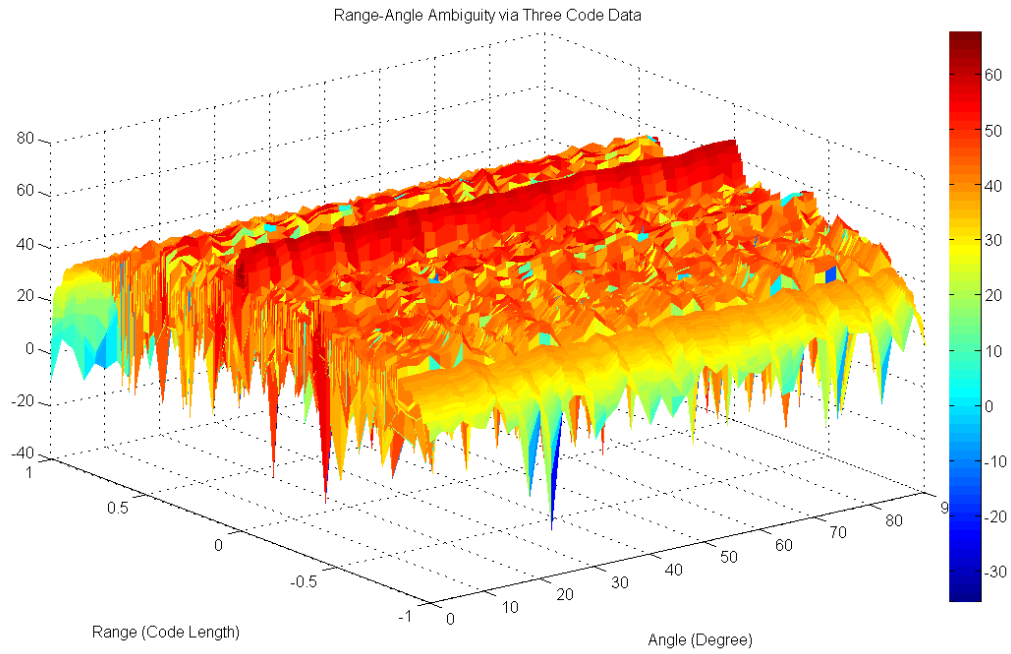


Figure 90.Range-Angle ambiguity function for array configuration 2

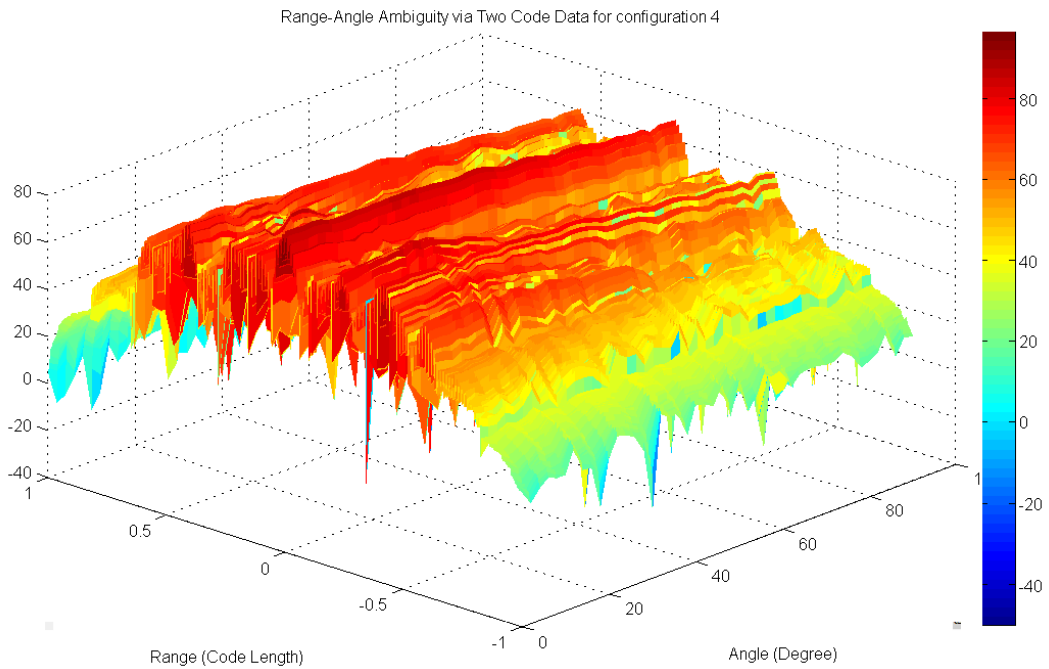


Figure 91.Range-Angle ambiguity function for array configuration 4

For the ideal case, we are expecting to see the peak for range equals to zero, which is due to the auto correlation of codes with themselves . It seems configuration 2 has better ambiguity plot. It is surprising, since mutual coupling in configuration 2 is more than configuration4.

This could be due to constructive/destructive combining of waveforms in far field of antennas.

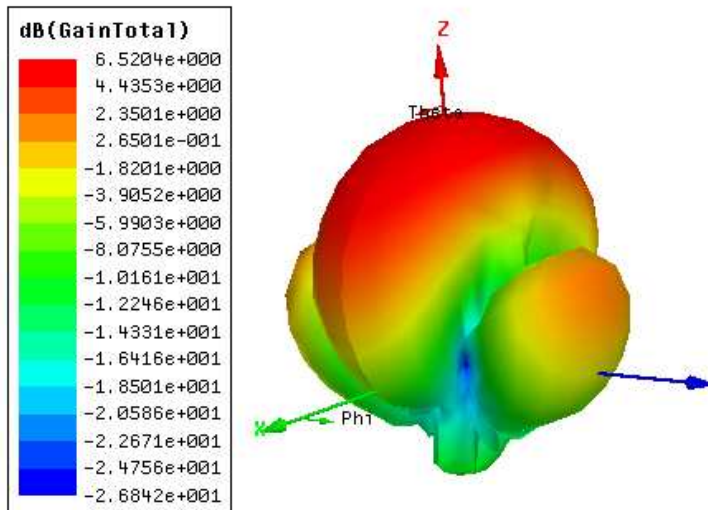


Figure 92.Radiation pattern of array with configuration2

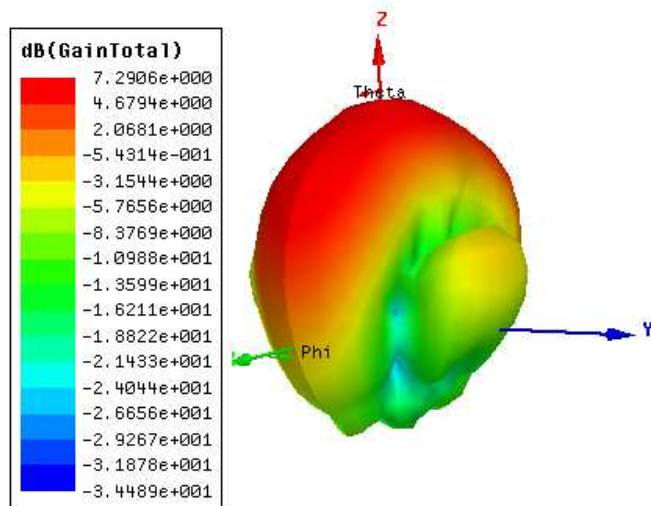


Figure 93.Radiation pattern of array with configuration4

5.4 Three Elements Array

Since in reality arrays may have more than two elements, mutual coupling between three elements have been measured in four different array configurations.

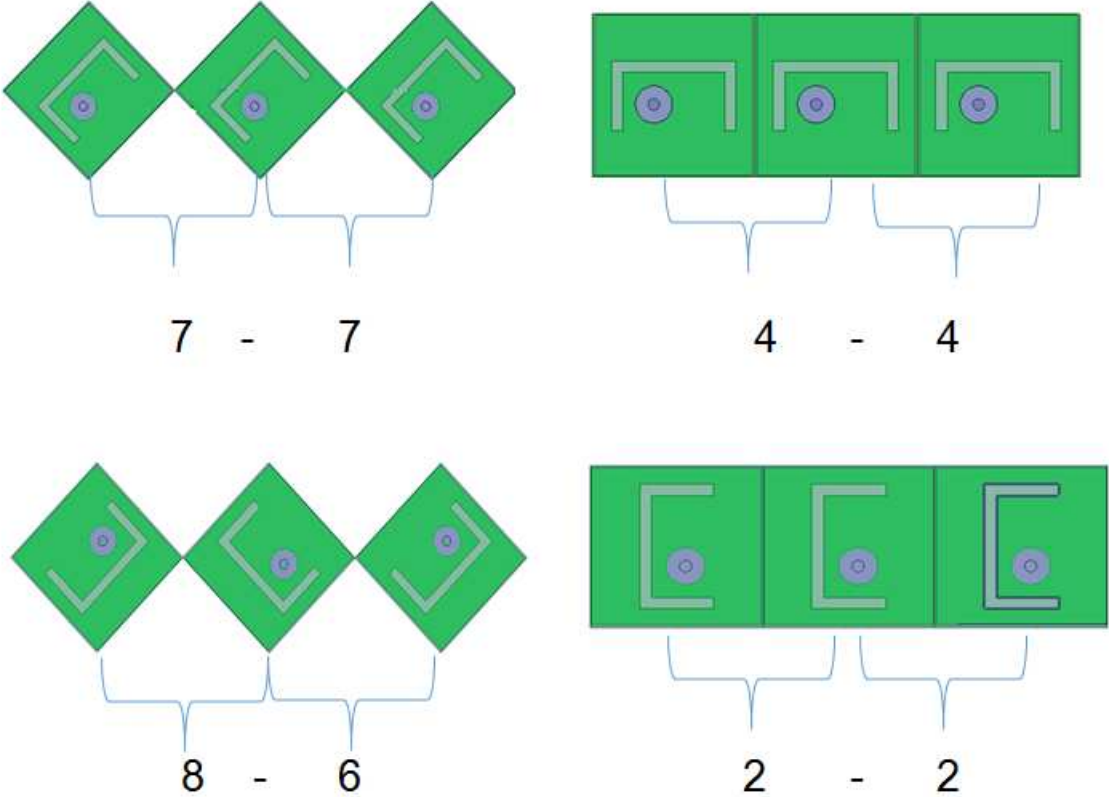


Figure 94 .Four different three element array configurations

Figure 97 shows measured S_{12} for above four configurations. It is obvious that for lower resonance frequency configuration 4-4 has the lowest mutual coupling between element 1 and 2. There is about 33 dB different between configuration 2-2 and 4-4 at 3.42 GHz.

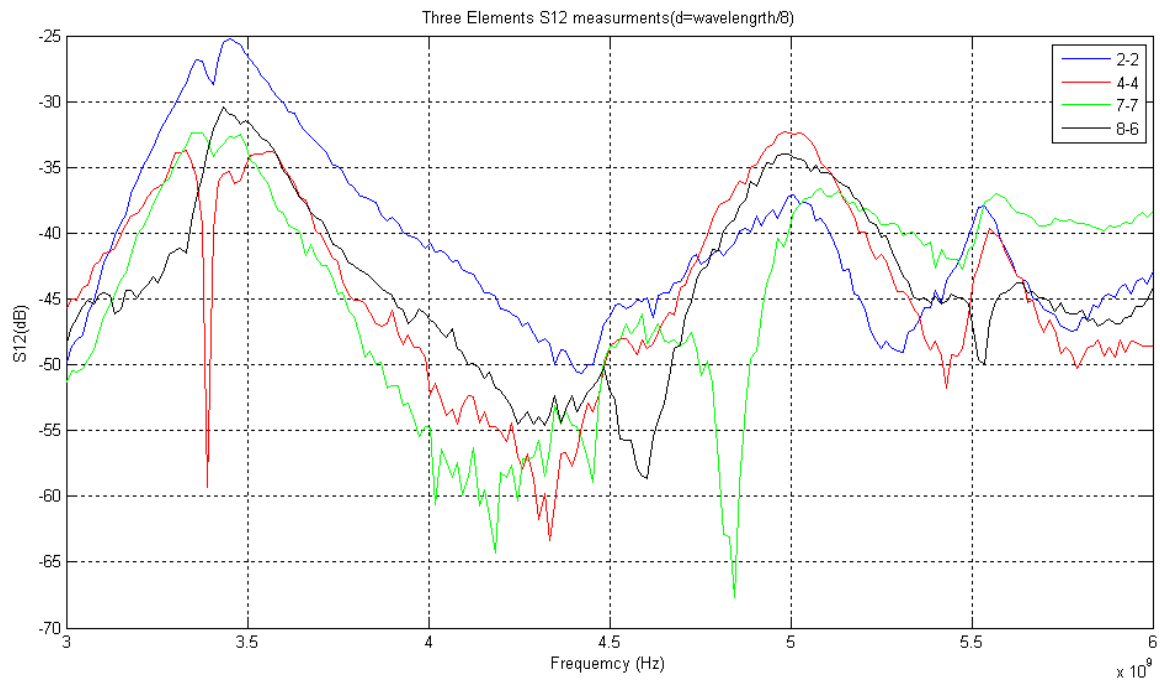


Figure 95. S_{12} measurements for four different configurations

As we expected all configurations shows very low mutual coupling between the first and third elements .This is because these two elements are far enough from each other compared to elements one and two or elements two and three.

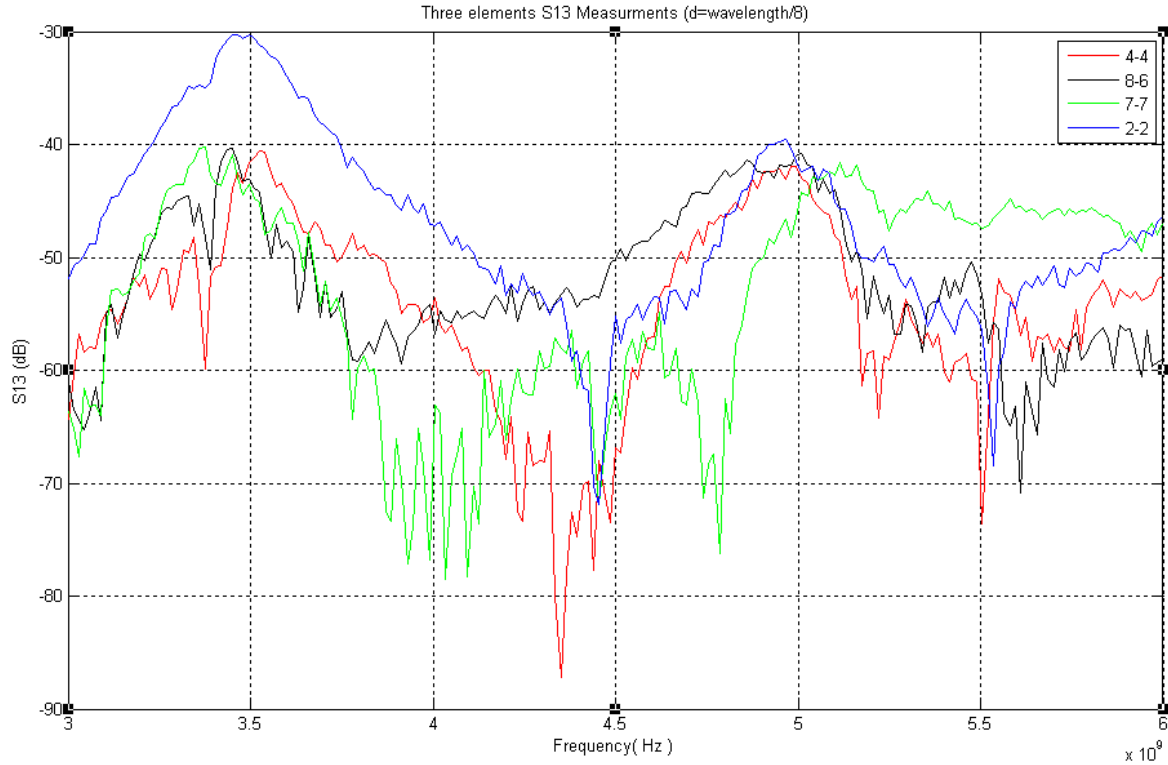


Figure 96. S_{13} measurements for four different configurations

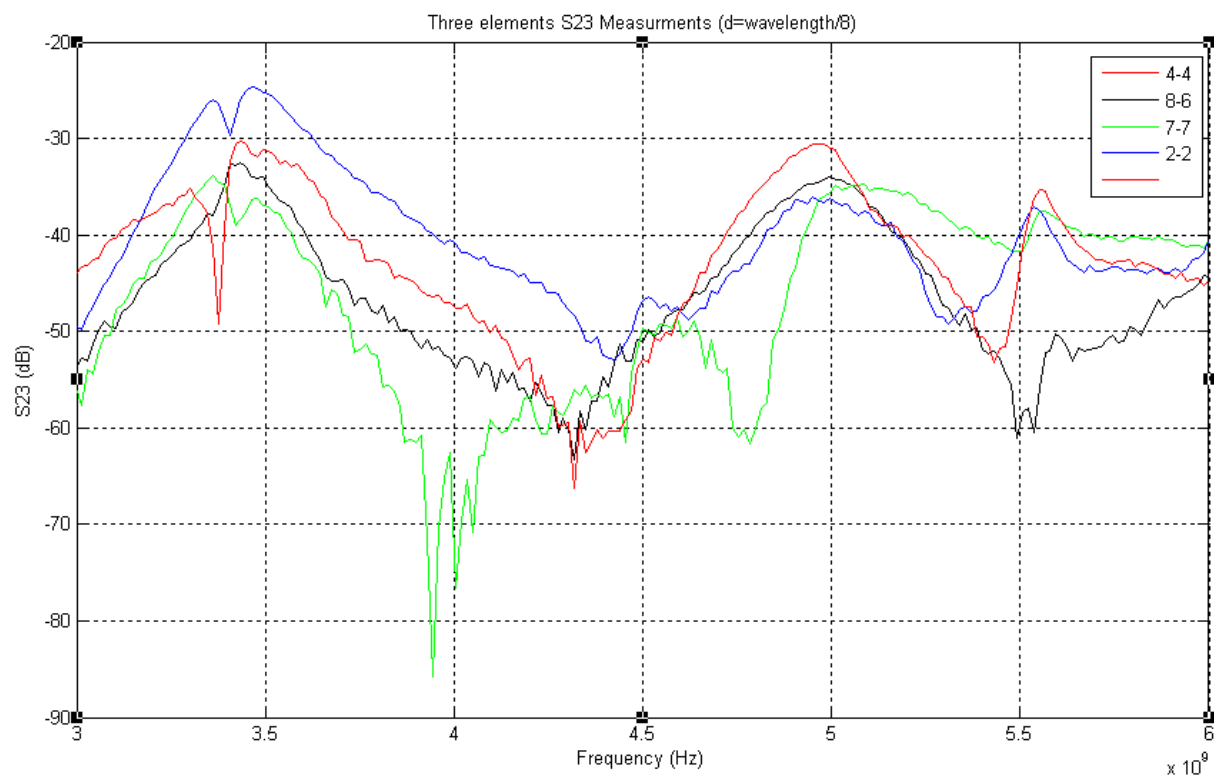


Figure 97. S_{23} measurements for four different configurations

Chapter 6

Conclusion and Future work

A simple but highly effective technique is proposed to reduce mutual coupling between antenna elements. Despite other techniques, in this method antenna structure remains unchanged and this leads to easier and more cost efficient fabrication.

In this thesis we investigated the behavior of U-slot patch antenna. It seems they are suitable choices to be used in MIMO applications. It was pointed out that different array configurations could have different amount of mutual coupling between elements. Eight different array configurations for two U-slot antennas have been considered.

Generally configurations 6, 8 and 4 are the configurations with the low mutual coupling. It has been shown that having low mutual coupling increases the MIMO capacity in Communication systems. And therefore a reconfigured antenna array in MIMO applications to get the lowest possible mutual coupling seems to be desirable.

Three U-slot antennas were fabricated, and mutual coupling was measured in different array configurations for an antenna array of two and three elements. In order to investigate the effect of mutual coupling on MIMO radar systems, the radar ambiguity function was been calculated for three different configurations. It is believed that choosing an antenna array configuration that shows lower mutual coupling between antennas has better radar performance. Simulation and experiment both confirm the possibility of getting low mutual coupling in an antenna array by using the best array configuration and without changing the antenna element's structure. It was also proven that this enhances the performance of MIMO systems in both communication and radar applications.

Bibliography

- [1] C. A. Balanis, "Antennas Theory: Analysis and Design", 3rd edition, John Wiley and Sons, 2005.
- [2] Tolga M. Duman, Ali Ghayeb, "Coding for MIMO Communication Systems", Wiley, December 10, 2007
- [3] Bassem R. Mahafza, Atef Z. Elsherbeni, "MATLAB Simulations for Radar Systems Design", 2004 by Chapman & Hall/CRC CRC Press LLC
- [4] Yi Huang , Kevin Boyle , "Antenna: From theory to practice", Wiley, 2008

- [5] Hofer, R.D. ; Oliver, D.E. ; Chatterjee, D. , "Analysis of Uslot, microstrip phased array radiator elements on electrically thick substrates", IEEE , 2007 .

- [6] Yan Wu, Linnartz, J.W.M. Bergmans Attallah, 'Effects of Antenna Mutual Coupling on the Performance of MIMO Systems', 29th Symposium on Information Theory in the Benelux, May 2008
- [7] LEE, R.Q., LEE, K.F., and BOBINCHAK, I.: 'Characteristics of a two-layer electromagnetically coupled rectangular patch antenna', Electron. Lett, 1987, 23, (20). pp. 1070-1072
- [8] GUPTA, K.C. "Multiport network approach for modelling and analysis of microstrip patch antenna and arrays"

- [9] CHEN, W., LEE, K.F., and LEE, R.Q. "Spectral-domain moment-method analysis of coplanar microstrip parasitic sub arrays", 1993, 6, (3), pp. 157-163

- [10] G. Foschini, "Layered space-time architecture for wireless communication in a fading environment when using multi-element antennas," Bell Labs. Technical Journal pp.41-59, 1996.
- [11] G. J. Foschini and M. J. Gans, "On limits of wireless communications in a fading Environment when Using Multiple Antennas ", Wireless Personal Communications: An International Journal , 1998

- [12] I. E. Telatar, "Capacity of multi-antenna Gaussian channels," *European Transactions on Telecommunications*, vol. 10, pp. 585-595, 1999
- [13] Pawandeep Singh Taluja, "Information-Theoretic Limits on Broadband Multi-Antenna Systems in the Presence of Mutual Coupling", PHD Dissertation
- [14] Tong, Chin Hong Matthew, "system study and design of broad-band u-slot Microstrip patch antennas for aperstructures and opportunistic arrays", thesis, December 2005,
- [15] Bhalla, R.; Shafai, L.; Rafi and Shafai, "Resonance behavior of single U-slot and dual U-slot antenna", *Antennas and Propagation Society International Symposium*, 2001. IEEE
- [16] Kin-Fai Tong and Ting-Pong Wong, "Circularly Polarized U-Slot Antenna", *IEEE transactions on antennas and propagation*, VOL. 55, NO. 8, AUGUST 2007
- [17] B. K. Lau, et al, "Impact of matching network on bandwidth of compact antenna arrays," *IEEE Trans. Antennas Propagation*, vol. 54, no. 11, pp. 3225–3238, Nov. 2006.
- [18] Y. Fei, et al, "Optimal single-port matching impedance for capacity maximization in compact MIMO arrays," *IEEE Trans. Antennas Propagation*, vol. 56, no. 11, pp. 3566–3575, Nov. 2008.
- [19] Luk, K.M.; Tong, K.F.; Shum, S.M.; Huynh, T.; Lee, R.Q. "Experimental and simulation studies of the coaxially fed U-slot rectangular patch antenna", Oct 1997, *Microwaves, Antennas and Propagation, IEE Proceedings (Volume:144, Issue: 5)*.
- [20] Mahmoud, M. "Improving the Bandwidth of U-slot Microstrip Antenna Using a New Technique" (Trough-Slot Patch), *IEEE conference publications*, 2008
- [21] Zhi Ning Chen; Xue Ni Low, "Configuration optimization of suspended plate antennas for reduction of mutual coupling" *Antenna Technology, 2011 International Workshop*
- [22] Clenet, M. and L. Shafai, "Multiple resonances and polarization of U-slot patch antenna," *Electron. Lett.*, Vol. 35, No. 2, 101–103, Jan. 21, 1999.
- [23] Kai Fong Lee; Yang, S.L.S.; Kishk, A.A.; Kwai Man Luk "The Versatile U-Slot Patch Antenna", *Antennas and Propagation Magazine, IEEE*, On page(s): 71 - 88 Volume: 52, Issue: 1, Feb. 2010

- [24] Cordill, B. ; Metcalf, J. ; Seguin, S.A. ; Chatterjee, D. ; "The impact of mutual coupling on MIMO radar emissions", Electromagnetics in Advanced Applications (ICEAA), 2011 International Conference , Publication Year: 2011
- [25] Gonzalez, A.N., Lindmark, B. "The effect of antenna orientation and polarization on MIMO capacity", Antennas and Propagation Society International Symposium, 2005 IEEE Publication Year: 2005 , Page(s): 434 - 437 vol. 3B
- [26] Huynh, T. and K. F. Lee, "Single layer single patch wideband microstrip antenna," Electronics Letters, Vol. 31, No. 16, 1310–1312, 1995
- [27] John Volakis, "Antenna Engineering Handbook", Fourth Edition McGraw-Hill Companies, Incorporated, 2007
- [28] Zhengyi Li ; Zhengwei Du ; Takahashi, M. ; Saito, K. ; Ito, K. "Reducing Mutual Coupling of MIMO Antennas With Parasitic Elements for Mobile Terminals", Antennas and Propagation, IEEE Transactions on , 2012 ,
- [29] http://course.ee.ust.hk/elec536/2013Fall_Notes/Lecture%208%20%20MIMO%201.pdf
- [30] Chatterjee, D., "Numerical modeling of scan behavior of finite planar arrays of wideband U-slot and rectangular microstrip patch elements". Phased Array Systems and Technology, IEEE , 2003.
- [31] G. Chi, L. Binhong, and D. Qi, "Dual band printed diversity antenna for 2.4/5.2 GHz WLAN applications," Microw. Opt. Technol. Lett, vol 45, no 6, June 2005
- [32] A. Diallo, C. Luxey, P. L. Thuc, R. Staraj, and G. Kossiavas, "Study and reduction of the mutual coupling between two mobile phone PIFAs operating in the DCS1800 and UMTS bands," IEEE Trans. Antennas Propag., vol. 54, no. 11, pp. 3063–3073, Nov. 2006.

